Failure and Degradation Modes of PV modules in a Hot Dry Climate:

Results after 4 and 12 years of field exposure

by

Jaya Krishna Mallineni

A Thesis Presented in Partial Fulfillment
of the Requirements for the Degree
Master of Science in Technology

Approved November 2013 by the
Graduate Supervisory Committee:

Govindasamy Tamizhmani, Chair
Devarajan Srinivasan
Narciso Macia

ARIZONA STATE UNIVERSITY

December 2013

ABSTRACT

This study evaluates two photovoltaic (PV) power plants based on electrical performance measurements, diode checks, visual inspections and infrared scanning. The purpose of this study is to measure degradation rates of performance parameters (Pmax, Isc, Voc, Vmax, Imax and FF) and to identify the failure modes in a "hot-dry desert" climatic condition along with quantitative determination of safety failure rates and reliability failure rates. The data obtained from this study can be used by module manufacturers in determining the warranty limits of their modules and also by banks, investors, project developers and users in determining appropriate financing or decommissioning models. In addition, the data obtained in this study will be helpful in selecting appropriate accelerated stress tests which would replicate the field failures for the new modules and would predict the lifetime for new PV modules.

The study was conducted at two, single axis tracking monocrystalline silicon (c-Si) power plants, Site 3 and Site 4c of Salt River Project (SRP).

The Site 3 power plant is located in Glendale, Arizona and the Site 4c power plant is located in Mesa, Arizona both considered a "hot-dry" field condition.

The Site 3 power plant has 2,352 modules (named as Model-G) which was rated at 250 kW DC output. The mean and median degradation of these 12 years old modules are 0.95%/year and 0.96%/year, respectively. The major cause of degradation found in Site 3 is due to high series resistance (potentially due to solder-bond thermo-mechanical fatigue) and the failure mode is ribbon-ribbon solder bond failure/breakage.

The Site 4c power plant has 1,280 modules (named as Model-H) which provide 243 kW DC output. The mean and median degradation of these 4 years old modules are 0.96%/year and 1%/year, respectively. At Site 4c, practically, none of the module failures are observed.

The average soiling loss is 6.9% in Site 3 and 5.5% in Site 4c. The difference in soiling level is attributed to the rural and urban surroundings of these two power plants.

DEDICATION

I dedicate this work to my parents Ranga Rao Mallineni, Satyavathi Mallineni and my sister Bindu Mallineni for their support throughout my study in Arizona State University.

ACKNOWLEDGMENTS

First, I would like to convey my heartfelt thanks to Dr.Govindasamy TamizhMani for his constant guidance and support throughout the project. I would also like to thank Dr.Narciso Macia and Dr.Devarajan Srinivasan for readily accepting to be on my advising committee.

My heartful thanks to Mr. Joseph Kuitche for giving me the opportunity to work at Arizona State University Photovoltaic Reliability Laboratory. I gained great knowledge while working under his supervision at PRL.

Thanks to SRP (Salt River Project) for funding support to execute the project successfully. I thank Mr. Bill Kazesta for the knowledge he shared during the site work. My appreciation goes to Brent Schuster, Hannoush Eric, Dan Wilson, Jeff for their support during the testing. I appreciate the joint working partnership with Karan Rao Yedidi on this project.

I will be grateful to Sai Tatapudi and Brett Knisely for their support and motivation through the course of my project.

Special thanks go out to my dearest friends Suryanarayana Vasantha Janakeeraman, Kolapo Olakonu, Jonathan Belmont, Cameron Anderson, Cassie Yan, and Sanjay Mohan Shrestha.

TABLE OF CONTENTS

Page

CHAPTER Page

LIST OF TABLES

LIST OF FIGURES

Figure Page

Figure Page

Figure Page

Figure Page

Figure Page

LIST OF VARIABLES

W/m^2= Watts / $Meter^2$

kW = Kilowatts

Isc = Short Circuit Current

V_{oc} = Open Circuit voltage

Imax= Maximum Current

Vmax= Maximum Voltage

FF = Fill Factor

Ft = Feet

STC = Standard Test Conditions (25^oC, 1000 W/m^2)

CHAPTER 1

INTRODUCTION

1.1 Background

In order for the photovoltaic (PV) industry to compete with the other power sources such as hydro, coal, nuclear, and natural gas and to also achieve grid parity, the cost of the module should be 0.5$/watt and the useful life of a module should be more than 20 years. More than 94% of PV modules in the world were installed in the last 5 years and the capability of these modules reaching their remaining useful life needs to be validated. The degradation and reliability issues found by evaluating old, existing power plants, helps to predict the useful life of newer power plants of the same technology.

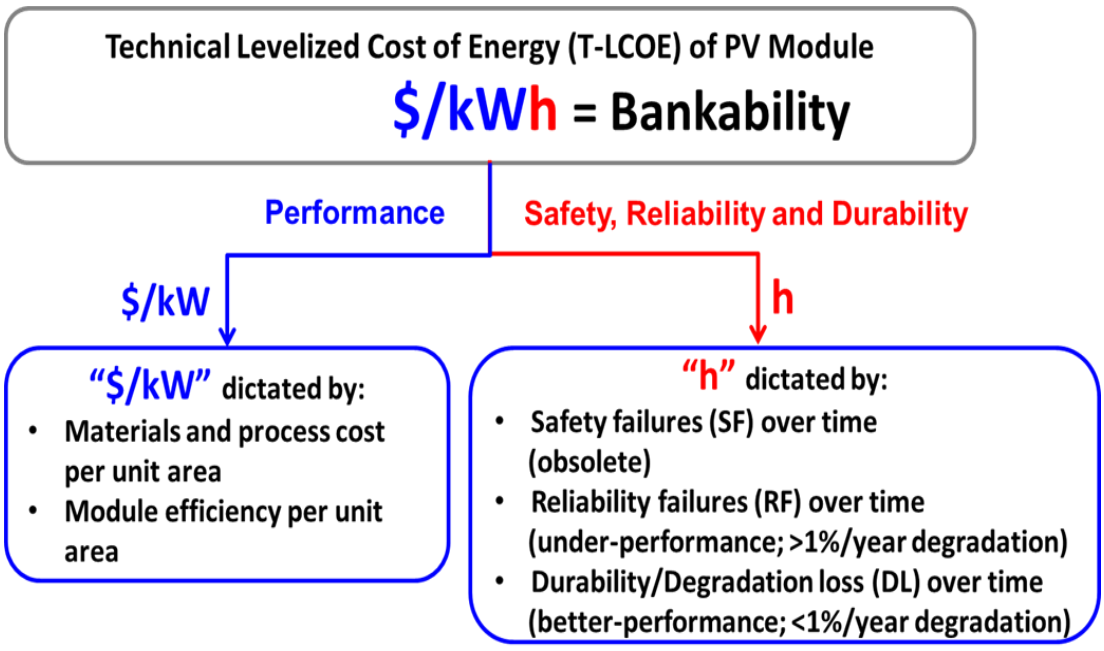

Figure 1 Overall goal of the industry to reduce levelized cost of energy

Currently the Salt River Project (SRP) has funded the Arizona State University-Photovoltaic Reliability Laboratory (ASU-PRL) to evaluate PV power plants. The degradation and the reliability failures found in the field from this project could be used to simulate accelerated life testing for "hot-dry desert" climatic conditions. The two PV power plants evaluated are the Site 3 power plant in Glendale, Arizona and the Site 4c power plant in Mesa, Arizona. Both of these power plants utilize a single axis tracking system with c-Si modules. Site 3 is a 12–year-old system with a 249.9 kW_{dc} output and Site 4c is 4-year-old system with a 243.2 kW_{dc} output.

1.2 Objective

The specific objectives of this study are to investigate the two PV systems at both the individual and string level. The main focus is to provide the following results

- Performance degradation of modules and strings;
- To confirm that Potential Induced Degradation(PID) does not exist in positive biased power plants in "hot-dry desert" climatic conditions;
- Soiling loss for single-axis tracking systems;
- Systematic wind direction effect on performance degradation;
- Durability issues and reliability failures found in a "hot-dry desert" climate.

The results and findings of this study will contribute to PV industry as follows

- To better predict the lifetime of the PV modules in "hot-dry desert" climatic conditions
- To improve materials used for the components of PV modules
- To help PV manufactures restructure their future warranty agreements.

- To help financial investors determine characteristics of future PV power plants.

1.3 Scope of the project

The scope of this project is presented in the Figure 2(below). The tests accomplished during this study are highlighted in green and the tests in blue are tests that could not be accomplished due to limited testing days. The two main goals for performing the tests include

- Safety and Reliability Evaluation - Identification of Safety Failures (SF) and Reliability Failures(RF)
- Durability and Reliability Evaluation – Identification of degradation rates.

The tests performed in Site 3 are:

- 84 soiled string level I-V measurements
- 367 cleaned individual modules I-V measurements
- Visual Inspection, IR imaging and diode check of all 2352 modules at Site 3.

The tests performed in Site 4c are:

- 158 soiled string level I-V measurements.
- 94 cleaned individual modules I-V measurements.
- Overview of visual inspection of all 1,280 modules
- Diode check of 640 modules.

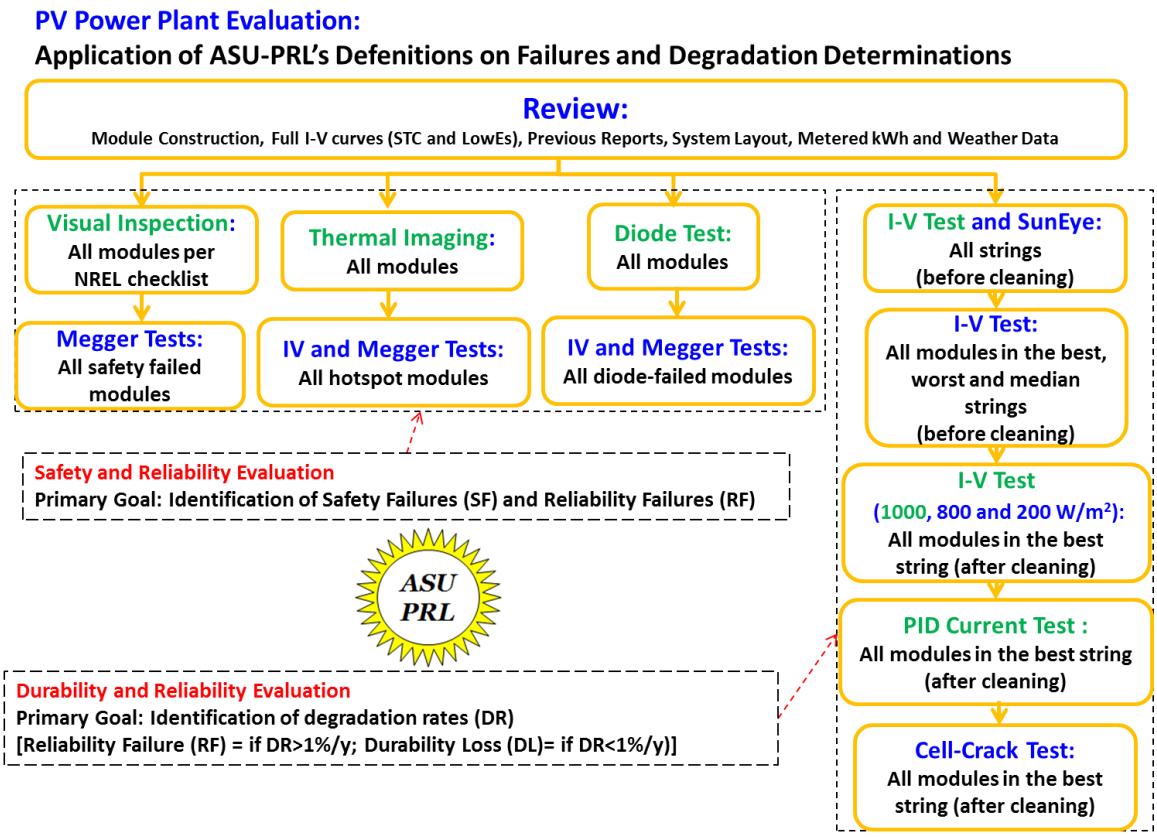

Figure 2 Scope of the project

CHAPTER 2

LITERATURE REVIEW

2.1 Durability and Reliability Definitions of PV modules

Durability: If the performance of PV modules degrades due to soft losses or degradative losses, but still meets the warranty requirements, then those modules are considered durable [1]. Durability issues could be attributed due to the materials or material systems used for manufacturing the PV modules. The degradation losses could be caused due to the gradual encapsulant degradation, slow corrosion and/or backsheet wrapping.

Reliability: A reliable PV module may be defined as a PV module that has a high probability of performing its intended function adequately for 30 years under the operating conditions encountered [2]. Reliability failures could be attributed to the design and production issues, and eligible for the warranty claims [1].

Figure 3 shows that 34 modules have experienced reliability issues such as delamination failures, diode failures and cell/circuit wear-out issues.

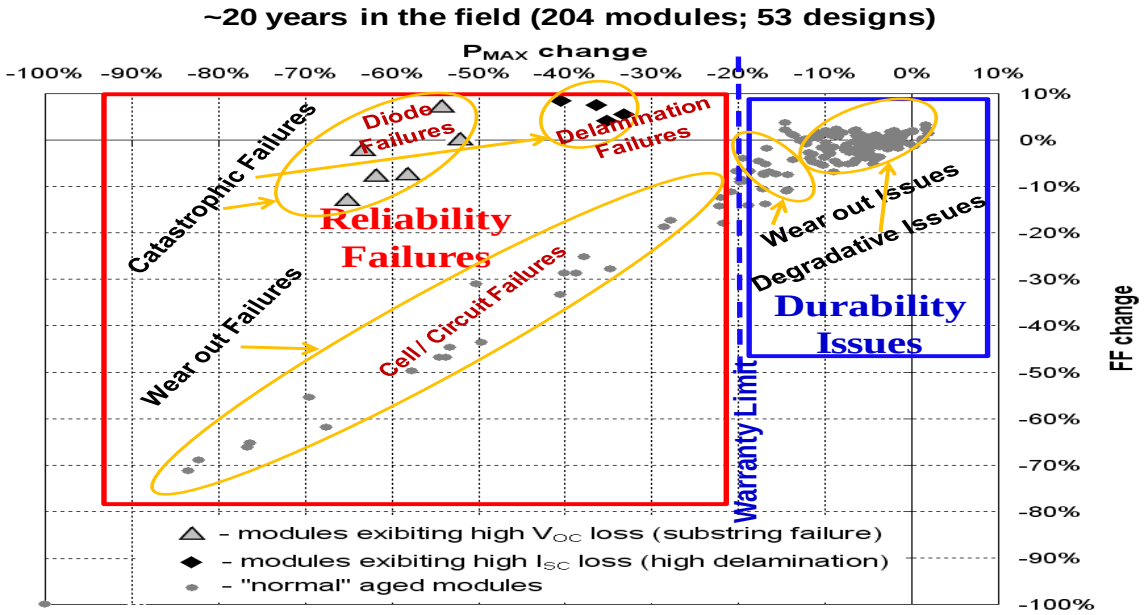

Figure 3 Reliability (failures) and Durability (degradative) issues of PV modules in field [1]

2.2 Failure modes and degradation modes

Failure and degradation modes and also mechanisms of PV modules are dictated by the design/packaging/construction and/or the field environment in which the modules operate [1]. Failure modes can have different causes and effects on PV modules.

The field failure analysis approach for PV modules may be represented as shown in the following sequence [1]:

Failure Mechanism (Cause) ⟶ Failure Mode (Effect)

Example:

Thermo-mechanical fatigue (Expansions-Contractions) ⟶ Broken interconnects (Arcing)

Broken interconnects, solder bond failures, hotspots, encapsulant delamination, backsheet warping are some of the failure modes. Thermal expansion and contraction is the major cause for broken interconnects and solder bond failures. Encapsulant delamination is caused by sensitivity of adhesive bonds to ultra violet light at higher temperature and/or to humidity in the field and also due to contamination from material(s) (Excess Na in glass or acetic acid from encapsulant). Hot spots are mainly caused due to shadowing, faulty cells, low shunt resistance and/or failure of bypass diodes.

Degradation Modes includes slow corrosion, gradual encapsulant discoloration and/or backsheet detaching/cracking/warping. Gradual encapsulant discoloration could be caused due to UV exposure at higher operating temperatures, reduced breathability and/or inappropriate additives in EVA. The major degradation modes experienced in “hot-dry” climates are found to be solder bond deterioration and encapsulant discoloration based on the research done on 1900 modules [15].

2.2.1 Solder bond failure

The modules ribbon wire is made of copper metal and soldered with SnPbAg as shown in Figure 4. The ribbon carries the current from the each solar cell to the junction box. The main cause for the cracks in the solder bond is caused by a mismatch of coefficient of thermal expansion between the module material and ribbon wire solder [7].

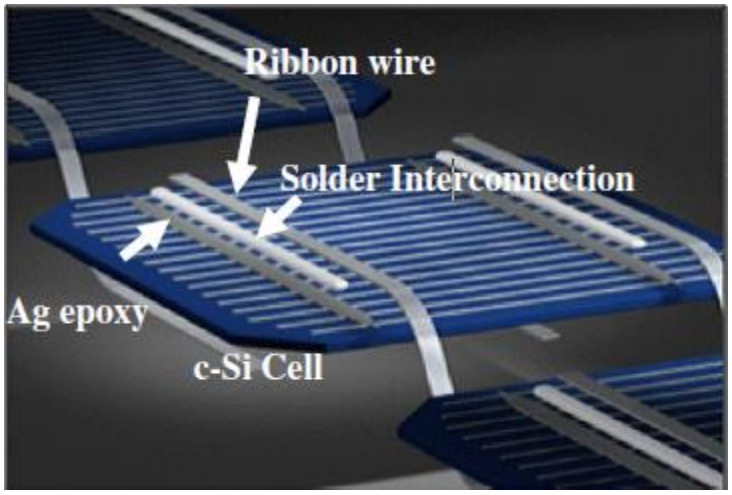

Figure 4 Solder interconnection between ribbon wire and silicon solar cell [7]

2.3 Degradation Rates

Arizona State University Photovoltaic Reliability Laboratory (ASU-PRL) researched 1,900 modules in the "hot-dry" climate of Tempe, Arizona and found that the degradation rates lie between 0.6%/year and 2.5%/year depending on the module model and manufacturer [4]. The major contributors of power degradation in glass/polymer modules appeared to be fill factor loss and short circuit loss. National Renewable Energy Laboratories (NREL) reported that the module degradation rate can be as high as 4%/year, but the median and average degradation rates are 0.5%/year and 0.8%/year, respectively [6].

2.4 Potential Induced Degradation (PID)

In a PV power plant, the modules in a string are connected in series or parallel to achieve higher output power. When modules are connected in series, the modules at different positions in the string will be at different voltages. This is especially true for the modules at the extreme ends of the strings which can experience a few hundreds of volts difference [5]. Figure 5 provides an example to determine the string biasing. If the negative end of the string is grounded the string is positive biased and if the positive end of the string is grounded the string is negative biased. When the insulation between the frame and the active layers is not perfect, the high bias voltage will produce a leakage current which affects the system's long term performance. These impacts have been named potential induced degradation (PID) [5].

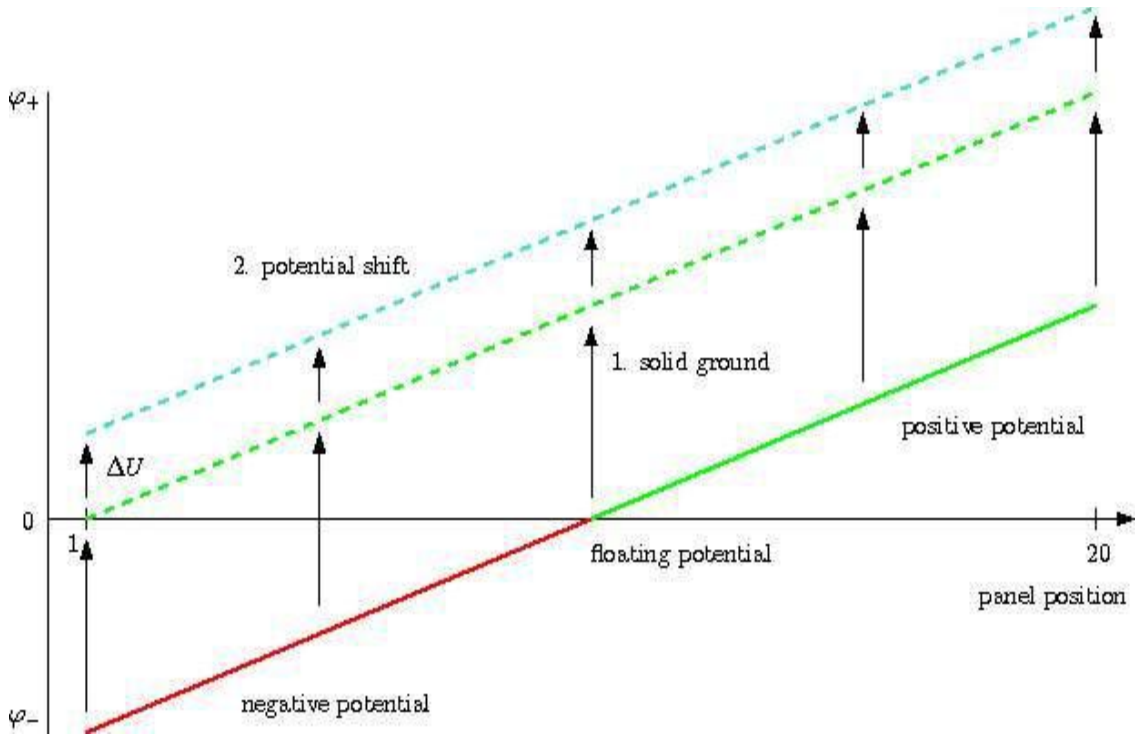

Figure 5 Biasing technique determination with ground [3]

PID depends on temperature and humidity [3]. Arizona state university Photovoltaic Reliability Laboratory (ASU-PRL) performed a PID investigation on more than 100 negatively grounded strings (with STC string voltage of about 500 V) and found that the c-Si modules did not experience the PID effect. The absence of the PID effect on the modules investigated in this project could possibly be attributed to the "hot-dry" climatic condition of the test site along with negative grounding of the system (Tempe, Arizona) [4].

2.5 Bypass diode Failures

Bypass diodes are triggered when a shadow is casted over a module or when there is a hotspot cell. If a bypass diode fails it could lead to safety issues. The "bypass diode

principle" is to use a diode in reverse paralleling with several solar cells. The bypass diode is blocked when all cells are illuminated, and conducts when one or several cells are shadowed [11]. The Figure 6 shows the bypass diode functioning.

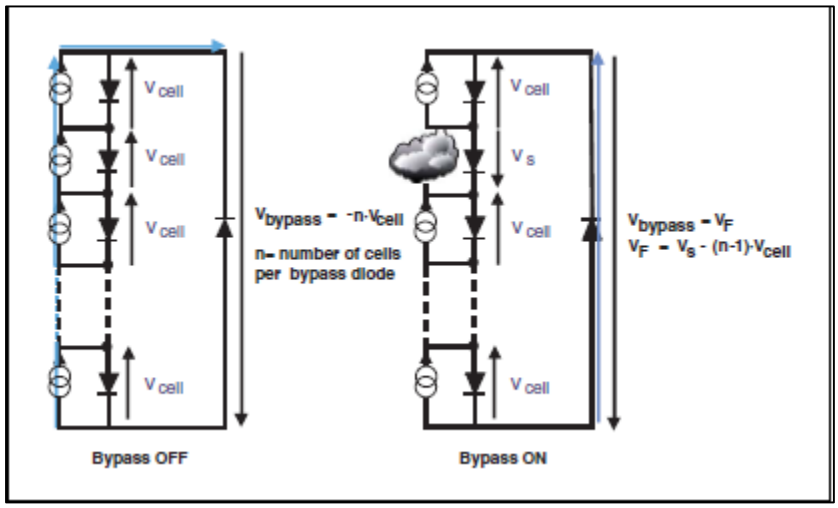

Figure 6 Bypass diodes working phases [11]

When the bypass diodes are are triggered due to a moving shadow they undergo thermal runaway[11] ,where the induced reverse leakage current could exceed the diode reverse leakage current rating. At high temperatures this condition can lead to failure as the high current diodes fail quickly in a run-away mode[12]. Figure 7 shows how the instantaneous leakage current passes through the diode at different reverse voltages at different temperatures. This problem could be overcomed by using low current diodes which cool down and stabilize safely at relatively low current[12].

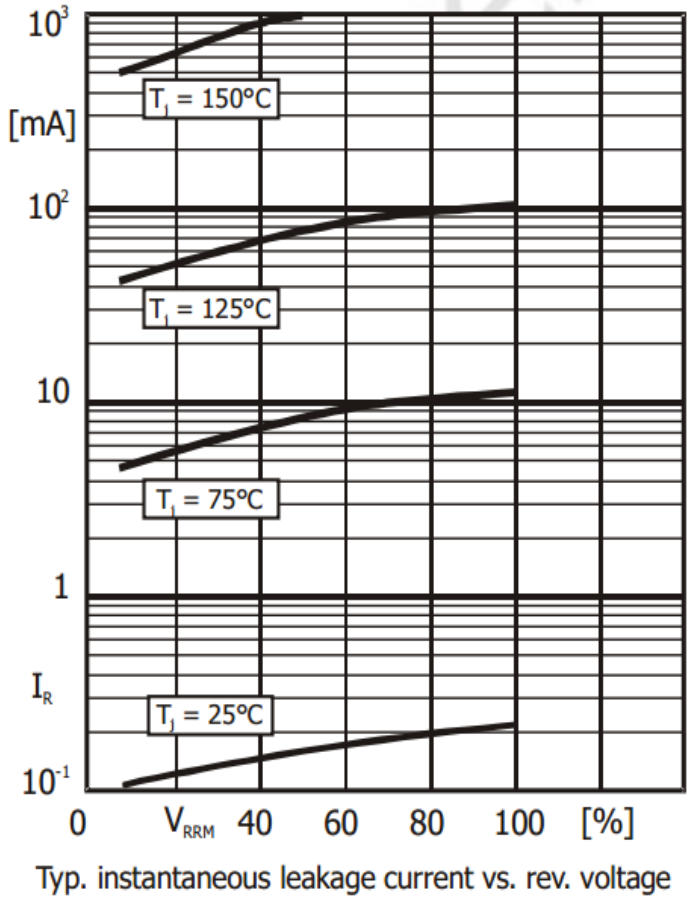

Figure 7 High reverse current diode instantaneous leakage current vs. reverse voltage [11].

2.6 Effect of Series and Shunt Resistance on I-V parameters

Series resistance in a solar cell has three causes: firstly, the movement of current through the emitter and base of the solar cell; secondly, the contact resistance between the metal contact and the silicon; and finally the resistance of the top and rear metal contacts [14]. FF is mainly reduced because of series resistance increase. Since FF = (Vmax x Imax)/ (Voc x Isc), as Voc and Isc do not increase in field aged modules, FF drop is dictated by only Vmax or Imax drop or both.

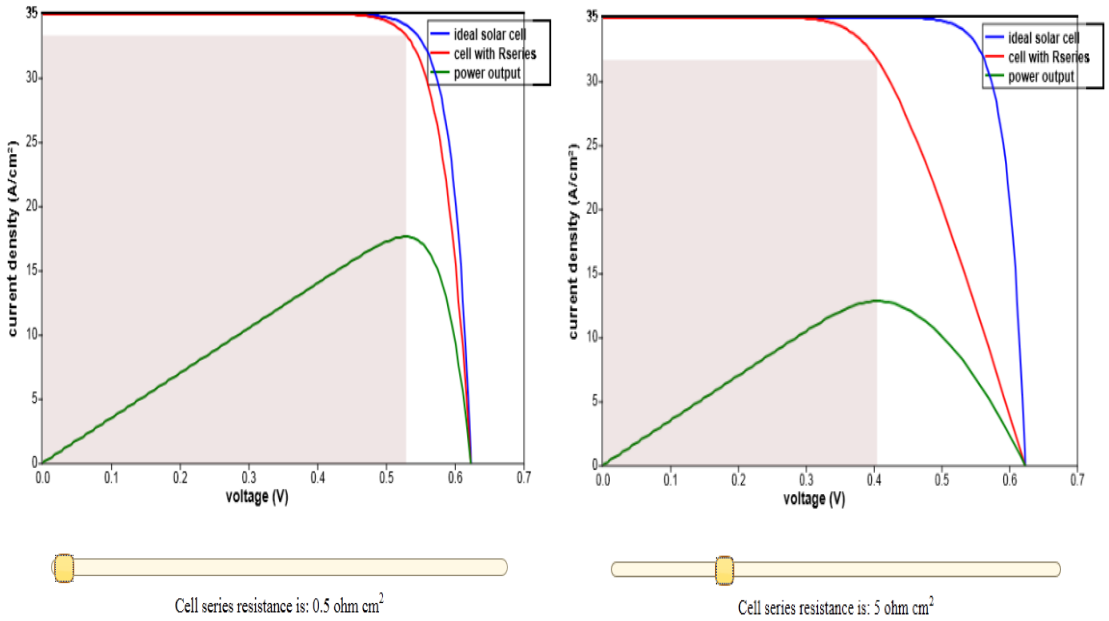

Figure 8 Cell series resistance [14]

In Figure 8, the graph on the left has series resistance of 0.5 ohms cm^{-2} and the graph on the right has series resistance increased to 5 ohms cm^{-2}. The parameters Isc and Voc has no change after the series resistance increased by 30 ohms cm^{-2}. Vmax has increased by 25% and Imax by 4%. When series resistance increases the major loss is seen in Vmax rather than Imax.

Shunt resistance drop is caused typically by manufacturing defects, potential induced degradation and severe hot spots. The drop in shunt resistance could decrease the voltage and have a severe impact on current at low light levels.

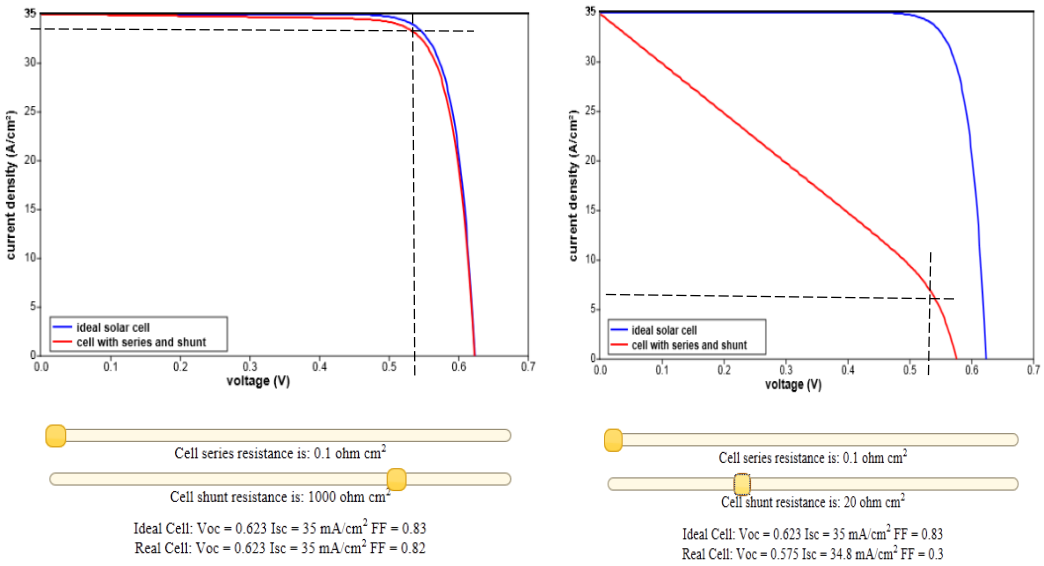

Figure 9 Cell shunt resistance [14]

In Figure 9, the graph on the left has shunt resistance of 1000 ohms cm^{-2} and the graph on the right has shunt resistance decreased to 20 ohms cm^{-2}. The parameters Isc and Voc have no change after the shunt resistance is decreased by 50 times. Vmax has decreased by 17% and Imax by 63%. So shunt resistance has more effect on Imax rather than on Vmax.

CHAPTER 3

METHODOLOGY

3.1 Site layout and description

The PV power plants analyzed in this study were the Site 3 and Site 4c photovoltaic power plants. The Site 3 power plant is located in Glendale, AZ and Site 4c power plant is located in Mesa, AZ. As and ASU-PRL policy, the names of the module manufacturers installed in these two power plants are not disclosed in this study. In both the systems, the modules are installed on single-axis tracking system.

Site 3 is a 249.9kW_{dc} and 200 kW_{ac} rated power plant and Site 4c is a 243.2kW_{dc} and 204.3kW_{ac} rated power plant.

Table 1 System Location

System	Location	Latitude	Longitude	Elevation	Year Commissioned
Site 3	Glendale, AZ	33.5° N	112.2 W	1160ft	2001
Site 4c	Mesa, AZ	33.4° N	111.7 W	1241ft	2009

Table 2 System description

System	Tilt/ Orientation	DC Rating (kW)	AC Rating (kW)	Years fielded	Module Type	No. of Modules	Inverter
Site 4c	Single-axis Tracking	243.2	204.3	4	H	1280	Xantrex-250U
Site 3		249.9	200	12	G	2352	Sunny Central

As shown in Figure 10 below, Site 3 consists of 14 rows/arrays, each with 6 strings of 28 modules connected in series.

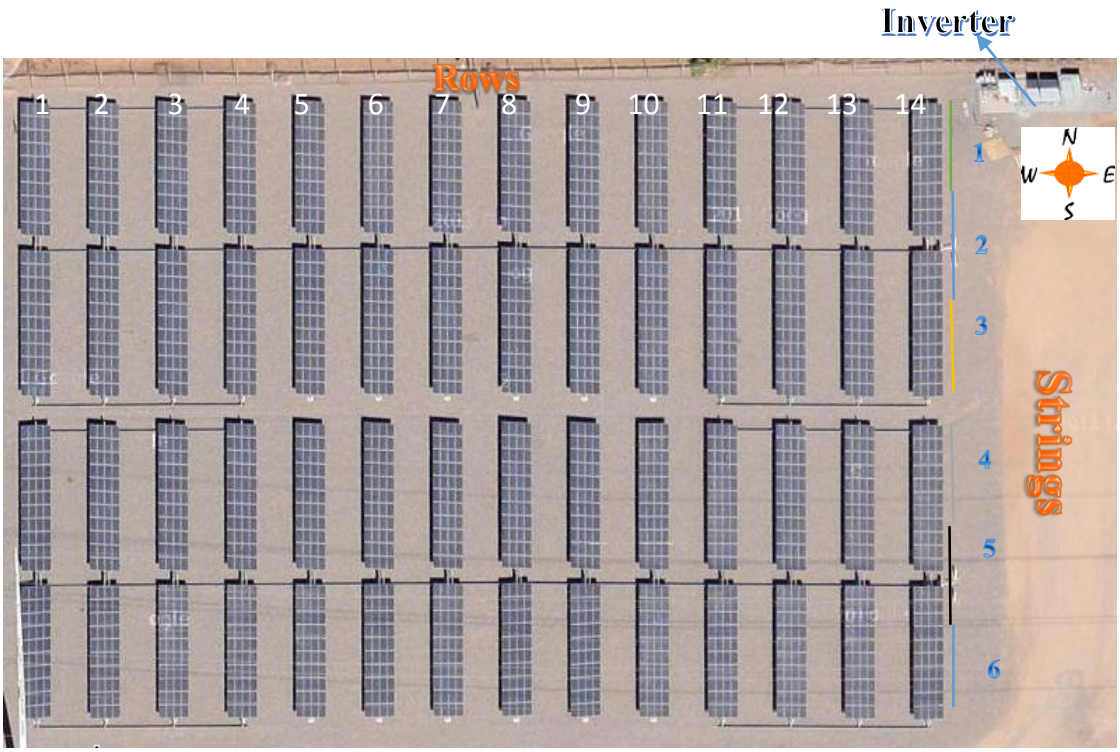

Figure 10 Site 3 site layout

As shown in Figure 11 below, Site 4c system consists of 32 rows/arrays, each with 5 strings of 8 modules connected in series.

Figure 11 Site 4c site layout

Table 3 Module and String nameplate rating

Model	**Design**	**Nameplate Rating**					
		Isc (A)	**Voc (V)**	**Imax (A)**	**Vmax (V)**	**Pmax (W)**	**FF (%)**
Module-G (Site 3)	Frameless Glass/polymer	7.3	20.6	6.4	16.6	106.3	70.6
Module-H (Site 4c)	Framed Glass/polymer	3.8	67.5	3.47	54.8	190	75.1
Site 3 String	28 modules per string	7.3	576.8	6.4	464.8	2975	70.6
Site 4c String	8 modules per string	3.8	540	3.47	438.4	1520	75.1

Figure *13* shows the string circuit diagram of the Site 3 power plant with the positive end and the negative end. The number in each box represents the modules and their position in the string. Figure 14 shows the string circuit diagram of Site 4c.

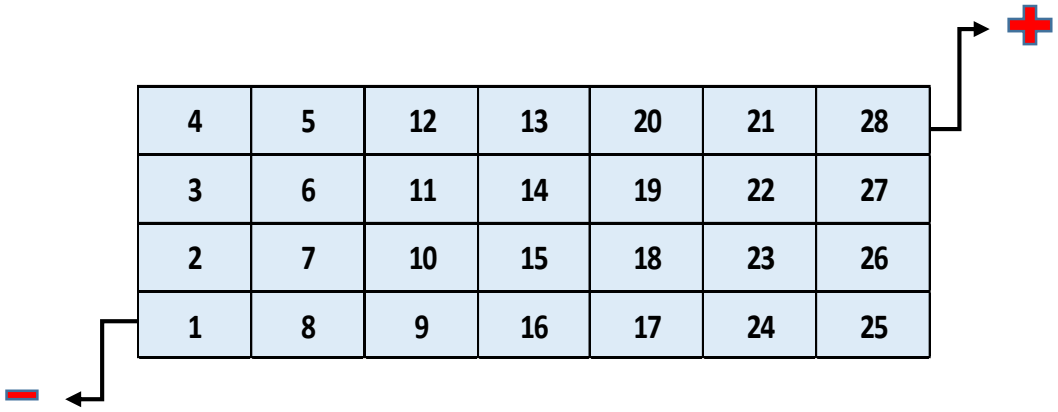

Figure 13 Site 3 string circuit diagram

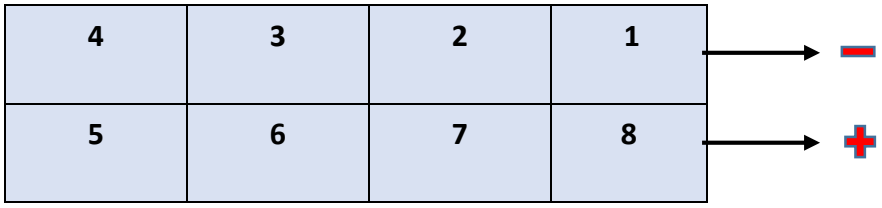

Figure 14 Site 4c string circuit diagram

A naming convention was followed for the strings. The strings were named in the R-S format, where R is the row and S is the string in that particular row. If a string number is 1-2, it indicates that the string is present in row 1 and the string number in this row is 2.

Figure 15 Picture of Module-G

Figure 16 Picture of Module-H

3.2 Data collection and processing

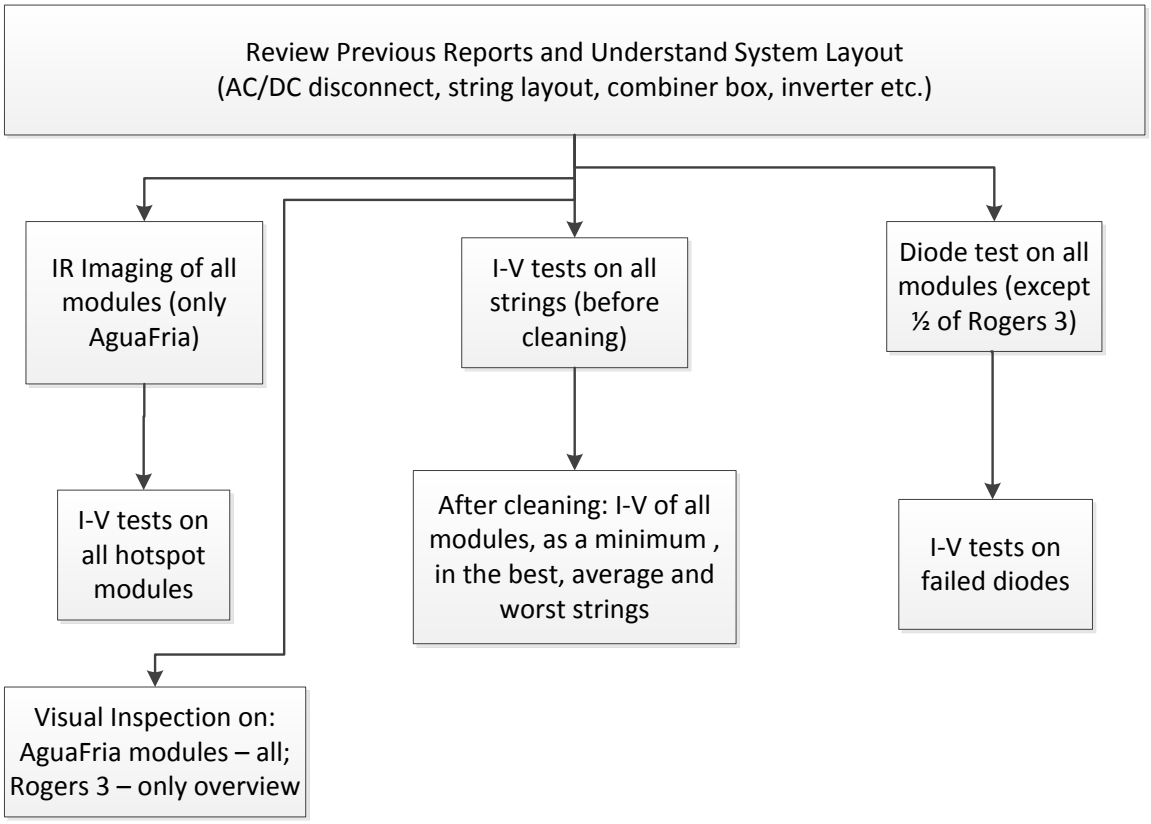

Figure 17 Flowchart of Tasks carried out.

The first step taken before the start of the testing at a PV power plant was to review the previous available reports of the plant. This helped in understanding the system layout, string layout, and to know the position of the combiner box, AC/DC disconnect and inverter.

Equipment Used

- Daystar DS-100C current-voltage (I-V curve tracer).
- Fluke TI-55 Infrared (IR) camera.
- Diode checker
- K-type and T-type thermocouples
- Two calibrated mono and poly reference cells

3.2.1 I-V measurements of modules and strings

The I-V curves of strings and modules provide the information related to the module and string performance parameters. First, the ac/dc disconnect switches were turned off and then the fuses were removed from the combiner box. At Site 3 the string IV measure ments were taken at module terminals in the string by disconnecting the string. However at Site 4c the string I-V measurements were done at the combiner box located at the start of each row. To measure each individual module, first the string to which the module belongs is disconnected and the I-V curve is taken at the module terminals. The reference cells were mounted co-planar to the modules being measured. The temperature of the module is directly recorded by the tracer and the thermocouple is placed in the center of the modules backsheet. All I-V measurements were taken at an irradiance of above $800W/m^2$.

3.2.2 Baseline I-V measurements

The measured I-V curves are required to be translated to Standard Test Conditions (STC). Temperature coefficients for voltage (β), current (α), and power are required for the translation. The modules to be tested at the power plant were cooled uniformly using ice

cubes and covering the top of the module with Styrofoam. The module's backsheet temperature was monitored and once the temperature fell between 12°C to 18°C, the ice cubes were removed and the module surface was dried using dry towels. Ten I-V curves were taken between 18°C to 45°C and with the irradiance approximately 1000 W/m^2.

Figure 18 Module cooled using ice and styrofoam.

3.2.3 Translation Procedure

The I-V measurements were taken at the ambient conditions that existed at the power plant. These measured curves were normalized to STC using an automated Microsoft Excel spreadsheet developed by ASU-PRL. The three I-V curves extracted from the IVPC software were entered in the Excel spreadsheet. These curves were translated using the temperature coefficients obtained from baseline measurements. The obtained STC data was used for further analysis.

4	**Manufacturer:**				**Model:**				**Test Date:** 6/27/2013									
5	**Project:**				**Sample:** 0016-A				**Test Location:**									
6																		
7		**Date**	**Isc**	**Voc**	**Imp**	**Vmp**	**FF**	**Pm**	**Time**	**W/m²**	**curves**	**Test Date**	**Isc**	**Voc**	**Imp**	**Vmp**	**FF**	**Pm**
8			A	V	A	V	%	W					A/°C	V/°C	A/°C	V/°C	%/°C	W/°C
9	**Measured @ STC**	6/27/2013	7.22	20.8	6.27	15.3	63.8	95.7	11:44:58	990.9	3	6/13/2013	-0.0026	-0.0746	-0.0156	-0.0651	-0.1771	-0.6630
10	**Rated @ STC**		7.20	20.10	6.20	16.10	68.97	100.00					-0.0042	-0.0802	-0.0041	-0.0962	-0.1664	-0.6249
11	**Rated @ NOCT**																	
12	**Temp. Coef. by ASU-PTL**			-0.0774		-0.0807	-0.1718	-0.6440										
13			*Values in italic are translated from rated values at STC and temperature coefficients.*															
14	**Test Data (ATC)**																	
15	CurveName		0016-A	0016-B	0016-C	**average**						**average**	**-0.0034**	**-0.0774**	**-0.0099**	**-0.0807**	**-0.1718**	**-0.6440**
16	Date		6/27/2013	6/27/2013	6/27/2013													
17	Time		11:44:58	11:45:10	11:45:20													
18	Tamb (°C)		44	44	44	**44.0**												
19	Tref1 (°C)		49.2	49.2	49.2	**49.2**												
20	Tm (°C)		61.6	61.6	61.9	**61.7**												
21	Tref2 (°C)		49.2	49.2	49.2	**49.2**												
22	G1 (W/m^2, T)		990	992	993	**991.7**												
23	G2 (W/m^2, T)		1,011	1,014	1,015	**1013.3**												
24	Isc (A)		6.889	6.904	6.901	**6.90**												
25	Voc (V)		17.74	17.726	17.7	**17.72**												
26	Imp (A)		5.662	5.873	5.784	**5.77**												
27	Vmp (V)		12.317	11.904	12.063	**12.09**												
28	Pm (W)		69.7	69.9	69.8	**69.80**												
29	FF (%)		57.1	57.1	57.1	**57.1**												
30																		

Figure 19 ASU-PRL template for I-V curves translation

3.2.4 Hotspot Determination

Hot spot heating occurs when a cell in a string of series connected cells is negatively biased and dissipates power in the form of heat instead of producing electrical power. This happens when the current produced by a given cell is lower than the string current. This can occur when the cell is shaded, damaged, or simply generates less current than the module. The Fluke TI-55 IR camera was used to take the IR images of all modules. The module's cells with a temperature difference of more than 15°C as compared to rest of the module's cells are determined as Hot spots cells.

3.2.5 Visual Inspection

Each individual module was inspected for defects such as encapsulant browning, encapsulant delamination, broken glass, interconnect breakages etc., using the National Renewable Energy Lab (NREL) check list of visual defects. An overview visual inspection was performed at Site 4c. This data was used to develop a defect table which was used to correlate with a drop in module performance.

3.2.6 Diode check and Interconnect failure detection

A diode checker instrument was used to detect failed diodes and broken interconnects on a PV module. The diode checker has two parts, a transmitter and a receiver. The transmitter is connected to the string terminals at the combiner box and the receiver was placed on the module busbars to detect the signal transmitted. The flow chart in Figure 20(below) illustrates the step by step procedure for the determination of failed diodes and interconnect failures. First, ensure the module is not shaded and the receiver is placed on bus bars of each string associated with diode. If no beeps are heard from the receiver, then there could be a possibility of a broken interconnect and/or a bypass diode failing in short circuit mode. Broken interconnects can be found visually by inspecting the busbar. If a broken interconnect is not seen, then a bypass diode failure should be suspected. It can be crosschecked with the I-V curve of the module and also with the IR scan of the diode. If the receiver beeps on all busbars then the next step is to shade half of the string of the module.

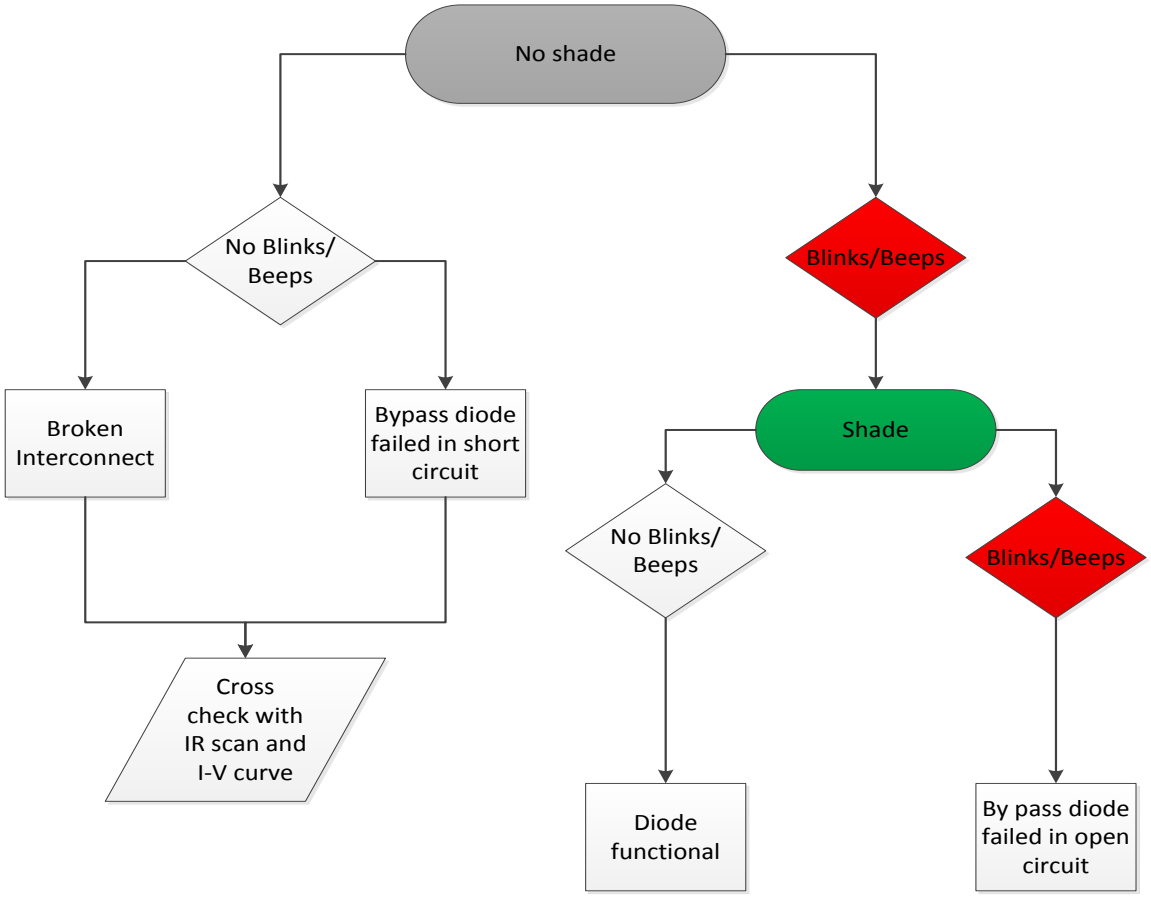

Figure 20 Flowchart for detection of failed diodes and broken interconnects using diode checker

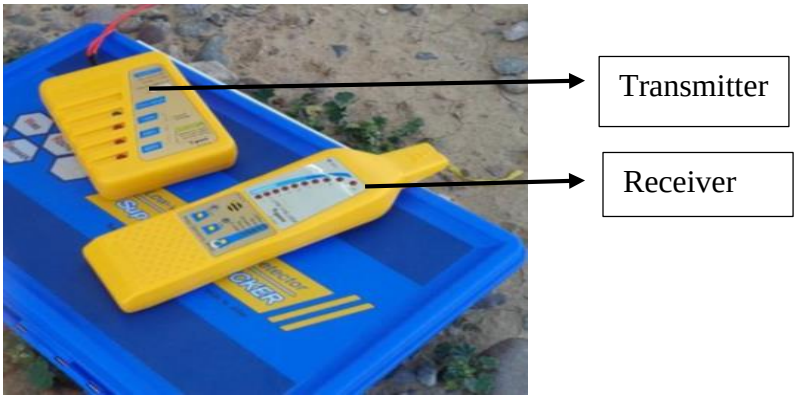

Figure 21 Transmitter and Receiver of diode checker

Place the receiver on the busbars of the shaded string, if the receiver does not beep then it indicates that the diode is functional and if the receiver beeps then diode failed in open circuit condition.

3.2.7 Soiling Loss

Soiling on the modules causes transmittance issues, which reduces the Isc of the modules The strings which were selected for individual module level analysis were cleaned with water. The strings were then allowed to dry for a few minutes. After drying, cleaned string level I-V curves and module level I-V curves were taken.

Figure 23 Cleaned and Soiled string comparison in Site 4c

3.2.8 Series resistance calculation

Series resistance is calculated by choosing 10 data points of I-V curve close to Voc. The slope of these selected points after normalizations gives the value of series resistance.

3.2.9 Classification of Defects into Failures and Cosmetic Defects

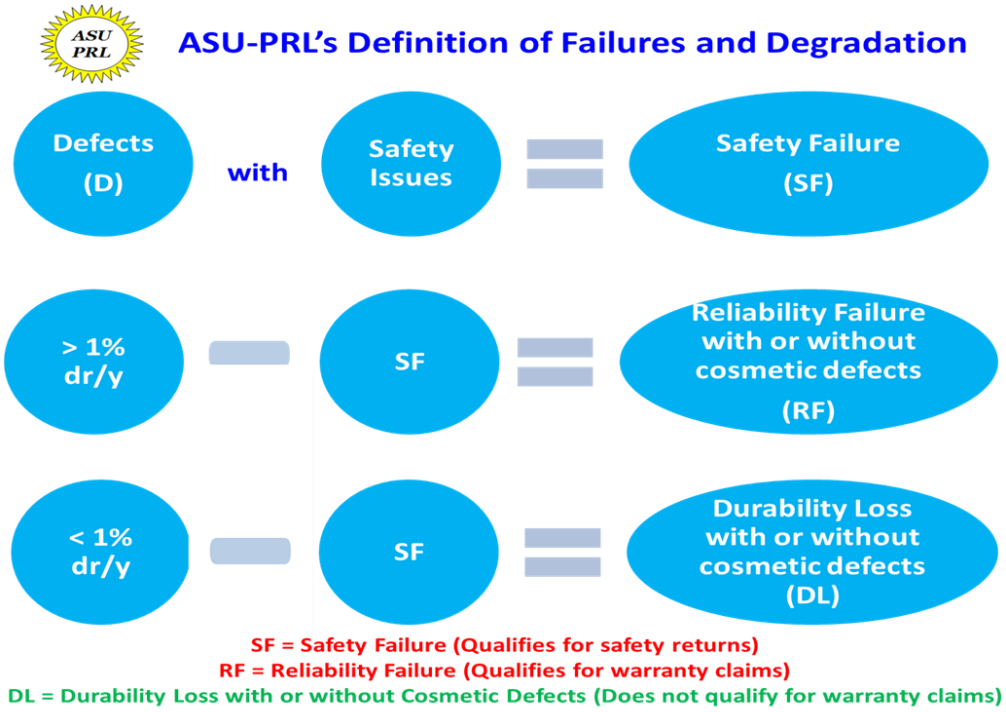

Figure 24 Classification of Defects into Failures and Cosmetic Defects

3.3 Data Analysis

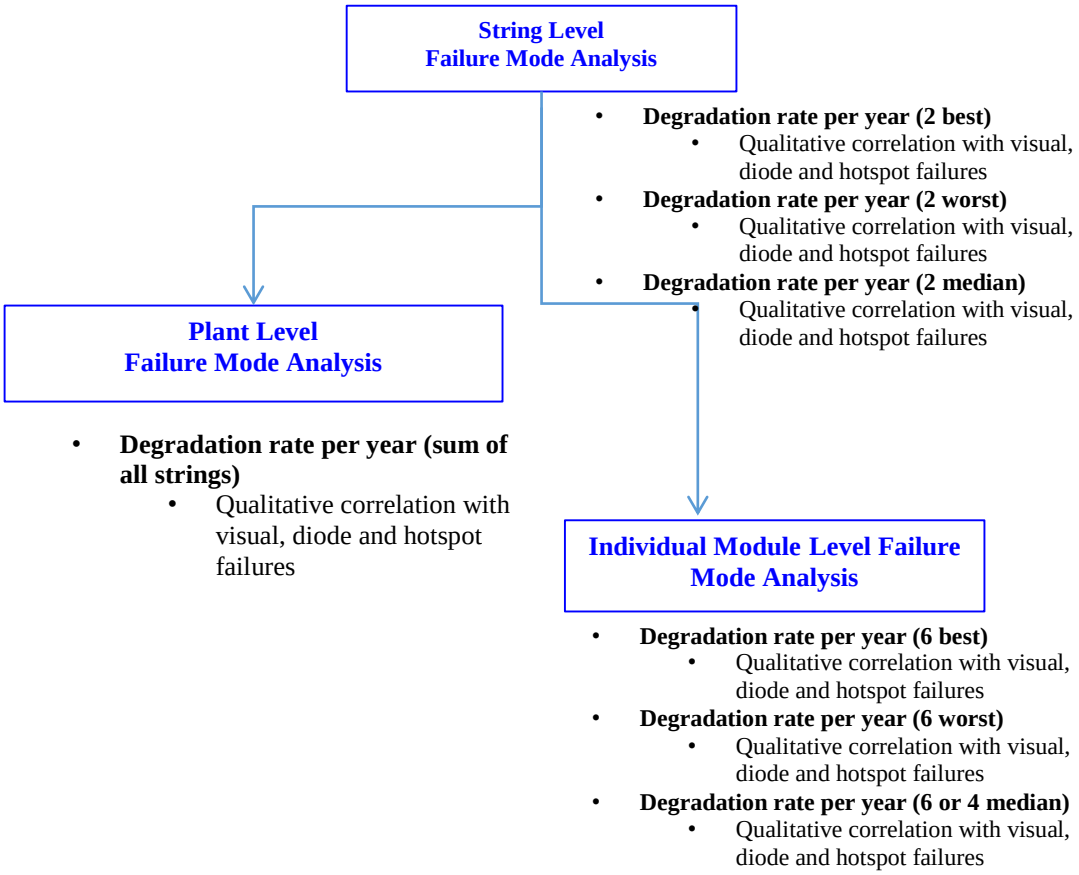

Figure 25 Flowchart of data analysis

The analysis for this study was carried out as shown in Figure 25(above). 2 Best, 2 Median and 2 Worst strings based on power were selected from each PV plant. From these 6 selected strings 3 Best, 3 Median and 3 Worst modules were selected. The degradation %/year for Isc, Imax, Voc, Vmax, FF and Pmax were calculated for the corresponding modules. In the case of 2 best strings 6 best, 6 median and 6 worst modules were analyzed by plotting box plot graph in Minitab. The primary parameter

responsible for the cause of power degradation is identified from the graph by choosing the median of the 5 parameters falling close to the median of the P_{max} degradation (%/year). This is correlated with the defects seen in the visual inspection and the responsible failure defect is identified as the cause of degradation in the particular parameter.

CHAPTER 4

RESULTS AND DISCUSSIONS

This chapter explains the I-V parameters responsible for the degradation of Pmax. The best,median and worst strings were selected. The modules from the selected strings were sepearated into best,median and worst modules. The best modules were analysed for durability issues and the worst modules were analysed for reliability failures. The detailed visual inspection results from the Site 3 power plant were presented and the durability issues such as potential induced degradation,soiling loss and systematic wind effect on the degradation of the strings were discussed.

4.1 Site 3 Performance Degradation Analysis

The performance degradation analysis was accomplished by selecting the best,median and worst strings as explained in Chapter 3. Figure 26(below) shows the Pmax of all the strings in Site 3. The name plate rating was used to calculating the performance degradation. Measured data from independent source database was not available for this model. However, other models measured data from the same manufacturer and when compared with measured data from independent source database, showed that some of the models are under rated. If under rated, the calculated degradation rate will be lower than that of the actual, which could be seen froma few Isc values in the best modules.The best modules form the best string were analysed to find the IV parameters responsible for the power degradation shown in Figure 27.

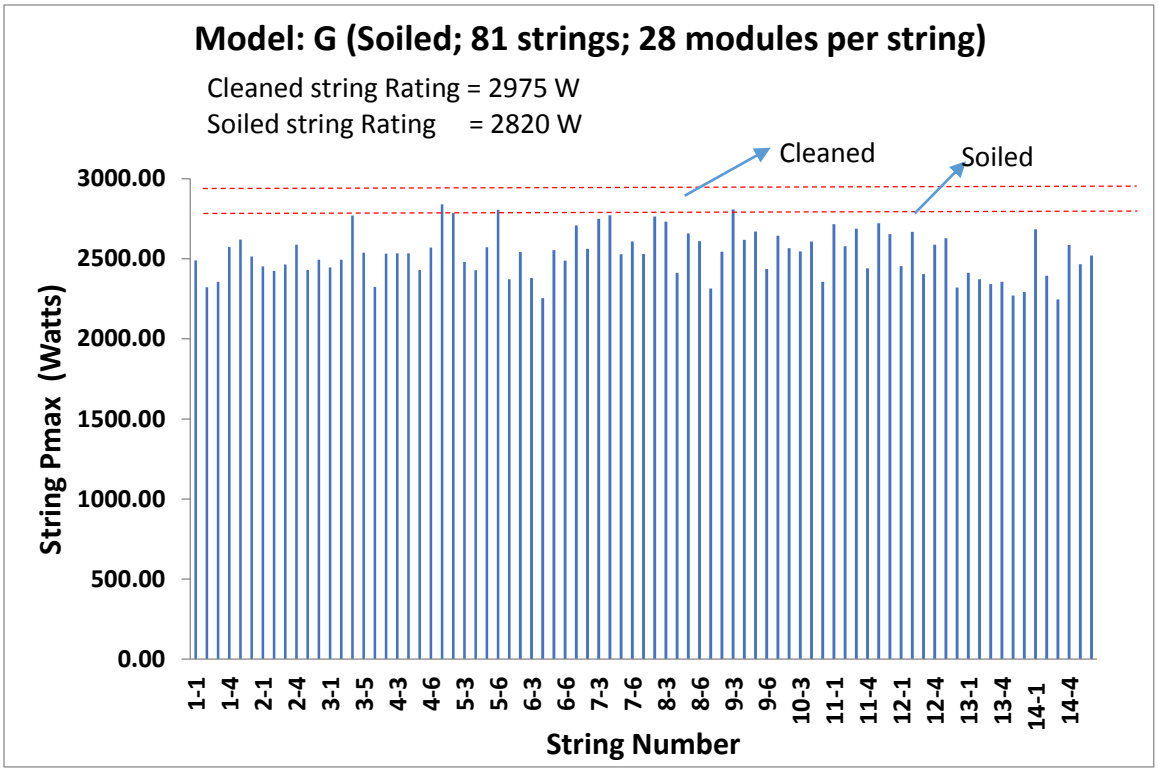

Figure 26 Strings Pmax in Site 3

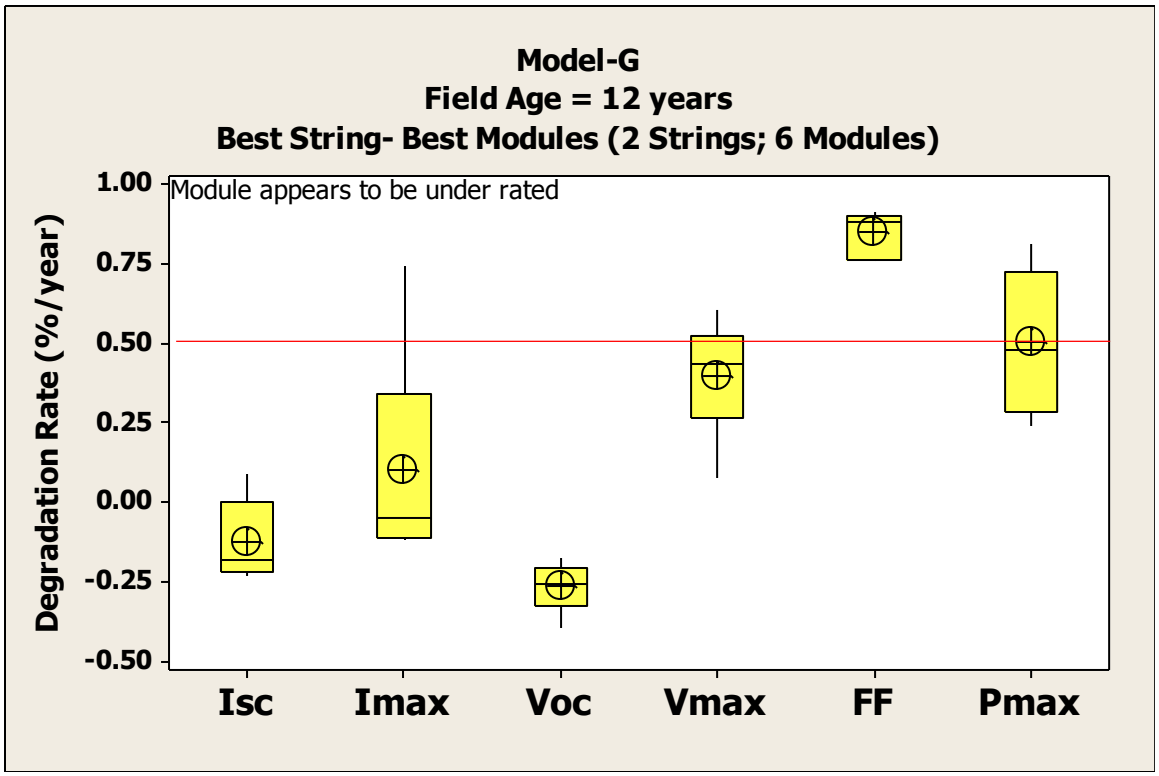

Figure 27 Plot for various I-V parameter degradation (%/year) for best string- best modules

The median of the Pmax degradation rate is close to the median of the Vmax degradation rate and followed by FF. Figure 28(below) also shows that Vmax is the main contributor for Pmax degradation and and Vmax drop influences the FF drop as shown in the Best modules of Best and Median strings. The Vmax contribution to the power drop could be associated with series resistance increase. Series resistance increase could arise from three interfaces/contacts:

- Cell and Metallization (C/M) contact
- Metallization and Ribbon (M/R) contact
- Ribbon and Ribbon (R/R) contact

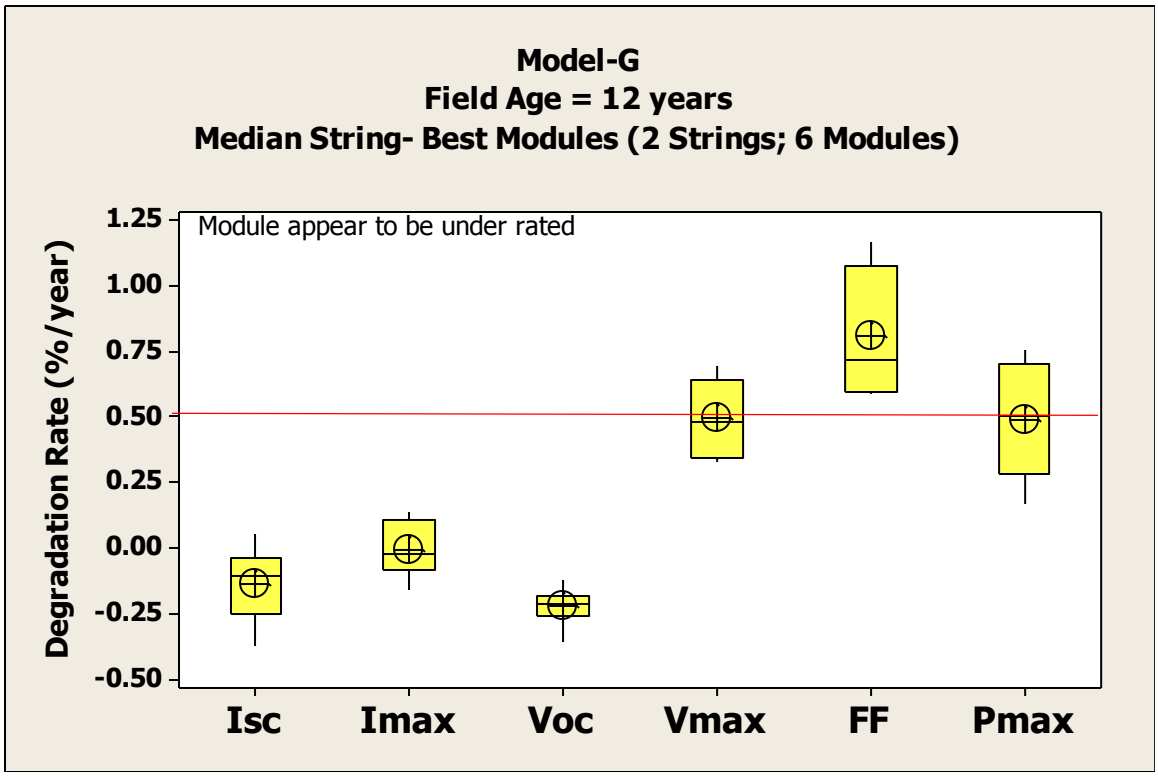

Figure 28 Plot for various I-V parameter degradation (%/year) for median string- best modules

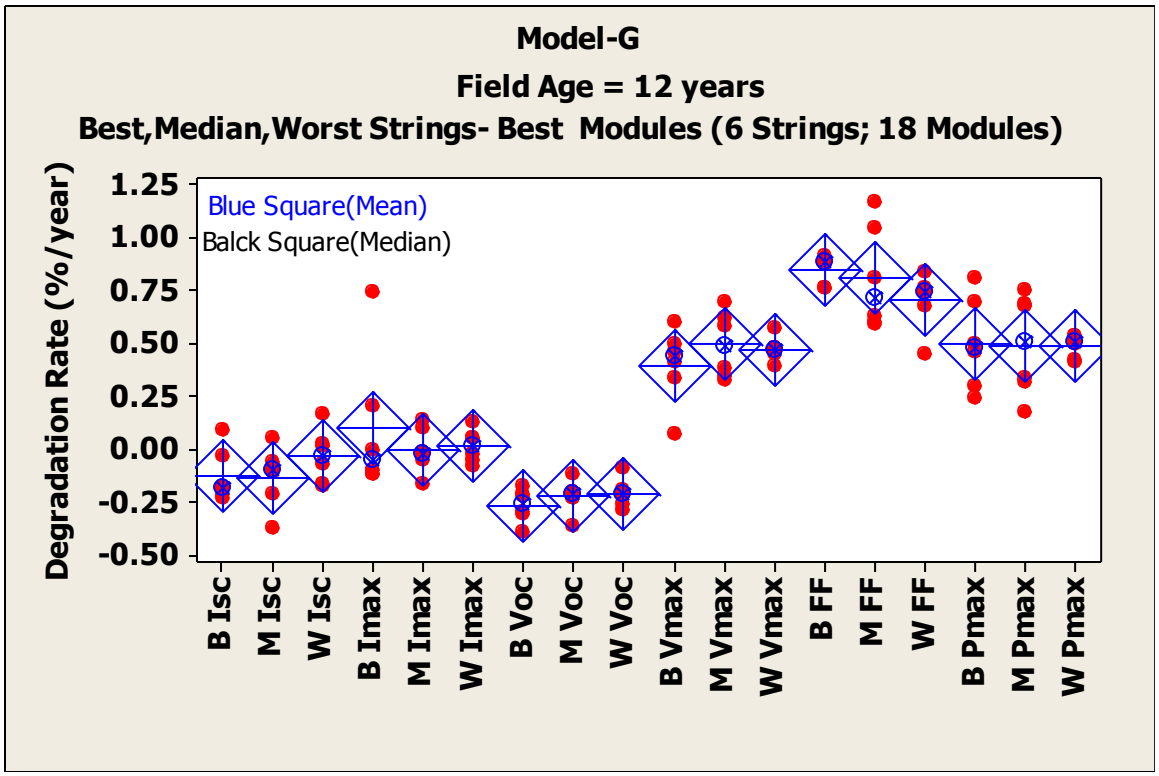

Figure 29 Summary plot for various I-V parameter degradation (%/year) for best modules in Best, Median and worst strings

The plot in Figure 29 is a summary of best modules performance degradation rate for various IV parameters of best, median and worst strings. Vmax and FF are the major contributors for Pmax degradation for the worst modules in the worst string. Vmax and Voc are affected due to the ribbon-ribbon solder bond failure shown in Figure 34 (below). Table 4 shows a comparison of series resistance between a fresh module and best modules with a field age of 12 years. Since the fresh module data for this specific model was not available, another model of the same manufacturer with closest nameplate rating has been assumed as the resistance of the fresh modules. The series resistance increased by about 21%.

Table 4 Comparison of series resistance

	Fresh Module	Field Modules (Median of 30 Best Modules)
Series Resistance	0.58	0.73
% Increase	-	21%

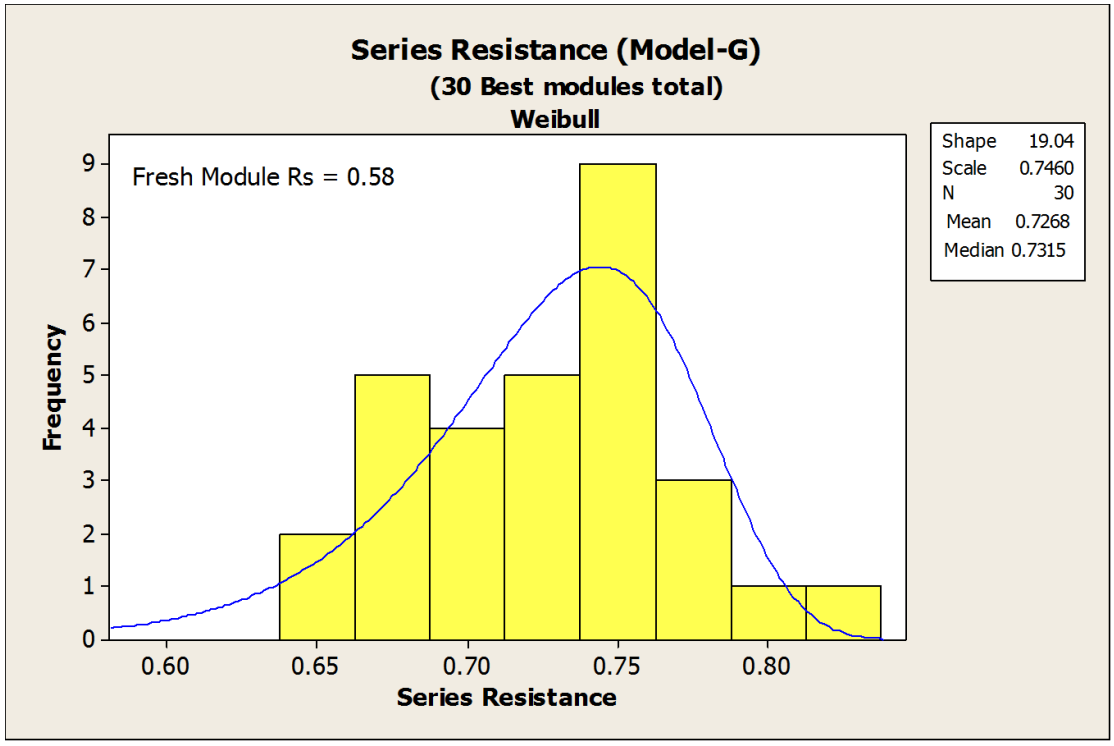

Figure 30 Series Resistance

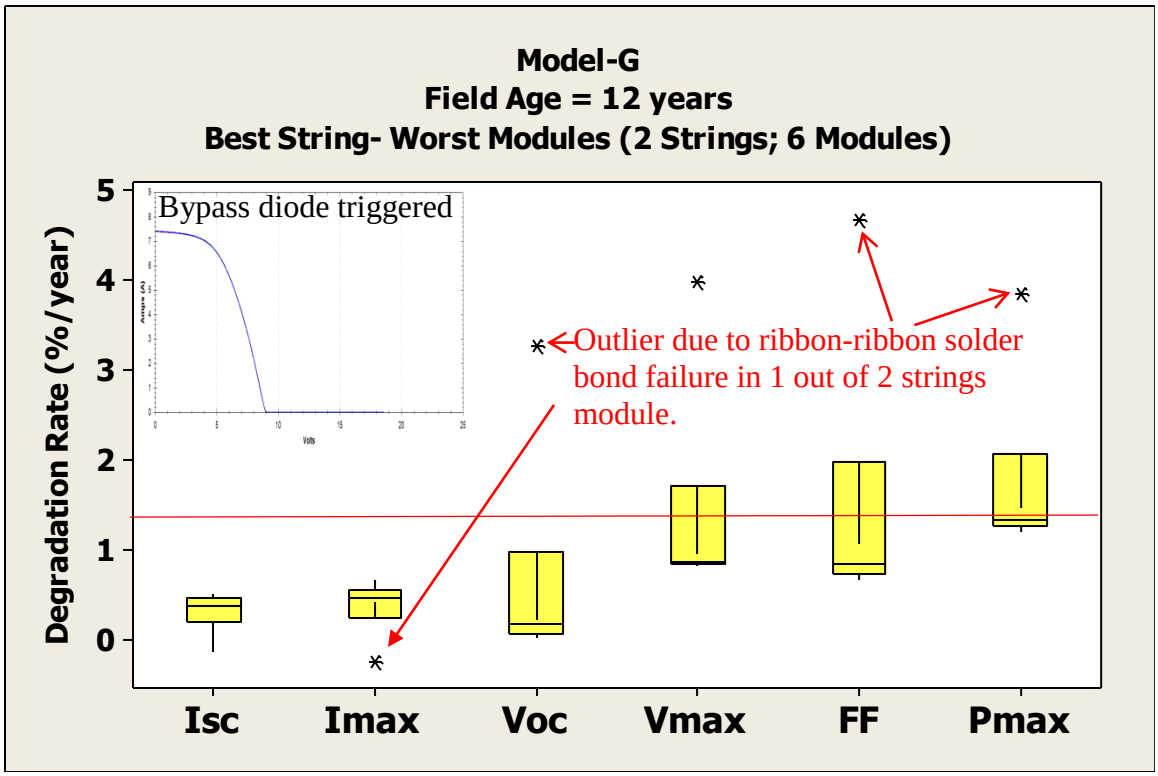

Figure 31 Plot for various I-V parameter degradation (%/year) for best string- worst modules

The worst modules in the best string have module with ribbon-ribbon solder bond failure, which triggered a diode in the corresponding string as shown in Figure 31. The module with ribbn-ribbon solder bond has a Imax outlier due to the ribbon-ribbon solder bond failure. Vmax and FF are the parameters responsible for the degradation of Pmax and the Vmax and is attributed to the series resistance increase of approximately 21% as compared to the fresh modules.

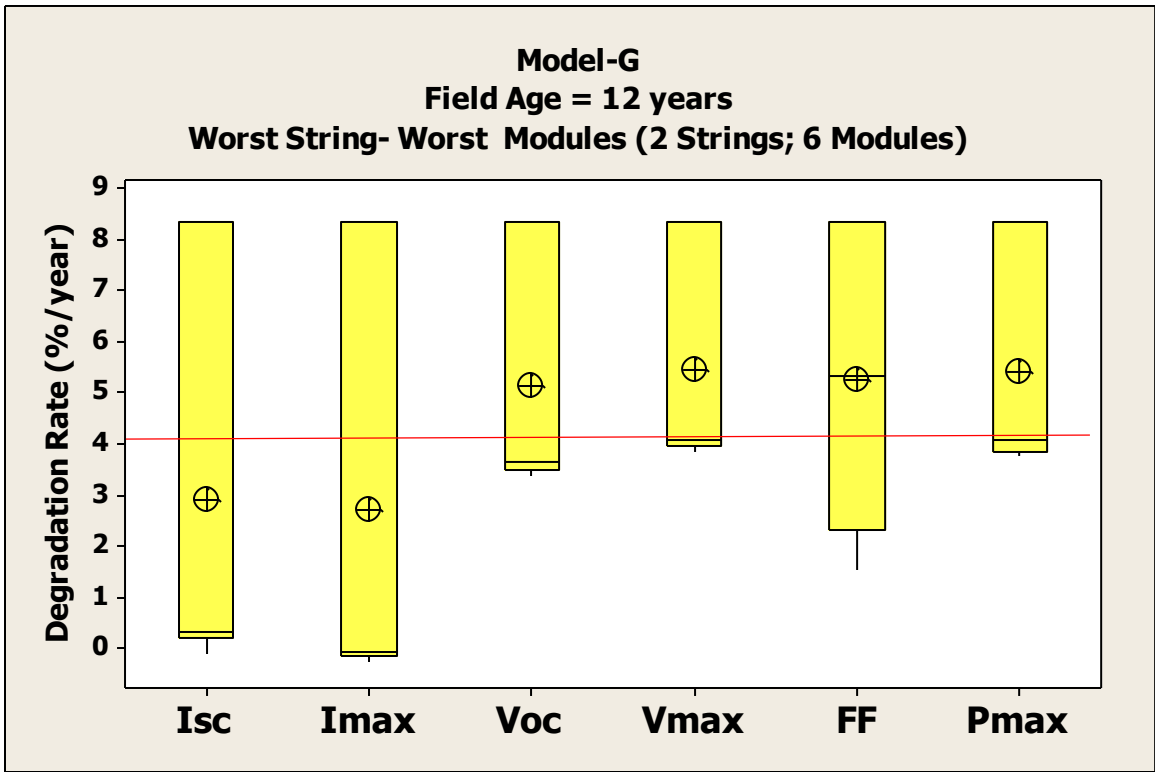

Figure 32 Plot for various I-V parameter degradation (%/year) for worst string- worst modules

Vmax, Voc and FF are the major contributors of Pmax degradation for the worst modules in the worst string. Out of the 6 modules, both ribbon-ribbon solder bonds failed in 2 modules which lead to zero power. These two modules contribute to the highest degradation rate in all parameters. The remaining 4 modules had 1 ribbon-ribbon solder bond failure. These modules contribute to a drop in Vmax, Voc and FF as one of the string in the module was disconnected due to the failure. The Isc and the Imax are not severely affected because the current bypasses the failed string through the bypass diode.

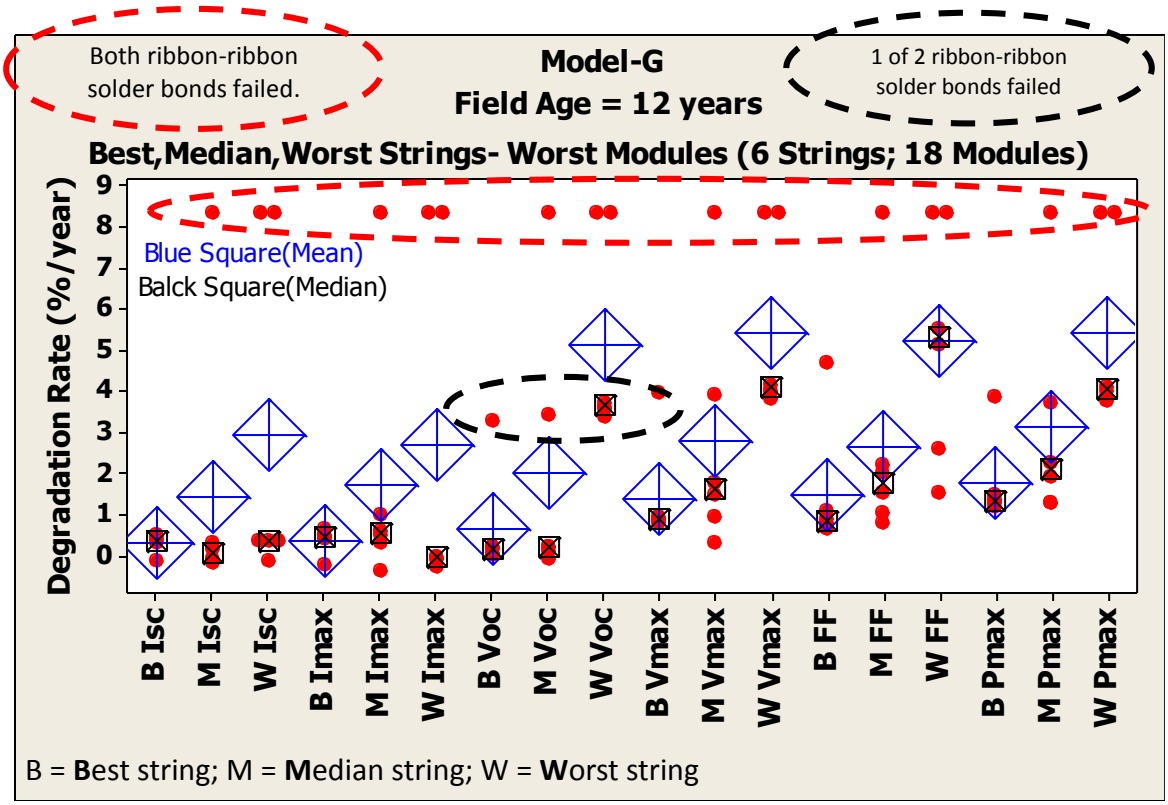

Figure 33 Summary plot for various I-V parameter degradation (%/year) for worst modules in Best, Median and worst strings.

The plot in Figure 33(above) is a summary of worst modules performance degradation rate for various IV parameters of best, median and worst strings. Vmax and Voc are the major contributors of Pmax degradation for the worst modules in the worst string. Vmax and Voc are affected due to the ribbon-ribbon solder bond failure shown in Figure 34 .

Table 5 shows the order of influence of the I-V parameters on the Pmax degradation.

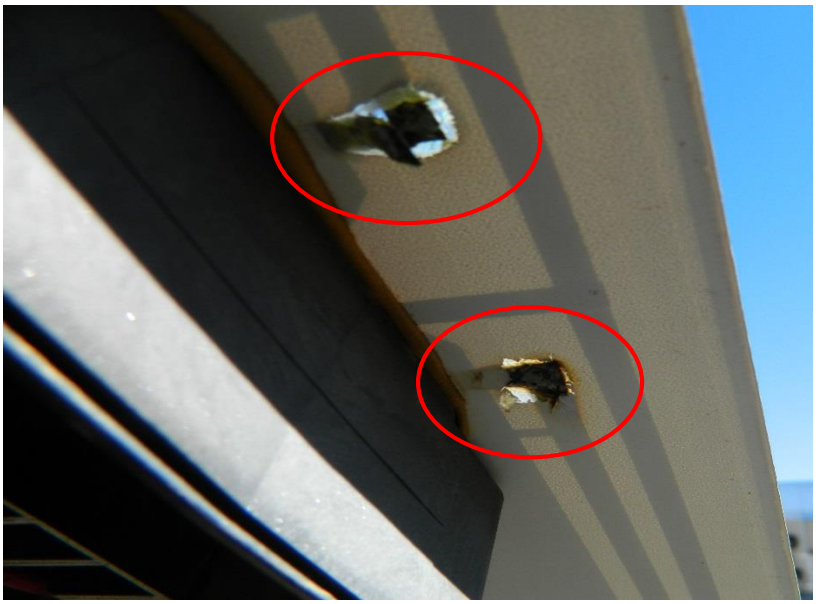

Figure 34 Ribbon-Ribbon solder bond failure

Table 5 I-V parameter order of Influence on Pmax degradation.

	6 Best Modules	6 Median Modules	6 Worst Modules
2 BEST STRINGS	Vmax~FF>>Imax ~Isc~Voc	Vmax~FF>>Imax ~Isc~Voc	Vmax>FF >Imax~Isc~Voc(1 ribbon-ribbon solder issue in 1 module)
2 MEDIAN STRINGS	Vmax~FF>>Imax ~Isc~Voc	FF~Vmax>>Imax ~Isc~Voc	FF>Vmax>Imax~Isc>Voc (1 ribbon-ribbon in 1 module and 2 ribbon-ribbon solder issue in 1 module)
2 WORST STRINGS	Vmax~FF>>Imax ~Isc~Voc	FF~Vmax>Imax~ Isc~Voc	Vmax>Voc>FF >Isc>Imax(1 ribbon-ribbon in 4 modules and both ribbon-ribbon solder issue in 2 modules)

As shown in Table 5, the best modules in all three different strings have the same order of influence of parameters on Pmax degradation. In the best modules Isc, Imax and Voc are do not affect the Pmax. Vmax and FF are the major contributors for Pmax loss. Since

Pmax = Voc * Isc * FF. Pmax drop could be due to drop in any one of the three parameters Isc, Voc, FF. Similarly FF = (Vmax*Imax)/ (Voc * Isc). So a FF drop could be due to an increase in Voc or Isc and due to a decrease in Vmax or Imax. Thus, it can be concluded that FF is affected primarily by Vmax loss which is attributed to series resistance increase. Series resistance in the best modules increased by approximately 30% compared to the fresh modules. The median modules in all three different strings have the same order of influence of parameters on Pmax degradation as that of the best modules. Vmax and FF are major contributors for the degradation of Pmax. Vmax loss could be attributed to series resistance increase. The worst modules in the best string had module with ribbon-ribbon solder bond failure and the worst modules in the median string had a module with ribbon-ribbon solder bond failure and a module with 2 ribbon –ribbon solder bond failures. In both the best and median strings, Pmax degradation was due to Vmax loss which is attributed to series resistance. All the worst modules in the worst string had ribbon-ribbon solder bond issues. Vmax, Voc and FF are the major contributors of Pmax degradation in the worst modules in the worst string. Voc loss is attributed to a ribbon-ribbon solder bond issue. Isc and Imax were not severely affected because the current bypasses the failed string through the bypass diode.

Table 6 Summary- Model G

Module Quality	Primary Parameter Affected	Primary Degradation/Failure Mode
Best Modules	**Vmax, FF**	**Solder bond fatigue (Degradation)**
Worst Modules	**Vmax, Voc**	**Ribbon-ribbon solder bond breakage (Failure)**

4.2 Site 4c Performance Degradation Analysis

Figure 35(below) shows the 158 strings Pmax. The same analysis performed on the Site 3 power plant was also performed on the Site 4c power plant

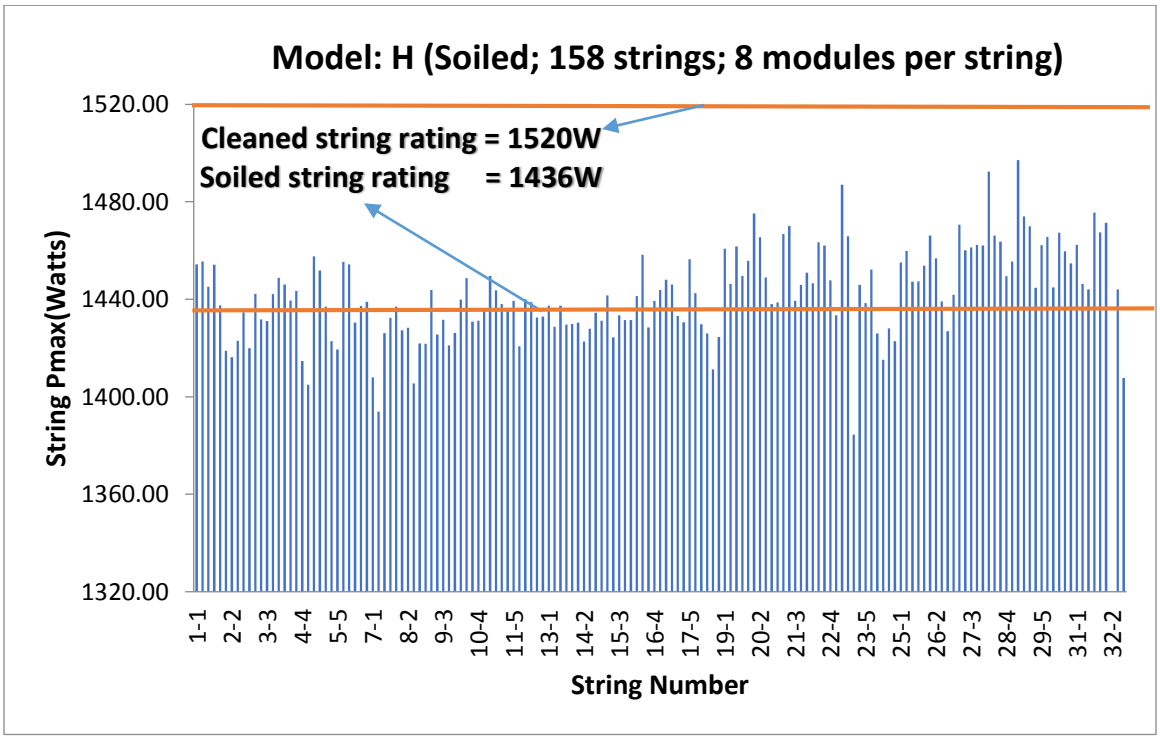

Figure 35 Strings Pmax in Site 4c

The plots from Figure 36(below) and Figure 37(below) show that FF, Voc and Imax are the main contributors for Pmax degradation in the best modules. The observed degradation is suspected to be due to the light induced effect in heterojunction technology**.** The Model-H seems to have thin a-Si layer on top of c-Si. Due to the Staebler-Wronski effect, it is suspected that the broken Si: H bonds in the a-Si layer seem to play a negative role (traps) on the observed effect of Voc [9].

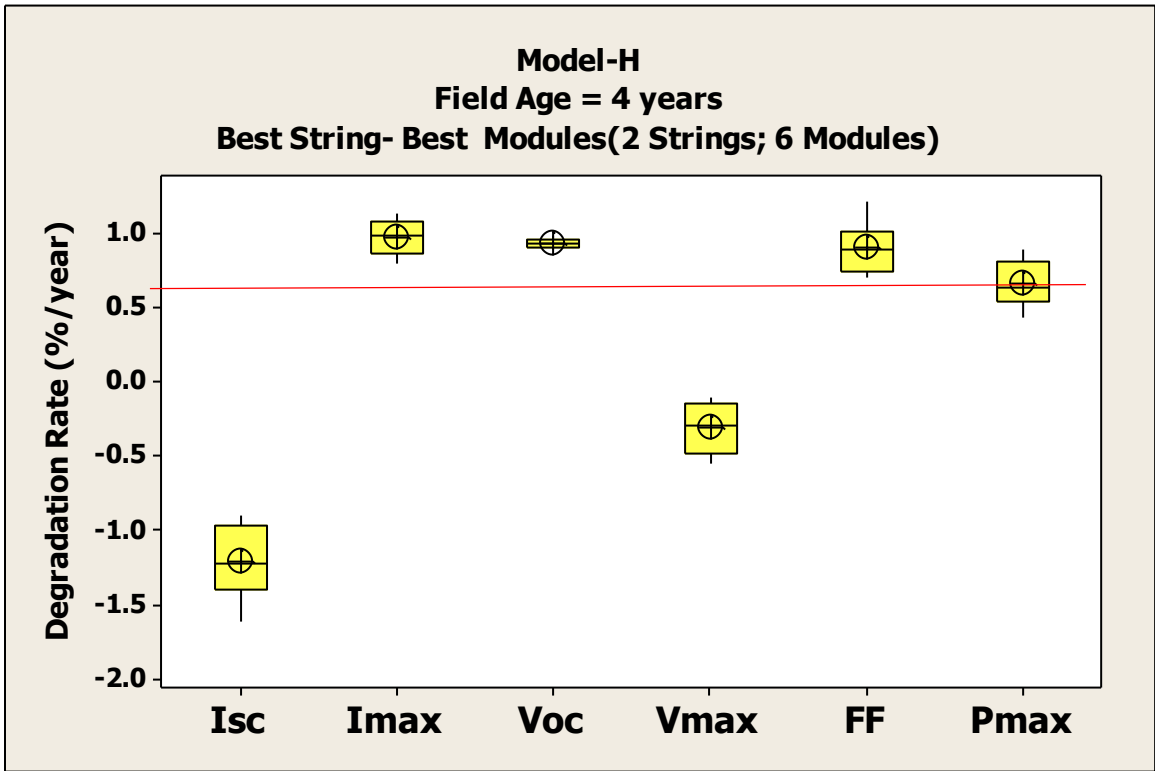

Figure 36 Plot for various I-V parameter degradation (%/year) for best string- best modules

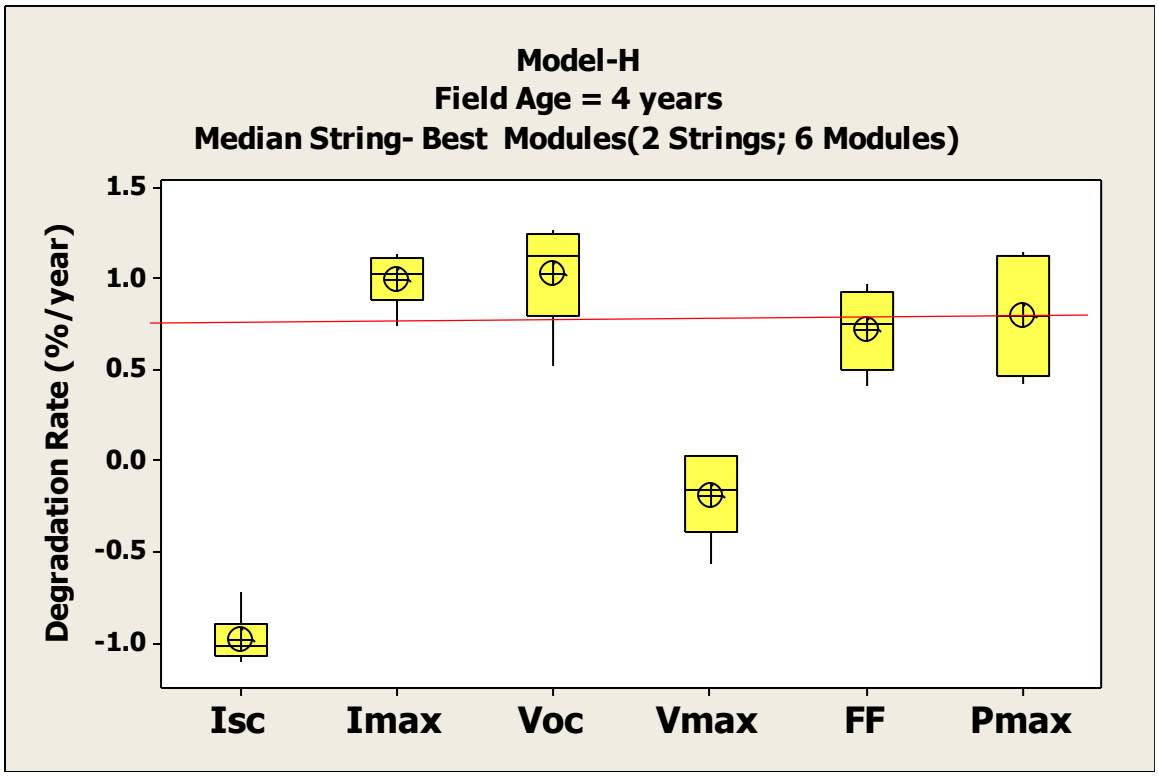

Figure 37 Plot for various I-V parameter degradation (%/year) for median string- best modules

The modules are on 1-axis tracking which means the temperatures may not typically exceed 65-70°. At these temperatures the annealing rate is expected to be lower. The broken Si-H bonds in the a-Si layer creates trap centers which lead to the drop in Voc [13]. The Imax drop is due to the decrease in shunt resistance which in turn is due to the generation of trap centers in the band gap [14].

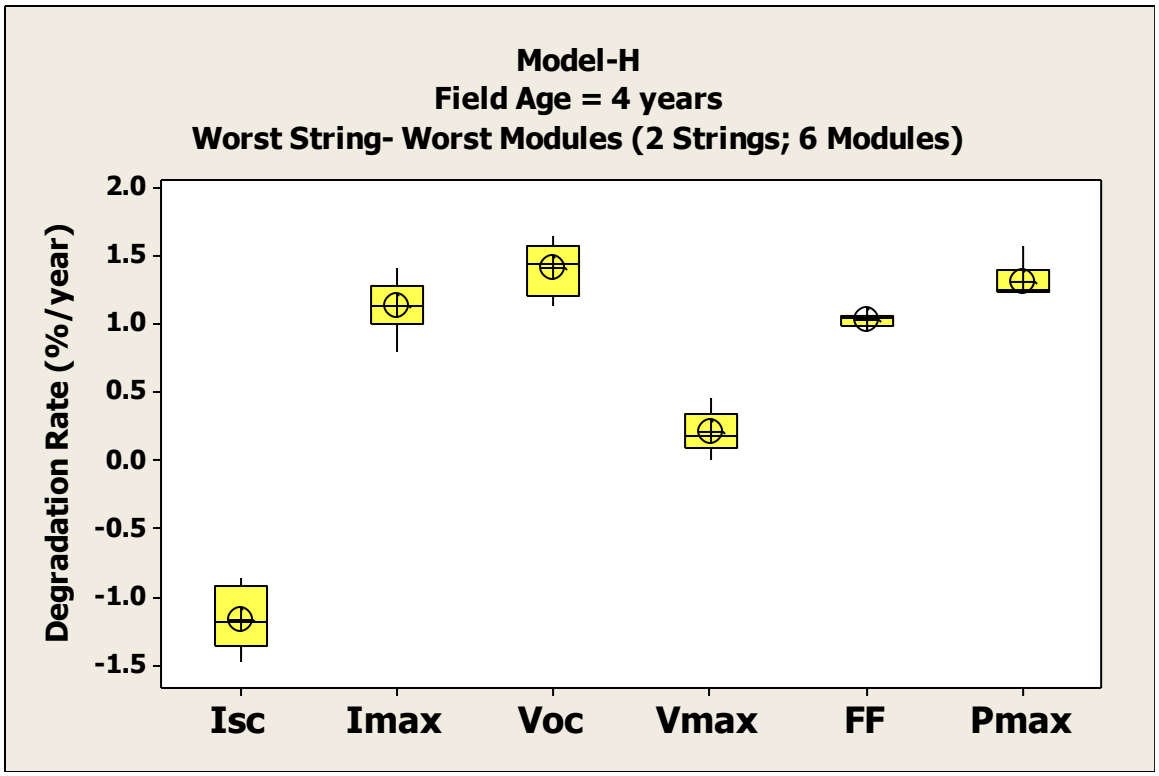

Figure 38 Plot for various I-V parameter degradation (%/year) for worst string- worst modules

For the worst modules in worst string the major contributors for the Pmax degradation are Imax, FF and Voc. Table 7 shows the order of influence of the I-V parameters on the Pmax degradation. In all the modules from the three different strings, Imax, FF and Voc are the major parameters causing the degradation in Pmax. FF drop is due to the Imax loss which is attributed to the decrease in shunt resistance. Voc drop is attributed due to the Staebler-Wronski (SW) effect of amorphous silicon layer of these heterojunction technology cell, leading to generation of recombination centers which lead to the decrease in quasi Fermi levels.

Table 7 I-V parameter order of Influence on Pmax degradation

	6 Best Modules	4 Median Modules	6 Worst Modules
2 BEST STRINGS	FF~ Voc~Imax>>Vmax>Isc	FF~ Voc~Imax>>Vmax>Isc	FF~ Voc~Imax>Vmax>Isc
2 MEDIAN STRINGS	FF~Imax~Voc>Vmax>Isc	Voc~FF~Imax >Vmax>Isc	Voc~Imax~FF>Vmax>Isc
2 WORST STRINGS	FF>Imax>Voc>Vmax>Isc	Imax>FF>Voc>Vmax>Isc	Imax>FF>Voc>Vmax>Isc

Table 8 Summary of degradation and failure Modes and their effects on performance parameters for Model H

Module Quality	**Primary Parameter Affected**	**Primary Degradation/Failure Mode**
Best Modules	**Voc, Imax**	**Practically, no failures observed are reported for these modules. The observed degradation is suspected to be due to the light induced effect in heterojunction technology.**
Worst Modules	**Voc, Imax**	

4.3 Degradation Rates

The histogram in Figure 39(below) shows the mean and median degradation rates of 0.95%/year and 0.96%/year for the Model-G modules. The histogram fits normal distribution. The histogram in Figure 41 shows the mean and median degradation rates of 1.17%/year and 1.15%/year, respectively, for the strings of Model-G. A slightly higher degradation rate of strings as compared to the modules may be attributed to intermodule cable loss and mismatch of modules in a string. The histogram in Figure 40 shows a mean and median of 0.41%/year and 0.41%/year of the 30 best modules.

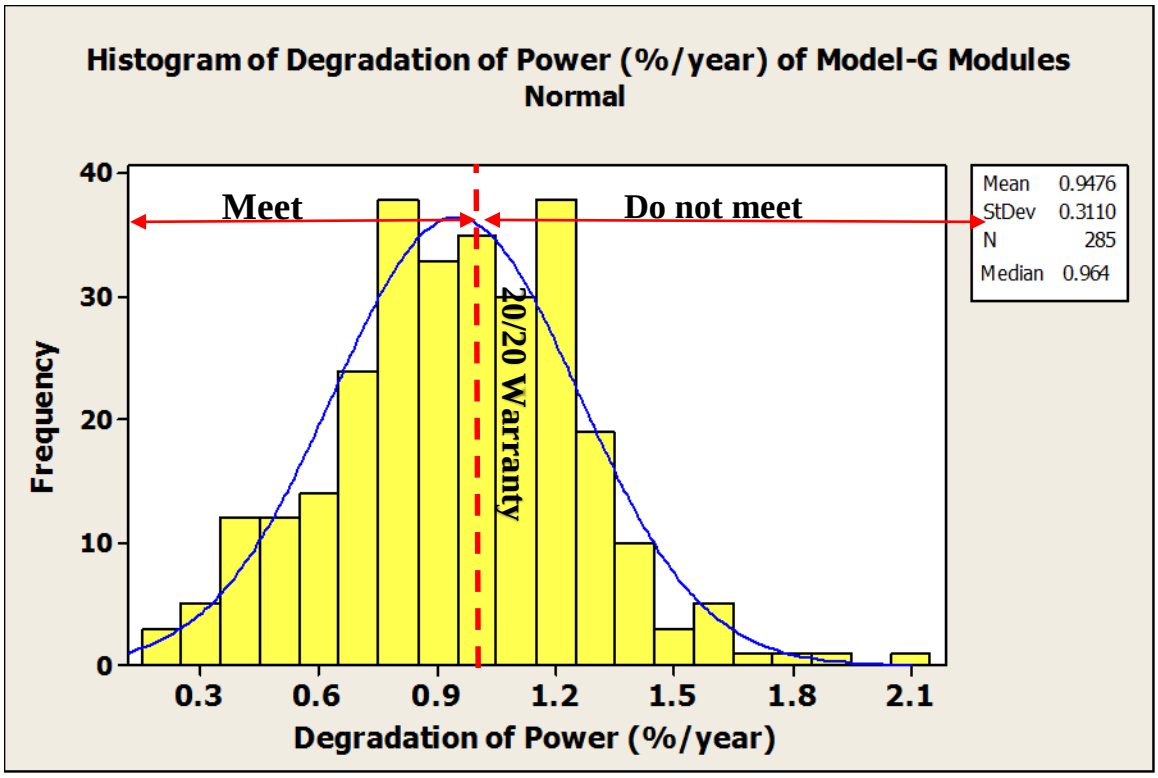

Figure 39 Histogram of Power Degradation (%/year) for Model-G Modules

The histogram in Figure 42(below) shows the mean and median degradation rates of 0.96%/year and 1.00%/year, respectively, for the modules of Model-H. The histogram in Figure 44 shows the mean and median degradation rates of 1.21%/year and 1.22%/year,

respectively, for the strings of Model-G. A slightly higher degradation rate of strings as compared to the modules may be attributed to intermodule cable loss and mismatch of modules in a string. The histogram in Figure 43 shows the mean and median rates of 0.63%/year and 0.62%/year for the 30 best modules.

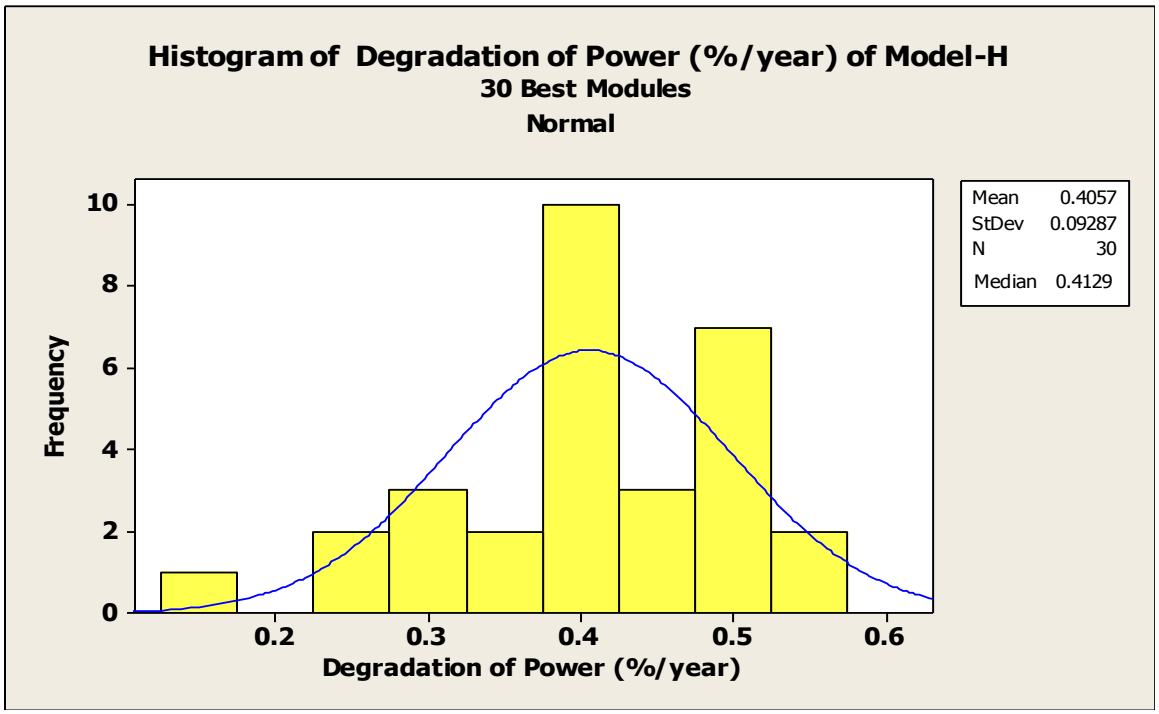

Figure 40Histogram of Power Degradation (%/year) for Model-G (30 Best Modules)

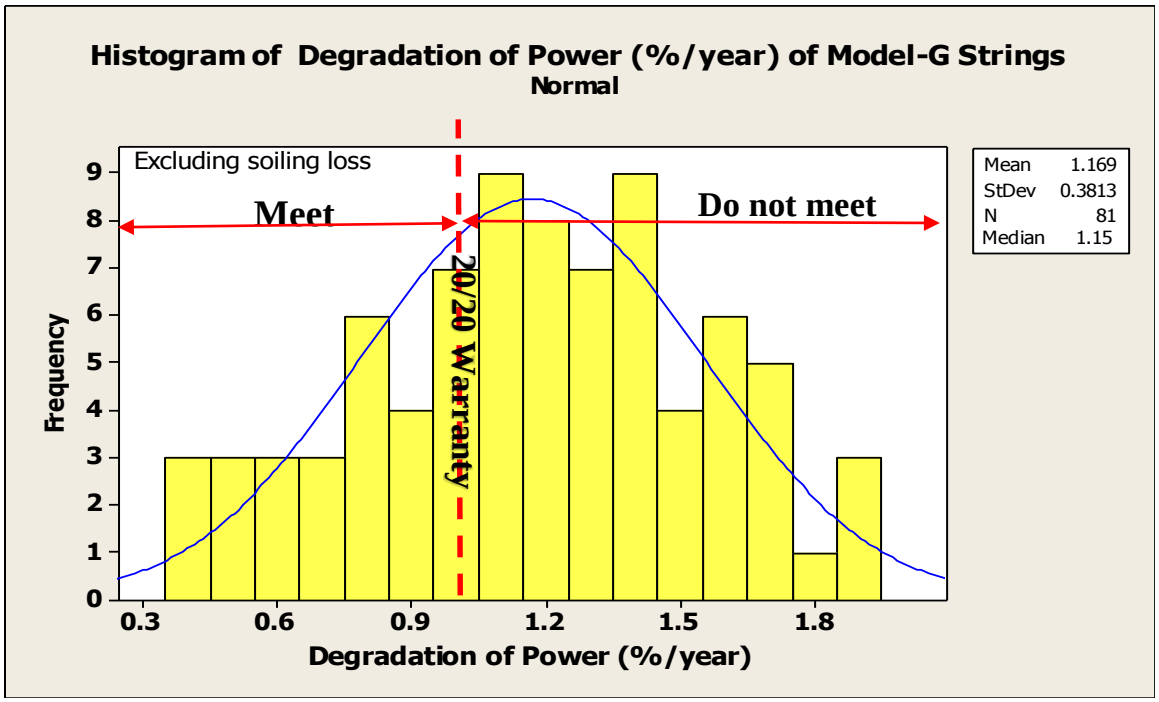

Figure 41 Histogram of Power Degradation (%/year) for Model-G All Strings

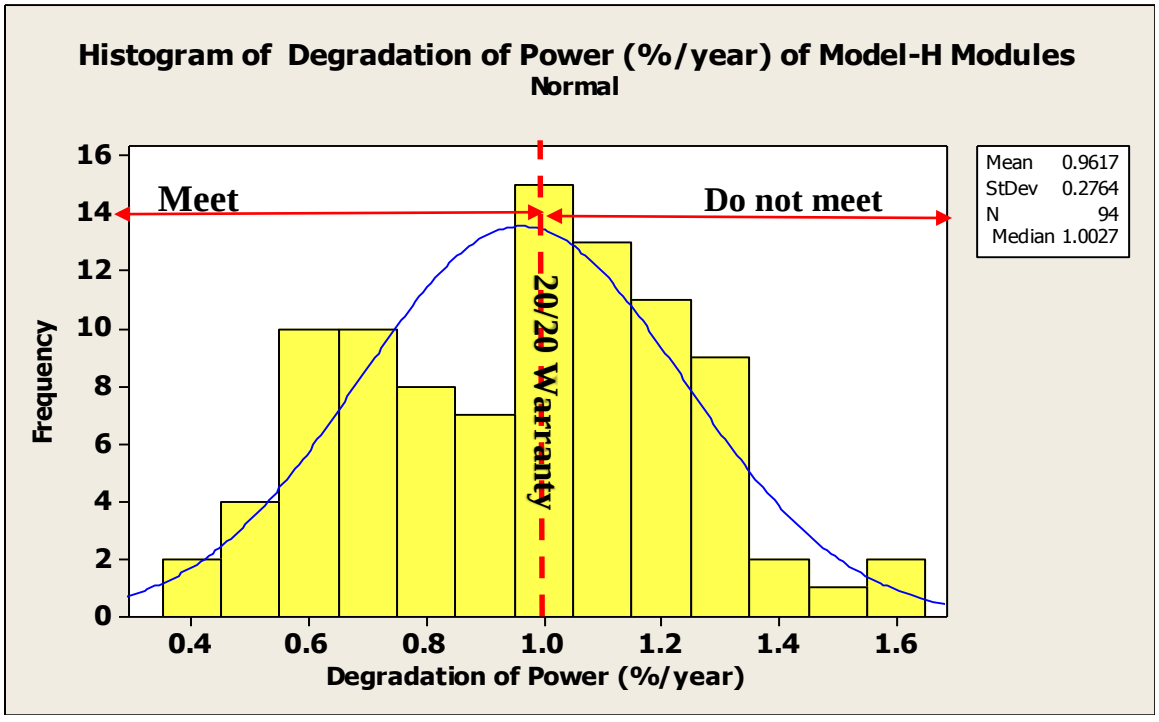

Figure 42 Histogram of Power Degradation (%/year) for Model-H Modules

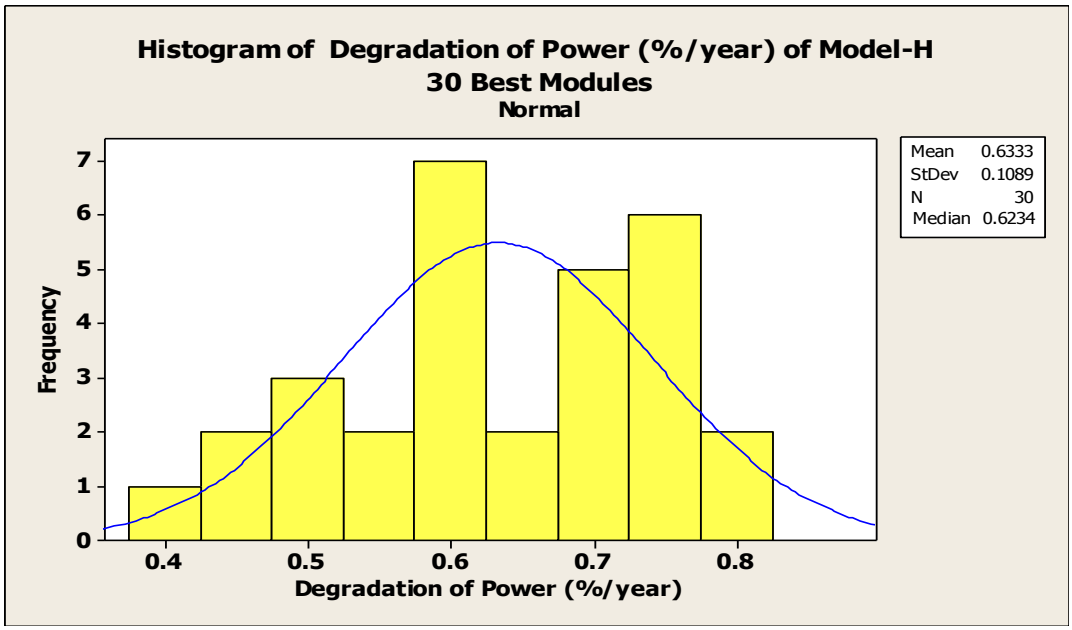

Figure 43 Histogram of Power Degradation (%/year) for Model-H (30 Best Modules)

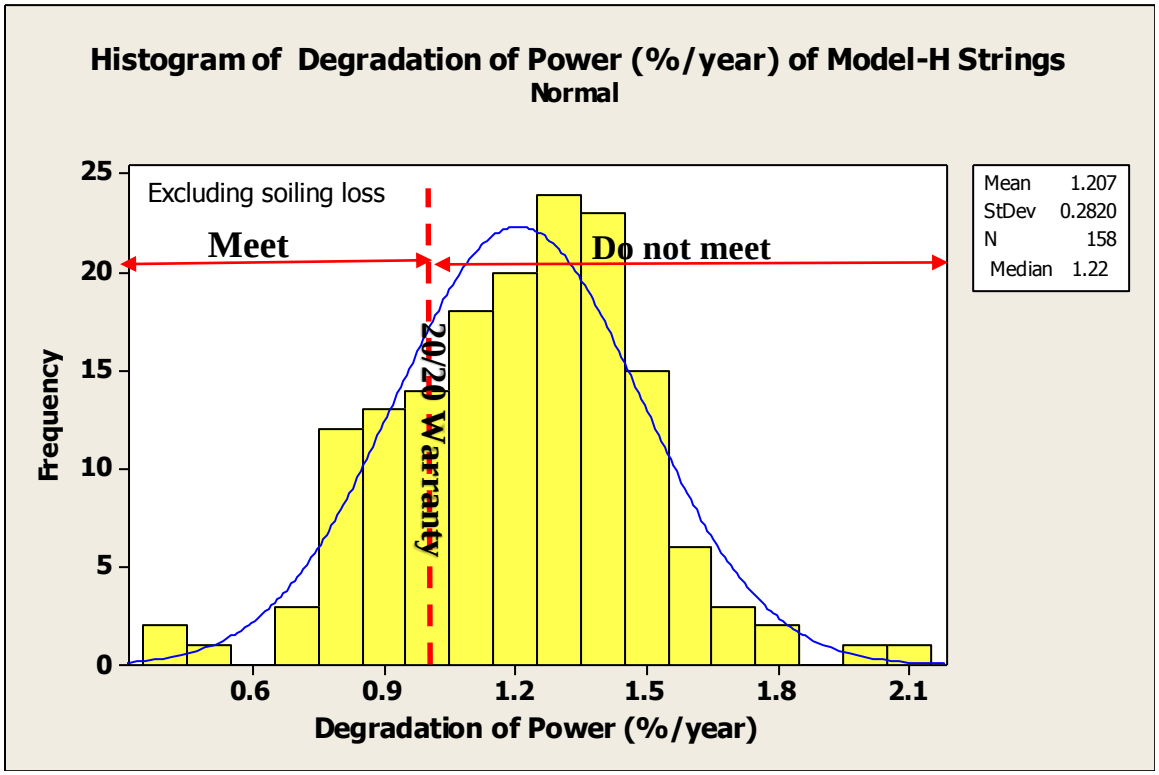

Figure 44 Histogram of Power Degradation (%/year) for Model-H All Strings

4.4 Visual Inspection

Since the Site 4c power plant is only 4 years old, no visual or diode failures were identified except for two broken modules. Based on the evidence found (crack propagation and impact location), it was confirmed that the modules were vandalized using golf balls. A detailed visual inspection was performed the in Site 3 power plant. The number of modules with defects (cosmetic or failure) is shown in Figure 45

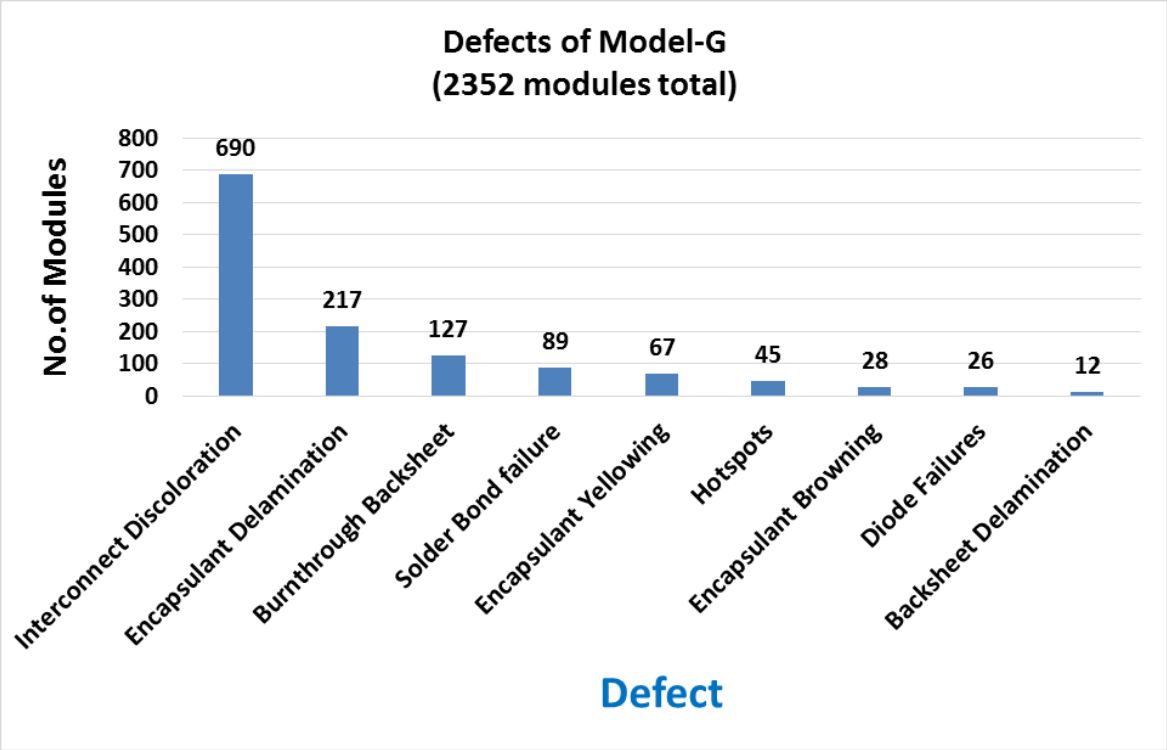

Figure 45 Defects of Model-G

The most predominant defects like interconnect discoloration, encapsulant delamination, encapsulant yellowing appear to be just cosmetic as there was no Isc degradation found for the best modules of Model G (see previous section of this chapter).

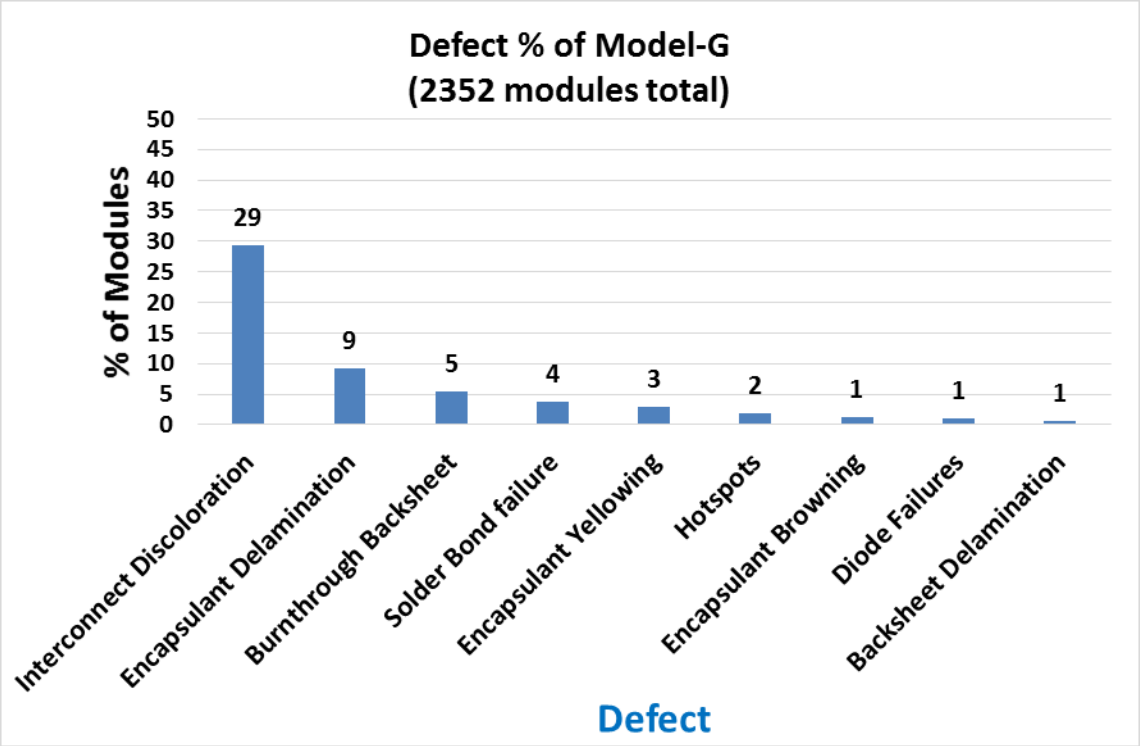

Figure 46 Defect % of Model-G

The reliability failures and durability loss percentage of the 285 total I-V based module distribution for the Site 3 power plant can be seen in Figure 48. Ribbon-Ribbon solder bond failure, hotspots leading to burnthrough backsheet and diode failures are the three safety failures found in Site 3.

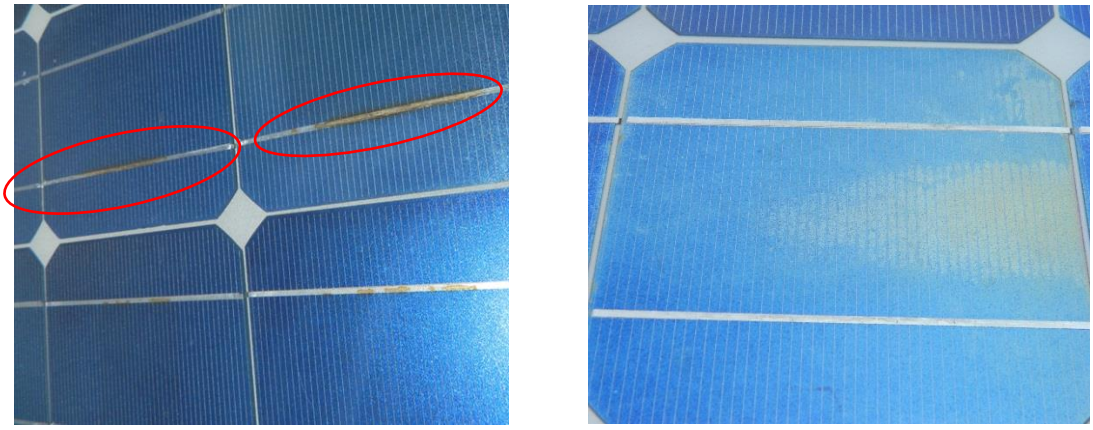

Figure 47 Left: Interconnect discoloration Right: Encapsulant Delamination

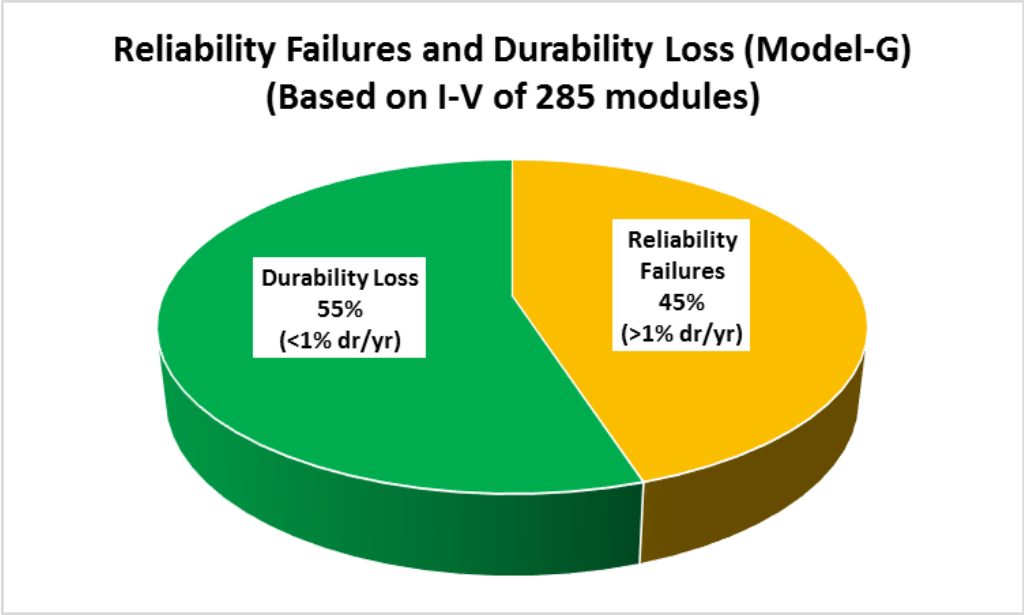

Figure 48 Reliability Failure, Durability loss (Rate %) – Total 285 I-V based modules

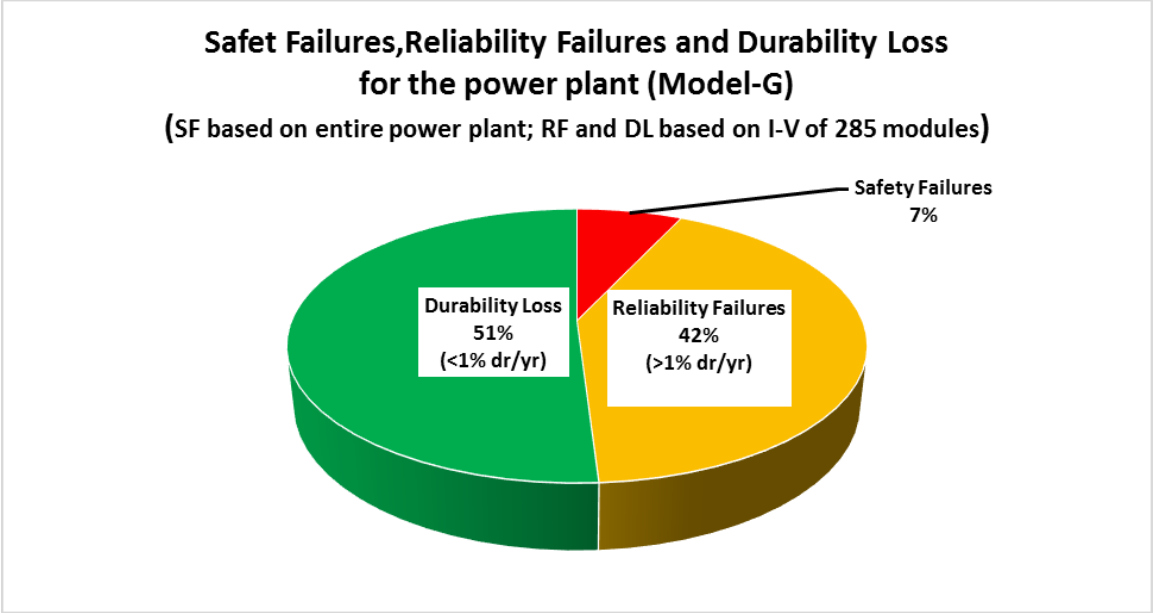

Figure 49 Safety Failures, Reliability Failures and Durability loss for entire power plant (Model-G)

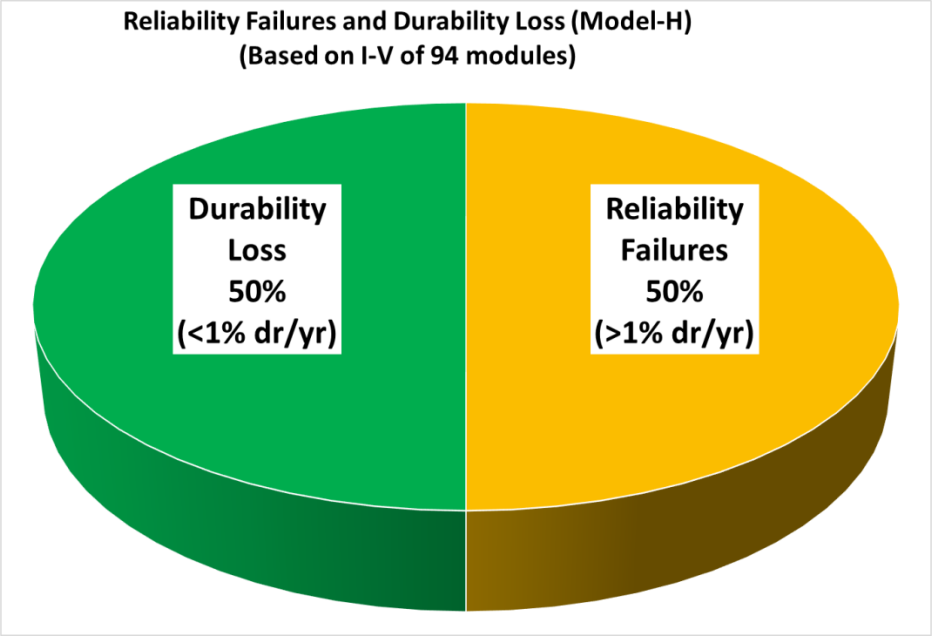

Figure 50 Reliability Failure, Durability loss (Rate %) – Total 94 I-V based modules

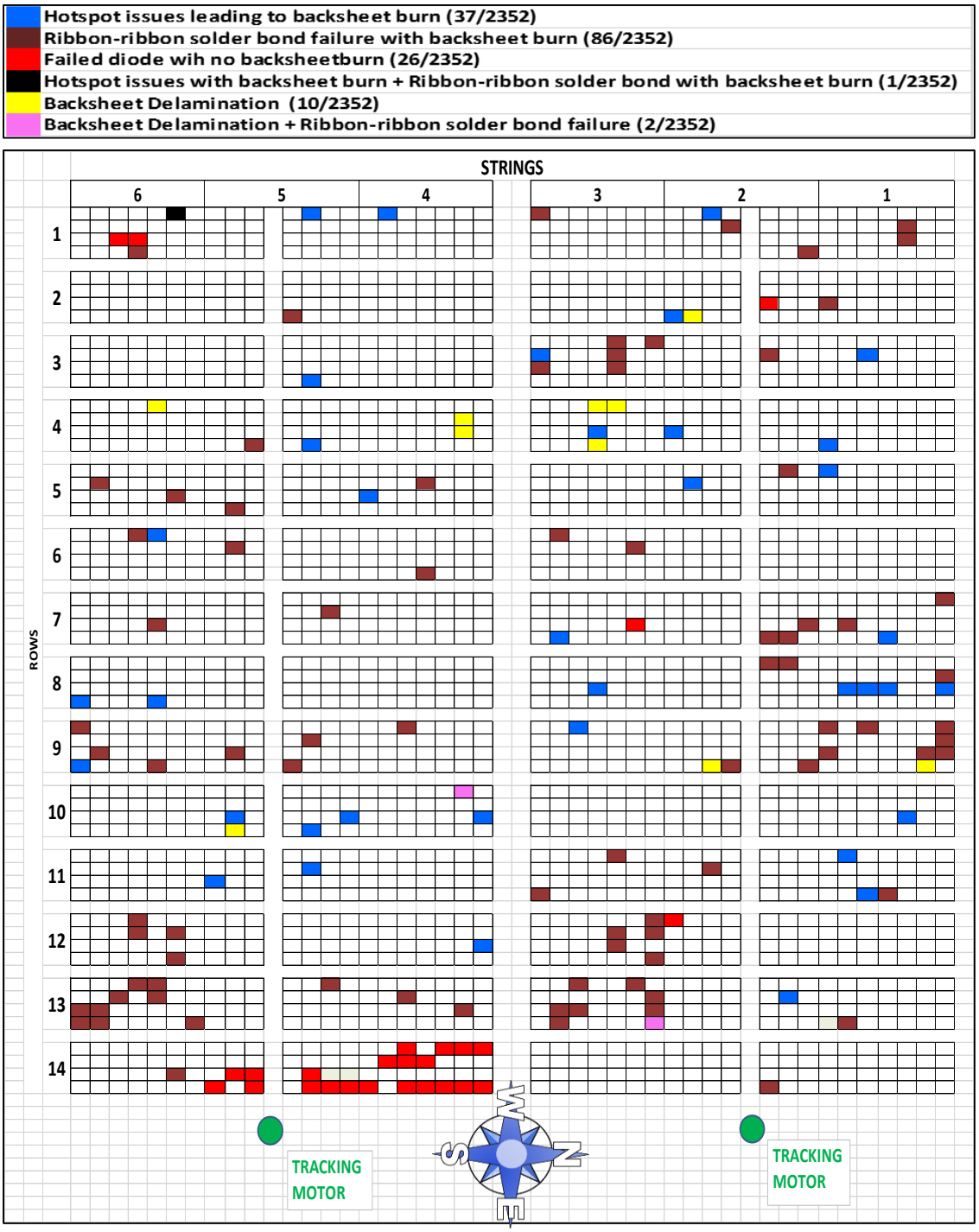

Figure 51 Layout of Safety Failures in Site 3 (Model-G)

In the whole power plant, 26 diodes failed (open circuited). Out of these failed diodes, as shown in Figure 51, only 19.3% failed randomly throughout the power plant and 80.7% failed in just two strings of 14-4 and 14-5. As shown in Figure 51, strings 14-4 and 14-5 are located next to one of the array's single-axis tracking motors. The reasons for these concentrated diode failures only in two strings are not known. It is known that the moving shadows can cause failures [12]. The possible reasons for these concentrated failures which occurred only in two strings near the tracking motor may be speculated as follows.

- The repair or other maintenance personnel of the power plant could have parked and moved their vehicles at that particular location. This could cause a moving shadow issue.
- During shaded state the diodes were forward biased and triggered and will reach a high temperature. After a shading occurrence and while the diode is still at a high temperature, the diode goes into a normal mode where it sees an operating voltage of 18 cells or roughly 10V. This induces a reverse leakage current that can exceed the diode reverse current rating at that temperature with the destruction of that diode most likely in the open circuit mode [12].
- The above explained phenomenon is thermal runaway, which results in the loss of temperature control, due to the inability to exhaust the power losses generated by the diode operation [11]. Figure 52 shows one of the failed diodes in the strings 14-4 and 14-5.

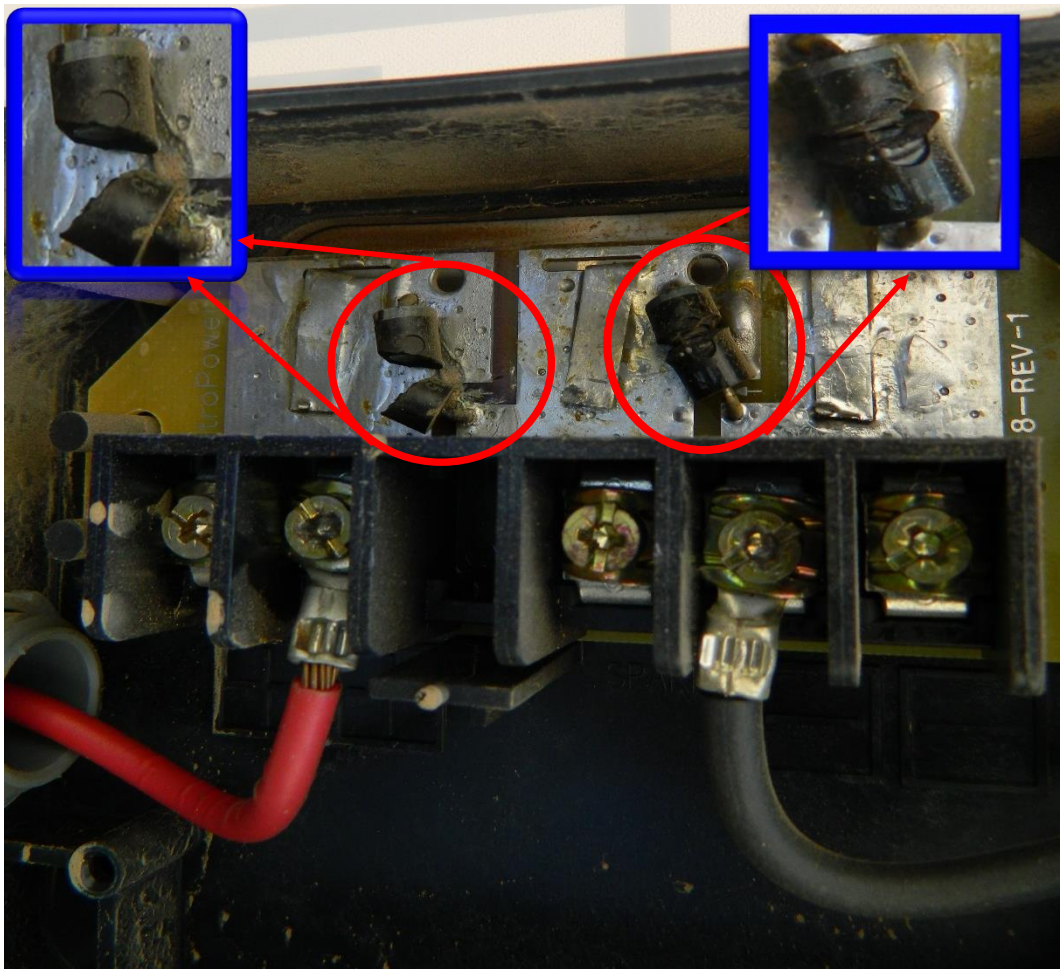

Figure 52 Failed diode

Figure 53, the hot spots in Site 3 array were found to invariably lead to backskin burning along the line of cell interconnect. The hotspot cells were found to operate at about 38°C higher than the average (55°C) of the other cells in the module. As shown in Figure 54, the hotspot modules degradation rate is 2.82 %/year which is more than the non-hotspot modules (0.94%/year). The modules are operating cooler by 3-5°C near the periphery of the support frames indicating they are acting as a heat sink.

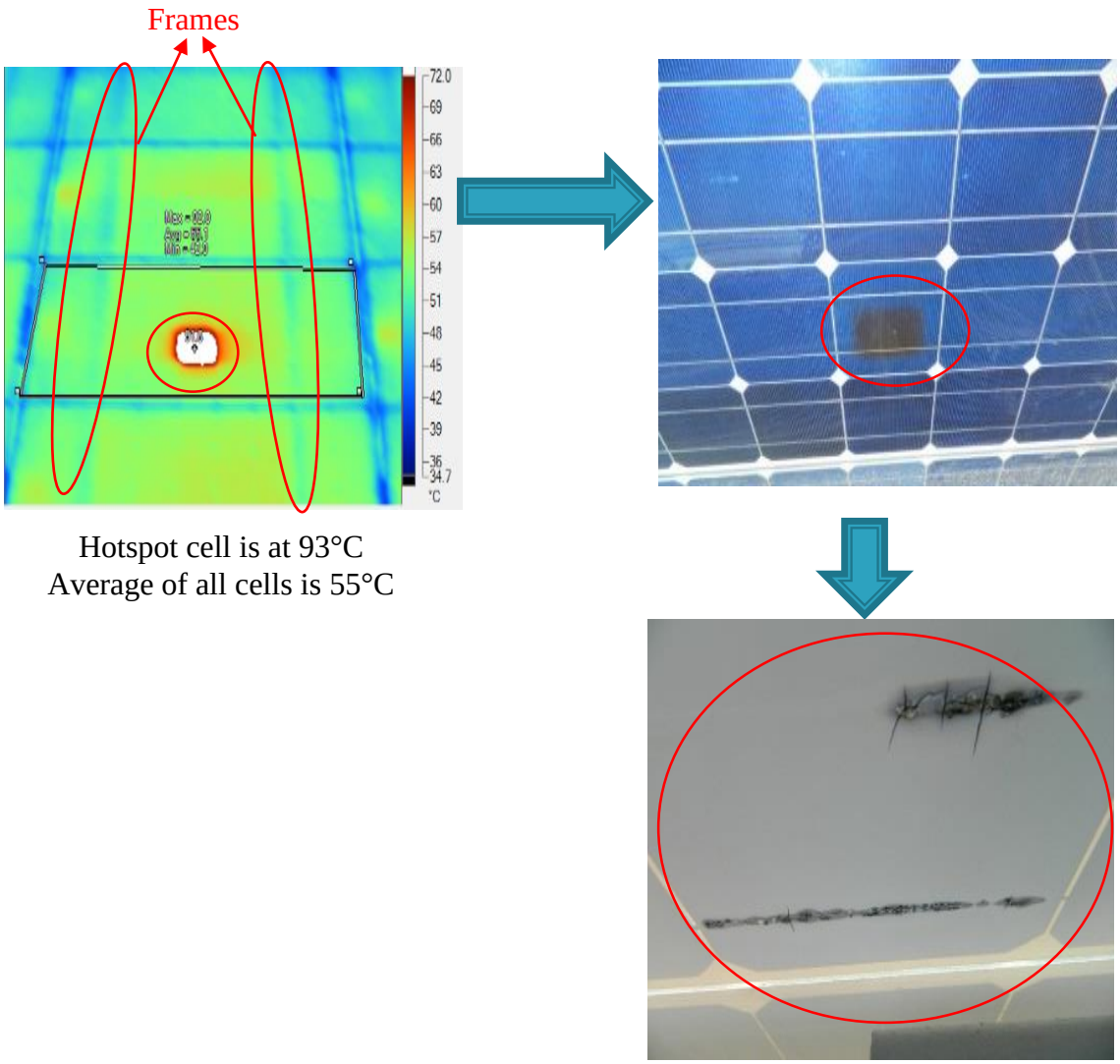

Figure 53 Hotspots leading to backsheet burning

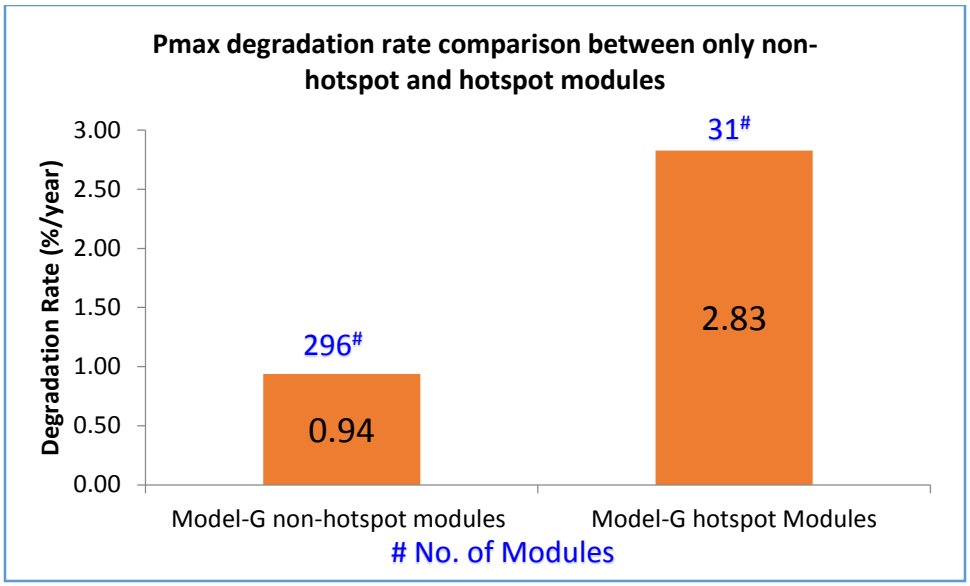

Figure 54 Degradation rate comparison between only non-hotspot and hotspot modules

4.5 Potential induced Degradation

Potential Induced Degradation (PID) is responsible for durability issues in modules. The degradation of modules operating at different voltages in a string was studied. All the strings at Site 3 and Site 4c are connected in series to obtain higher voltage levels. All the strings are positively biased with centralized negative grounding at the inverter. This study helps to understand the influence of voltage on module degradation in hot and dry climatic conditions. The percentage of degradation for each module in the string were arranged according to the position of the module in the string and a scatter plot was plotted. All the modules considered for the PID study in a string were free from reliability failures.

Two random best strings from Site 3 are presented in Figure 55 and Figure 56 . The last module in the string at the positive end experiences higher degradation than does the

module at position 1(grounded). In Figure 56 the first and the last modules have almost same percentage of degradation and the trend line suggests the degradation appears more on the negative side.

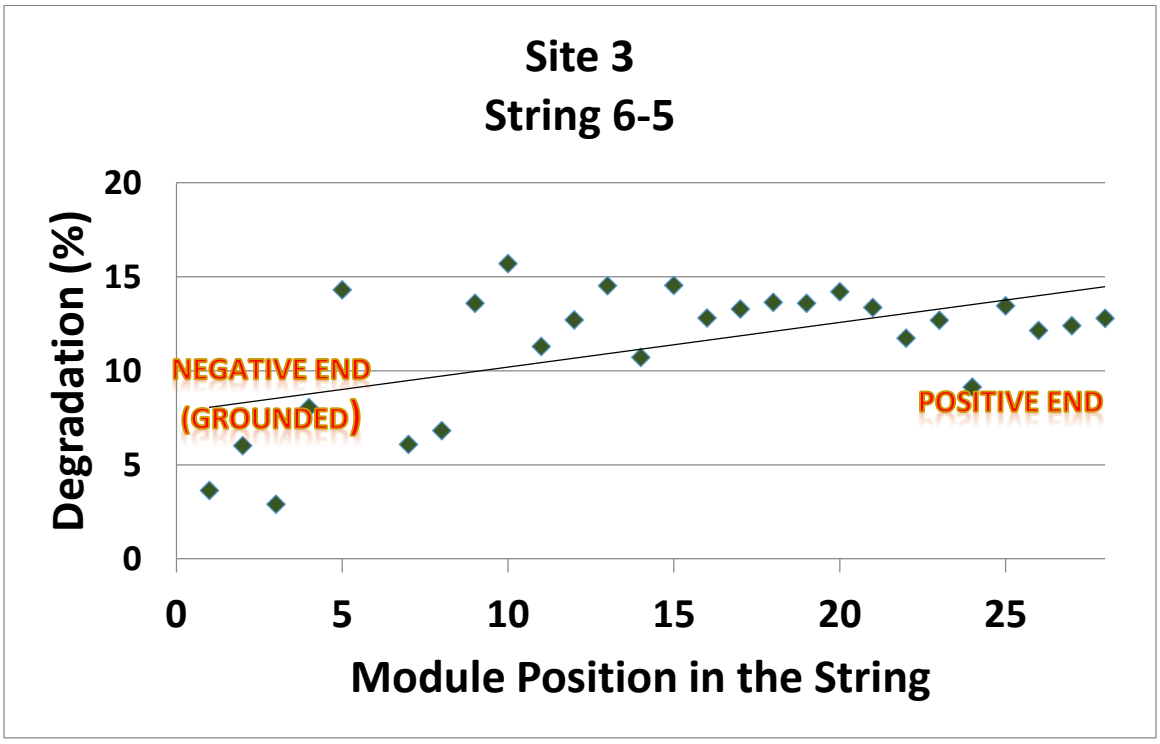

Figure 55 Higher degradation percentage at positive end of string (Model-G)

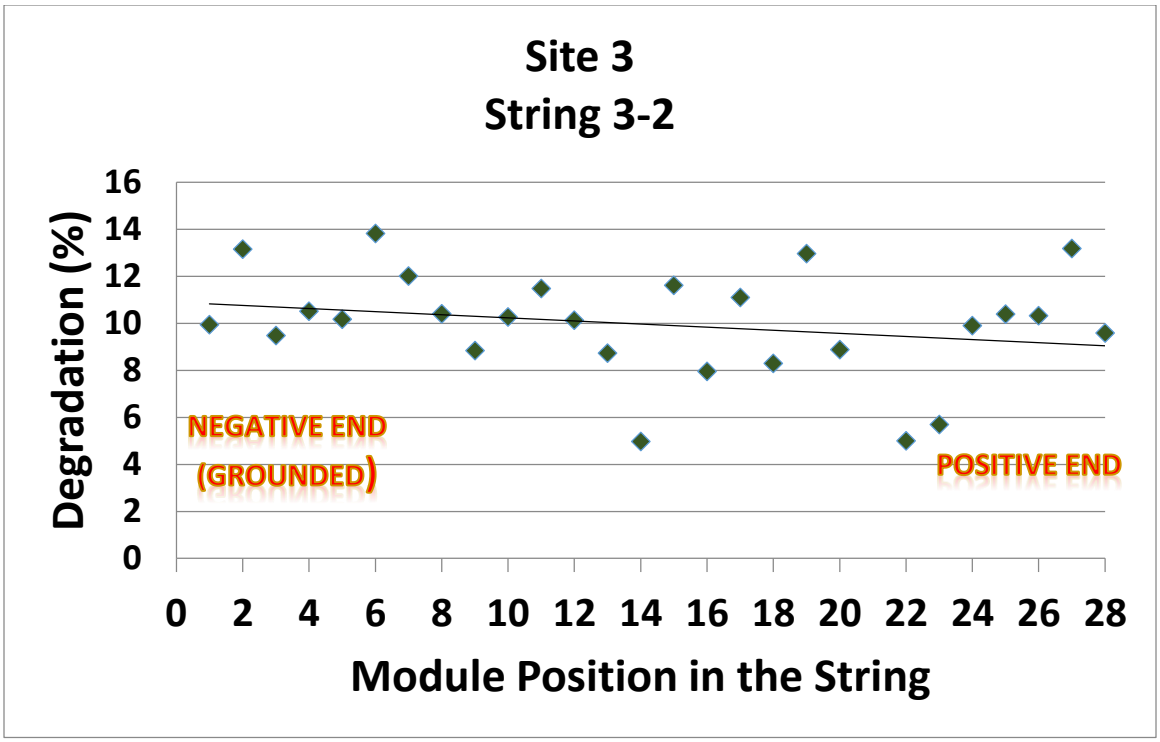

Figure 56 Higher degradation percentage at negative end of the string (Model-G)

The same analysis performed on Site 3 data is also performed on Site 4c data. Figure 57 and Figure 58 show there is no systematic trend in the degradation of modules with respect to their positioning in the string. These trends seen in Site 3 and Site 4c demonstrate the absence of PID.

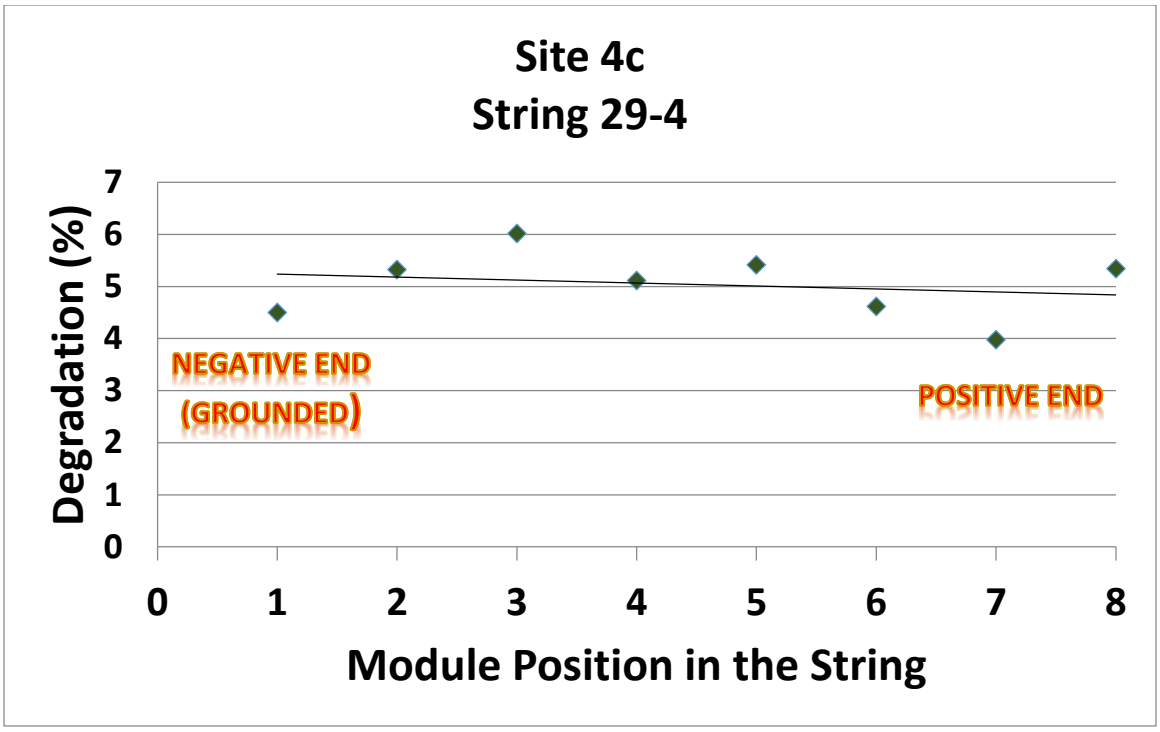

Figure 57 Higher degradation percentage at negative end of the string (Model-H)

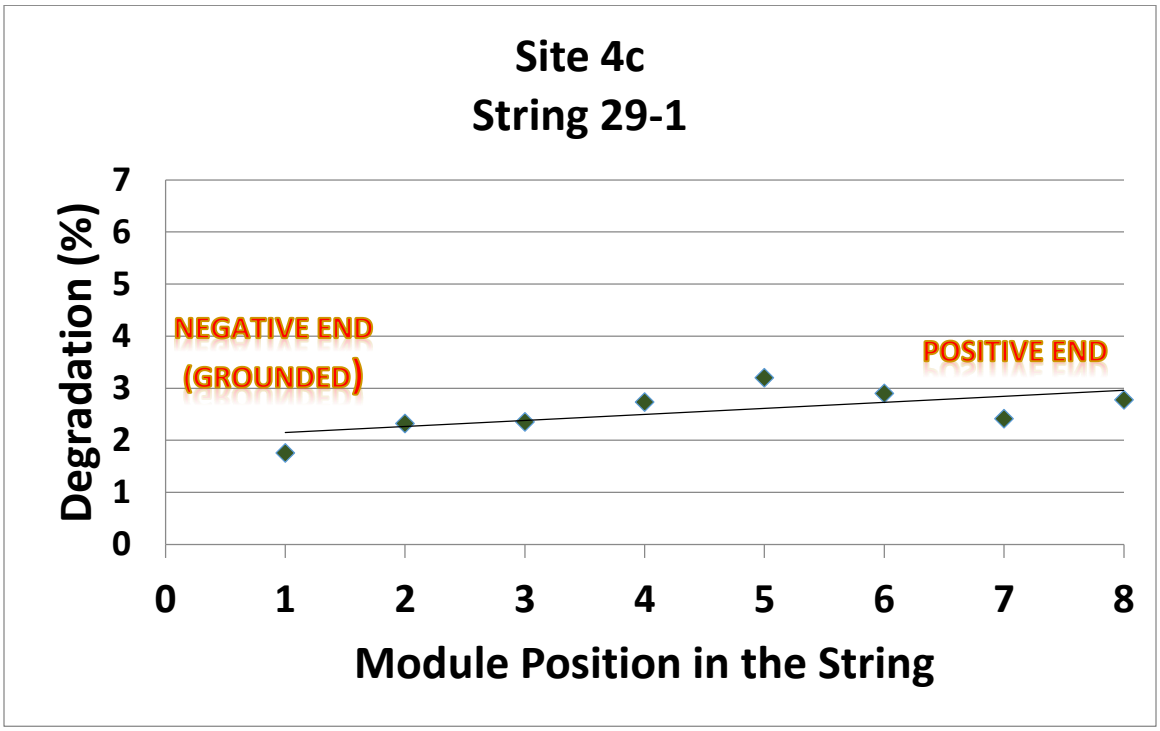

Figure 58 Higher degradation percentage at positive end of the string (Model-H)

4.6 SOILING STUDY

Soiling on PV modules causes a drop in the performance of the module. Soiling is a durability issue. Soiling reduces the transmittance of the light onto the solar cells which decrease Isc. String IV curves were taken in a soiled state which reflected the power plant's state of operation at that time. These strings were then cleaned with water and dried before taking another set of IV curves. Figure 59 and Figure 61 shows the soiling loss in Site 3 and Site 4c respectively. The Site 3 power plant had an average of 6.9 % soiling loss and the Site 4c power plant experienced a 5.5% soiling loss. The more soiling loss in site 3 than site 4c could be because site 4c is in urban area where there are no dust roads, but site 3 is in rural area where it is surrounded by dust roads with farmland.

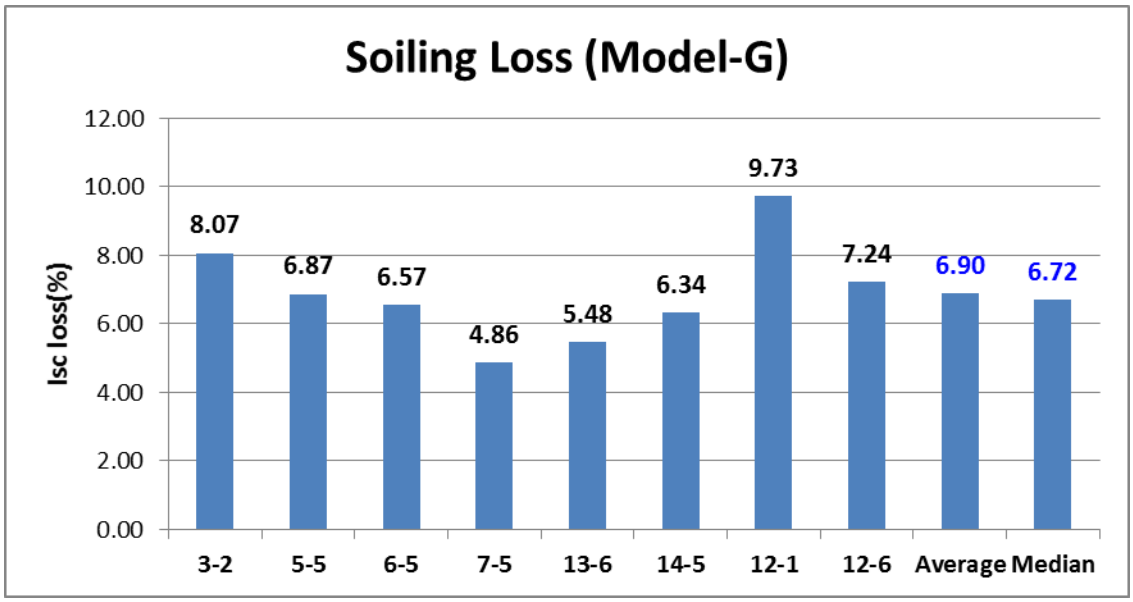

Figure 59 Soiling loss in Site 3

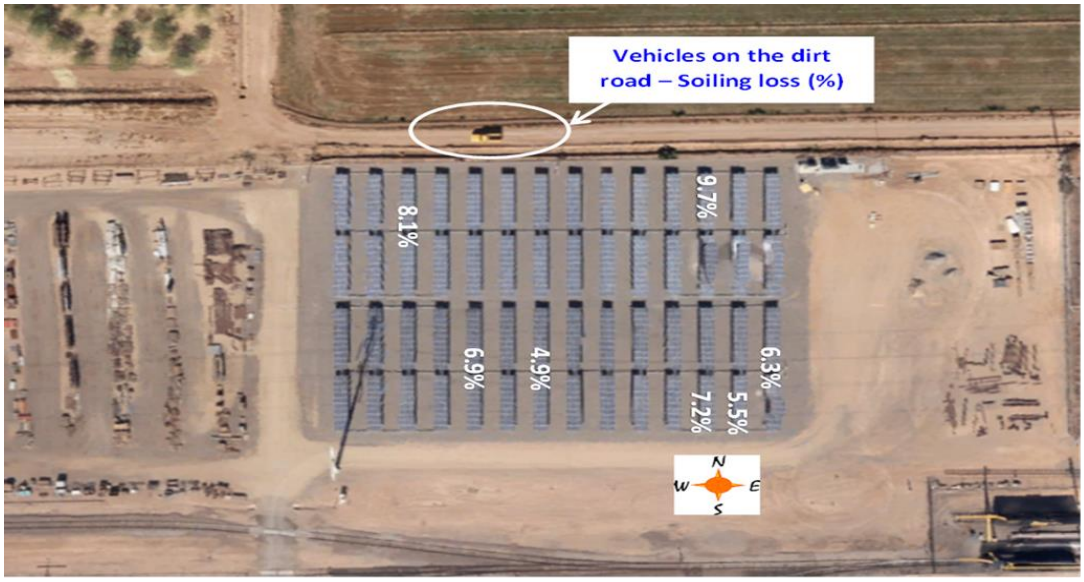

Figure 60 Soiling distribution in Site 3

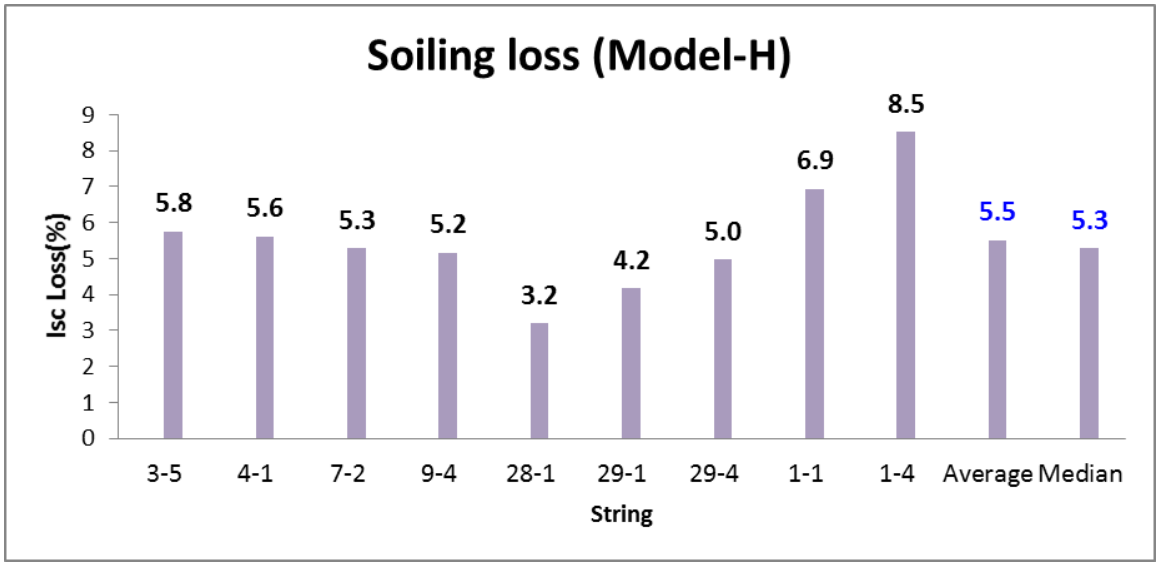

Figure 61 Soiling loss in Site 4c

4.7 Wind Effect on Durability

The modules performance is dictated by the temperature under which they are operating. Wind flow will help cool the modules. The wind direction in and around Phoenix Arizona is typically from the south –west. If there is a wind direction effect due to nearby wind obstructing objects, the south-west strings are expected to degrade at a lower rate than the north-east array. In Site 3 the surroundings are open with a farm land on the north and scrap yard (30 ft.) on the west and two big tanks far away (175 ft.) on the east and south sides . This can be seen in Figure 62. Due to an absence of barriers which obstruct the wind flow, no systematic wind direction effect on the module performance was observed. Figure 64 shows the string power distribution in Site 3. Site 4c has a wall on the south side, a building on the east side and Site4a, 4b situated about 5 feet from ground level of Site 4c on the north. No systematic wind effect on module performance was observed due to a lack of wind barriers.

Figure 65 indicating the absence of wind direction effect on the degradation rate of the PV modules in these power plants.

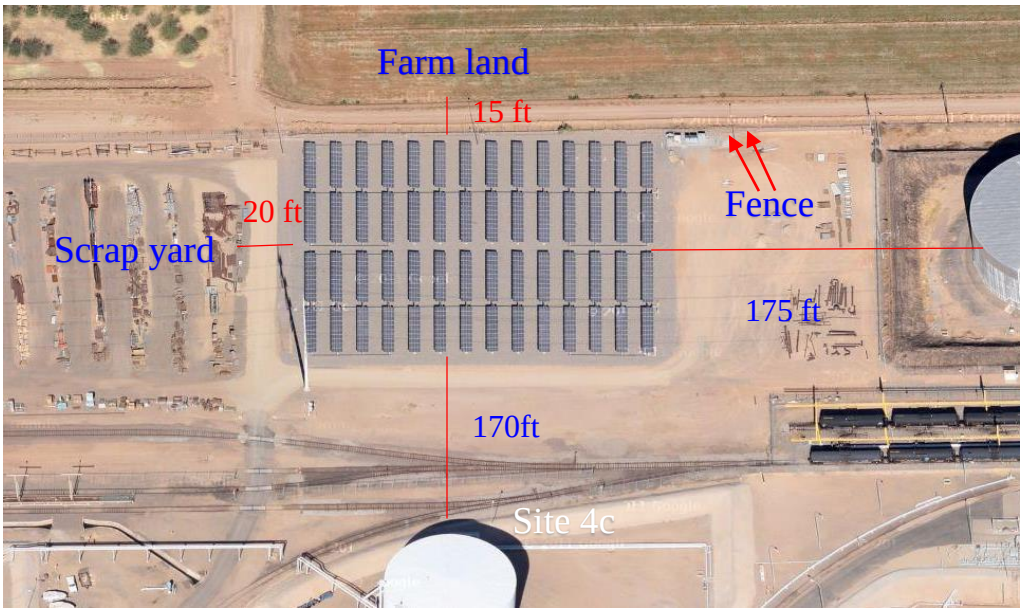

Figure 62 Site 3 google satellite image

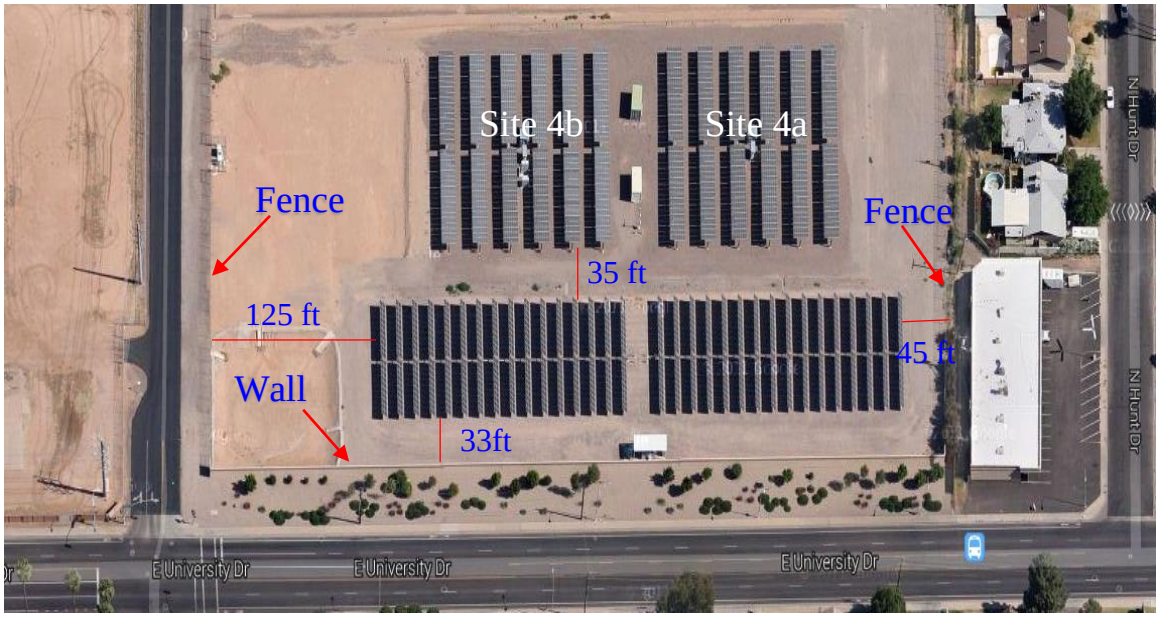

Figure 63 Site 4c google satellite image

Figure 64 Site 3 string power distribution to see if there is any systematic wind direction effect on degradation rates of strings

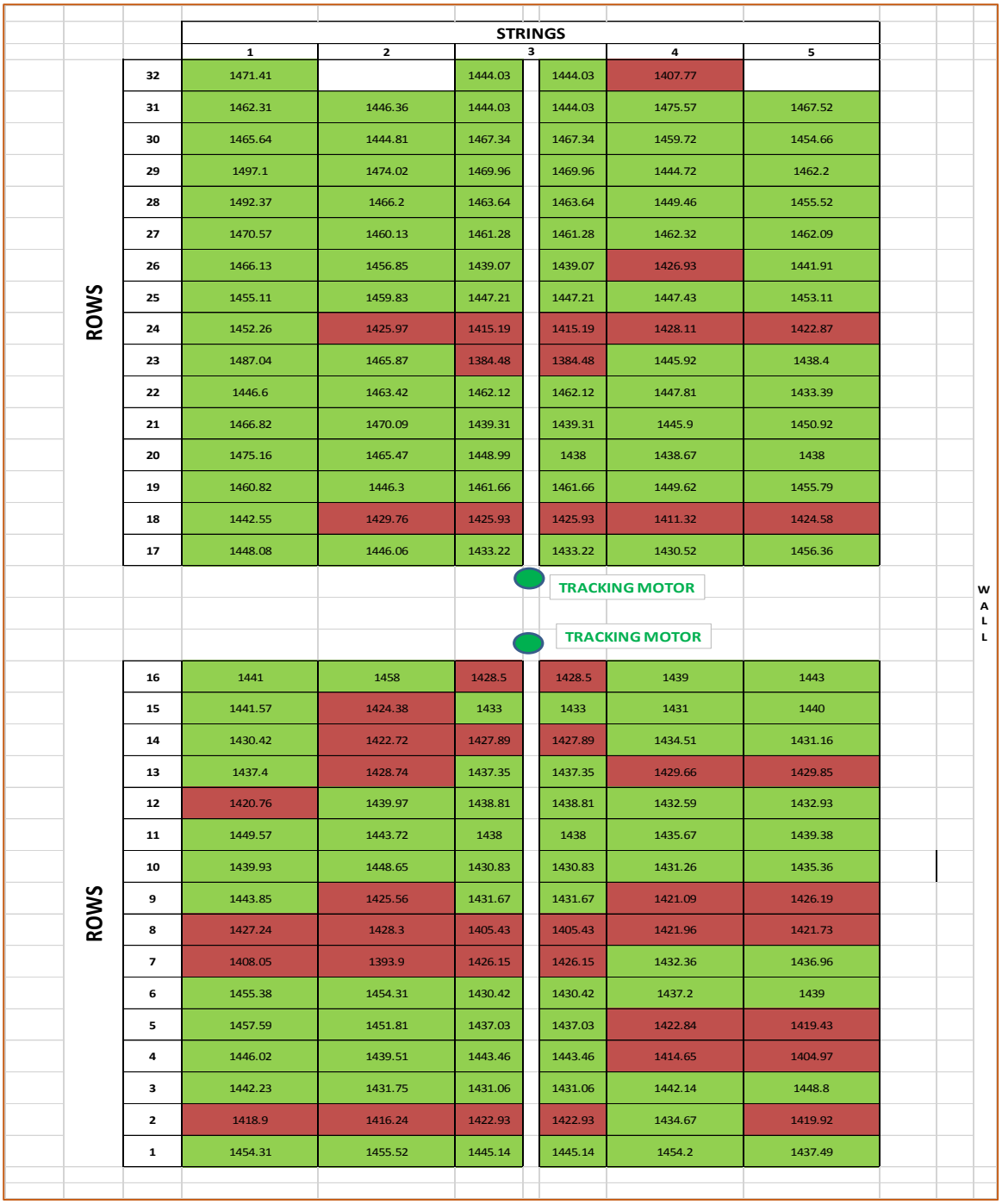

ROWS	STRINGS 1	2	3		4	5
32	1471.41		1444.03	1444.03	1407.77	
31	1462.31	1446.36	1444.03	1444.03	1475.57	1467.52
30	1465.64	1444.81	1467.34	1467.34	1459.72	1454.66
29	1497.1	1474.02	1469.96	1469.96	1444.72	1462.2
28	1492.37	1466.2	1463.64	1463.64	1449.46	1455.52
27	1470.57	1460.13	1461.28	1461.28	1462.32	1462.09
26	1466.13	1456.85	1439.07	1439.07	1426.93	1441.91
25	1455.11	1459.83	1447.21	1447.21	1447.43	1453.11
24	1452.26	1425.97	1415.19	1415.19	1428.11	1422.87
23	1487.04	1465.87	1384.48	1384.48	1445.92	1438.4
22	1446.6	1463.42	1462.12	1462.12	1447.81	1433.39
21	1466.82	1470.09	1439.31	1439.31	1445.9	1450.92
20	1475.16	1465.47	1448.99	1438	1438.67	1438
19	1460.82	1446.3	1461.66	1461.66	1449.62	1455.79
18	1442.55	1429.76	1425.93	1425.93	1411.32	1424.58
17	1448.08	1446.06	1433.22	1433.22	1430.52	1456.36
			TRACKING MOTOR			
			TRACKING MOTOR			
16	1441	1458	1428.5	1428.5	1439	1443
15	1441.57	1424.38	1433	1433	1431	1440
14	1430.42	1422.72	1427.89	1427.89	1434.51	1431.16
13	1437.4	1428.74	1437.35	1437.35	1429.66	1429.85
12	1420.76	1439.97	1438.81	1438.81	1432.59	1432.93
11	1449.57	1443.72	1438	1438	1435.67	1439.38
10	1439.93	1448.65	1430.83	1430.83	1431.26	1435.36
9	1443.85	1425.56	1431.67	1431.67	1421.09	1426.19
8	1427.24	1428.3	1405.43	1405.43	1421.96	1421.73
7	1408.05	1393.9	1426.15	1426.15	1432.36	1436.96
6	1455.38	1454.31	1430.42	1430.42	1437.2	1439
5	1457.59	1451.81	1437.03	1437.03	1422.84	1419.43
4	1446.02	1439.51	1443.46	1443.46	1414.65	1404.97
3	1442.23	1431.75	1431.06	1431.06	1442.14	1448.8
2	1418.9	1416.24	1422.93	1422.93	1434.67	1419.92
1	1454.31	1455.52	1445.14	1445.14	1454.2	1437.49

WALL

Figure 65 Site 4c string power distribution to observe any systematic wind direction effect on degradation of strings

Chapter 5

CONCLUSIONS

5.1 Degradation Rates and Failure Modes

- The mean and median degradation rate of Site 3 (Model G; 12 years on 1-axis tracker) modules in a hot-dry (desert) climate is 0.95%/year and 0.96%/year, respectively.
- About 7% of the Site 3 (Model G) modules qualify for the safety returns. Assuming a linear degradation and a 20-year warranty with less than 20% degradation from nameplate rating (20/20 warranty), about 51% of the tested modules of Site 3 do not qualify for warranty claims and about 42% of the tested modules of Site 3 (Model G) qualify for the warranty claims proportional to the rate of degradation above 1%
- The mean and median degradation rate of Site 4c (Model H; 4 years on 1-axis tracker) modules in a hot-dry (desert) climate is 0.96%/year and 1.00%/year, respectively.
- The Site 4C modules have not experienced any safety failures. About 50% of the tested modules of Site 4c meet the typical 20/20 warranty expectations while the other 50% of the modules do not.
- The primary cause of degradation in the best modules of Site 3 is solder bond fatigue leading to increase in series resistance. The primary failure mode in the worst modules is ribbon-ribbon solder bond failure.

- The observed degradation is potentially attributed to the light induced degradation.

5.2 Other Durability Issues

- PID does not seem to be responsible for the degradation of negative grounded systems in the hot-dry desert climatic condition of Phoenix, Arizona.
- The average soling loss observed in Site 3 and Site 4c are 6.9% and 5.5%, respectively.
- Systematic wind direction effect on the degradation of strings due to possible non-uniform thermal distribution of the power plant does not seem to be occurring in both the power plants.

REFERENCES

[1] G. Tamizhmani and J. Kuitche, "Accelerated Lifetime Testing Of Photovoltaic Modules," Solar America Board for Codes and Standards, 2013.

[2] T. J. McMahon, D. L. King, M. A. Quintana, G. J. Jorgensen and R. L. Hulstrom, "Module 30 Year Life : What Does it Mean and Is it Predictable/Achievable?," 2000.

[3] W. Richardson, "Potential Induced Degradation," in *Solon Corporation, NREL Photovoltaic Reliability Workshop*, 2011.

[4] J. Singh, J. Belmont and G. TamizhMani, "Degradation Analysis of 1900 PV modules in a Hot-Dry Climate: Results after 12 to 18 years of field exposure," in *39th IEEE PVSC* , 2013.

[5] M. Schütze, M. Junghänel, M. Koentopp, S. Cwikla, S. Friedrich, J. Müller, J. Wawer, S. Q-Cells and Sonnenallee 17-21, "LABORATORY STUDY OF POTENTIAL INDUCED DEGRADATION OF SILICON," in *37th IEEE PVSC*, 2011.

[6] D. Jordan and S. Kurtz, "Photovoltaic Degradation Rates — An Analytical Review," *Progress in Photovoltaics: Research and Applications*, 2012.

[7] J. Jeong, N. Park and C. Han, "Field failure mechanism study of solder interconnection for crystalline," *Microelectronics Reliability*, pp. 1-5, 2012.

[8] K. Kato, "PV module failures observed in the field-solder bond and bypass diode failures," in *NREL PVMRW2012*.

[9] D. Staebler and C. Wronski, "Reversible conductivity changes in dischargeproduced amorphous Si," *Applied Physics Letters*, pp. 1-4, 1977.

[10] D. King, A. Kratochvi and W. Boyson, "STABILIZATION AND PERFORMANCE CHARACTERISTICS OF," in *IEEE*, 2000.

[11] "How to choose a bypass diode for a silicon panel junction box," STMicroelectronics, 2011.

[12] R. a. A. Posbic.J, "High Temperature Reverse By-Pass Diodes Bias and Failures," in *NREL PVRM*, 2013.

[13] L. R. S. W. Y. Jiang.L, "Open-Circuit Voltage Physics in Amorphous Silicon Solar Cells," *Materials Research Society,* pp. 1-11, 2000.

[14] H. Bowden.S, "PV Education," [Online]. [Accessed October 2013].

[15] Suryanarayana.V.J, "Angle of Incidence and Power Degradation Analysis of pholtovoltaics," Arizona State University, 2013.

[16] Olakonu.K, "26+ Year Old Photovoltaic Power Plant: Degradation and Reliability - Evaluation of Crystalline Silicon Modules – South Array," Arizona State university, 2012.

[17] Belmont.J, "26+ Year Old Photovoltaic Power Plant: Degradation and Reliability Evaluation of Crystalline Silicon Modules - North Array," Arizona State University, 2013.

[18] Singh.J, "Investigation of 1,900 Individual Field Aged Photovoltaic Modules for Potential Induced Degradation (PID) in a Positive Biased Power Plant," Arizona State University.

[19] Suleske.A, "Performance Degradation of Grid-Tied Photovoltaic Modules in a Desert Climatic Condition," Arizona State University, 2010.

APPENDIX A

SITE 3 PLOTS FOR VARIOUS I-V PARAMETERS

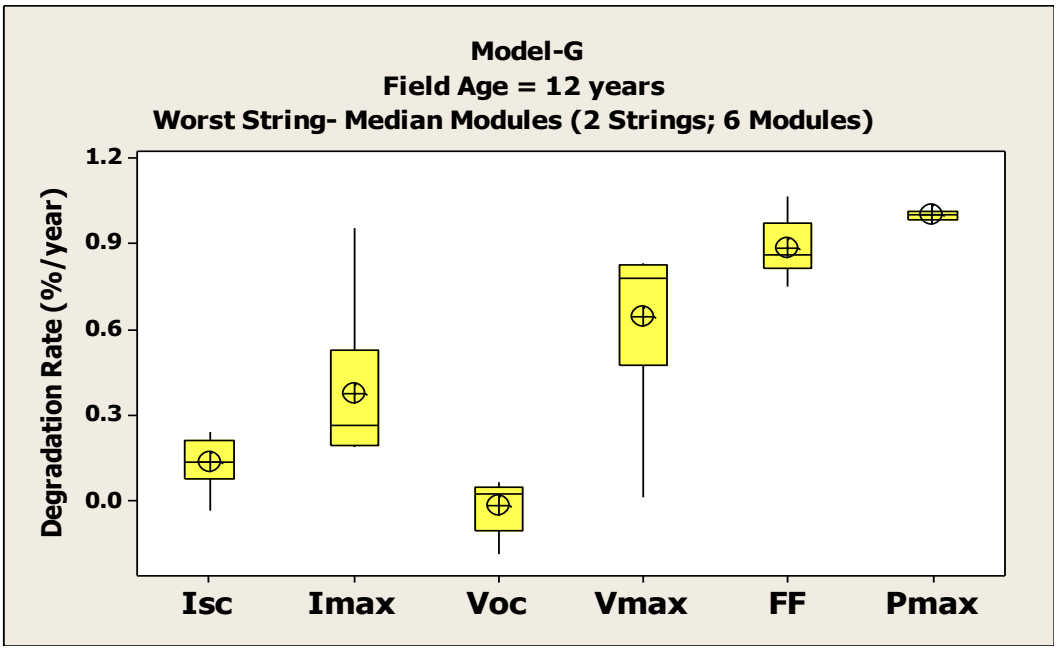

Figure A 1 Plot for various I-V parameter degradation (%/year) for worst string- median modules

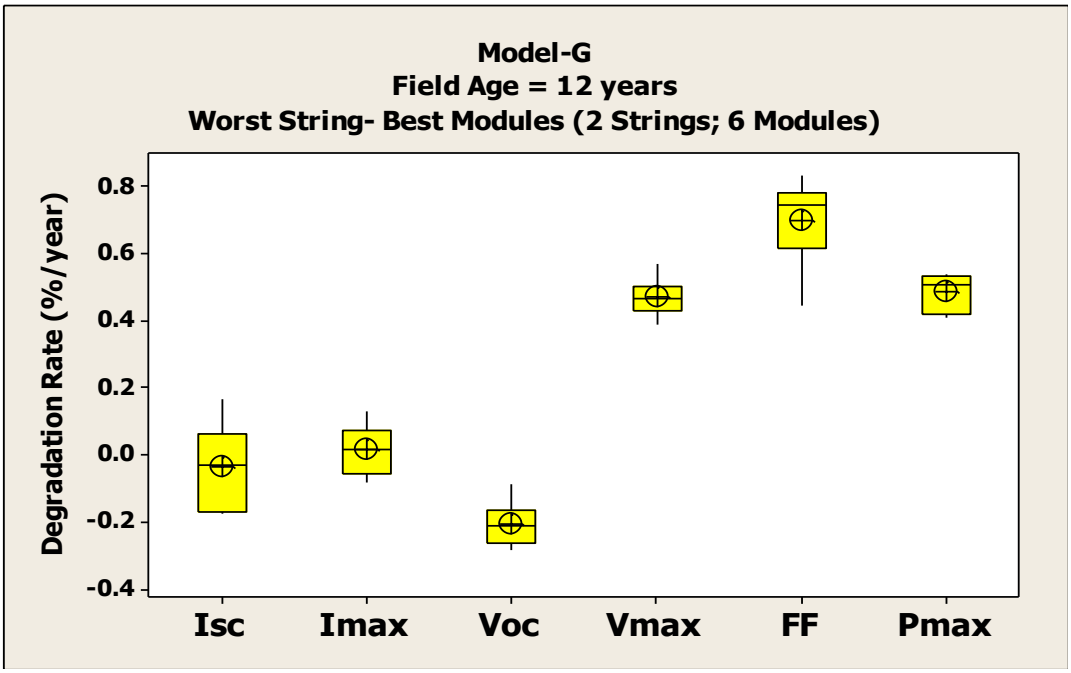

Figure A 2 Plot for various I-V parameter degradation (%/year) for worst string- best modules

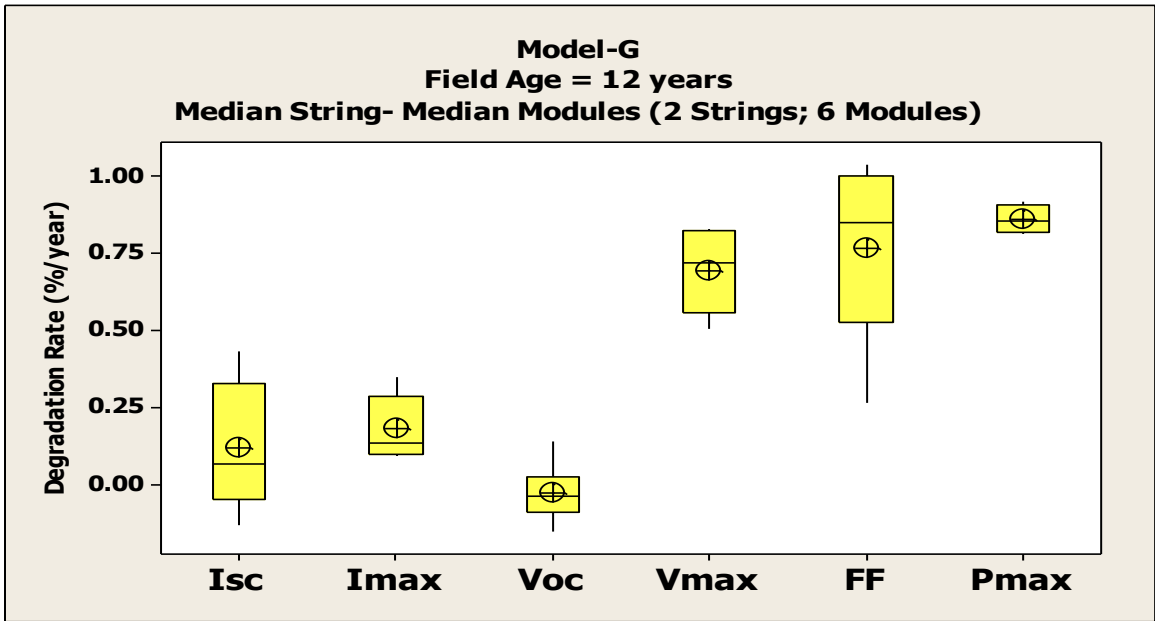

Figure A 3 Plot for various I-V parameter degradation (%/year) for median string-median modules

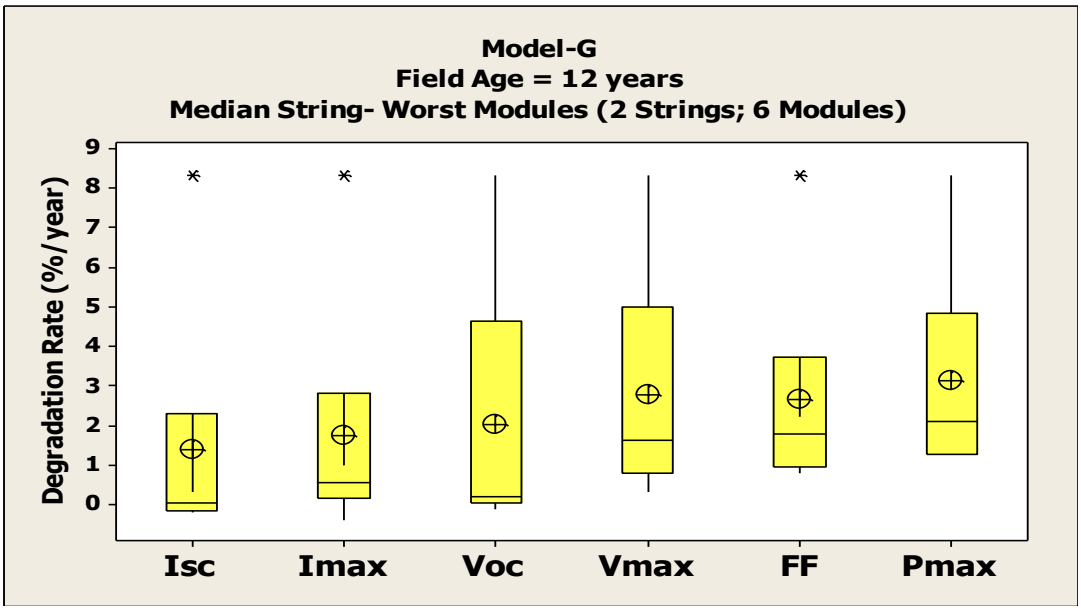

Figure A 4 Plot for various I-V parameter degradation (%/year) for median string- worst modules

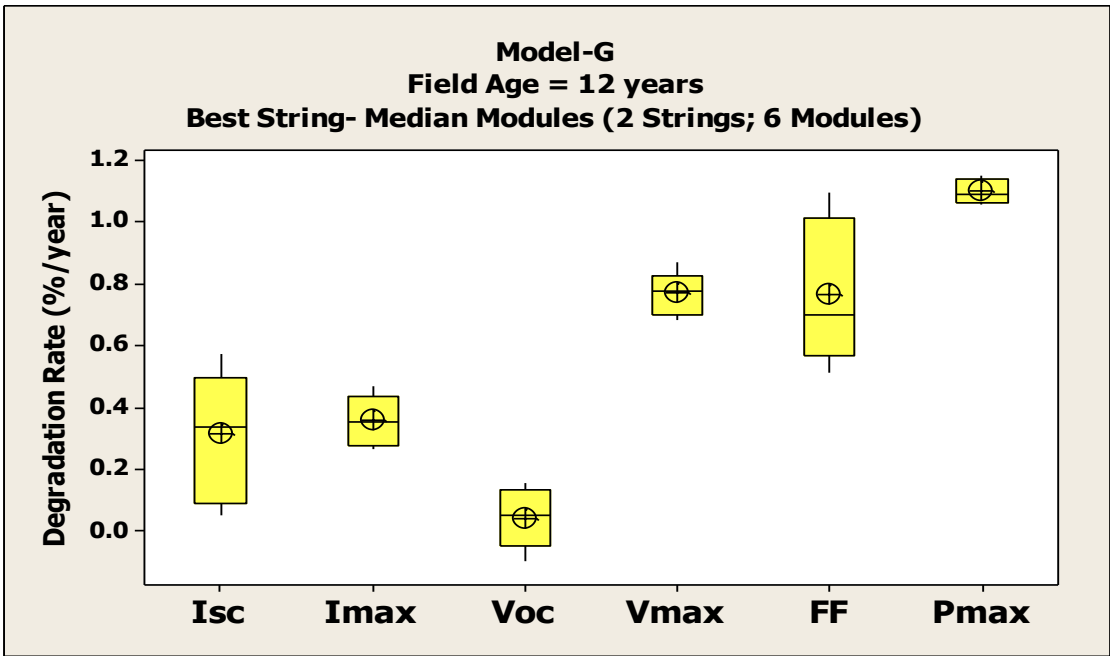

Figure A 5 Plot for various I-V parameter degradation (%/year) for best string- median modules

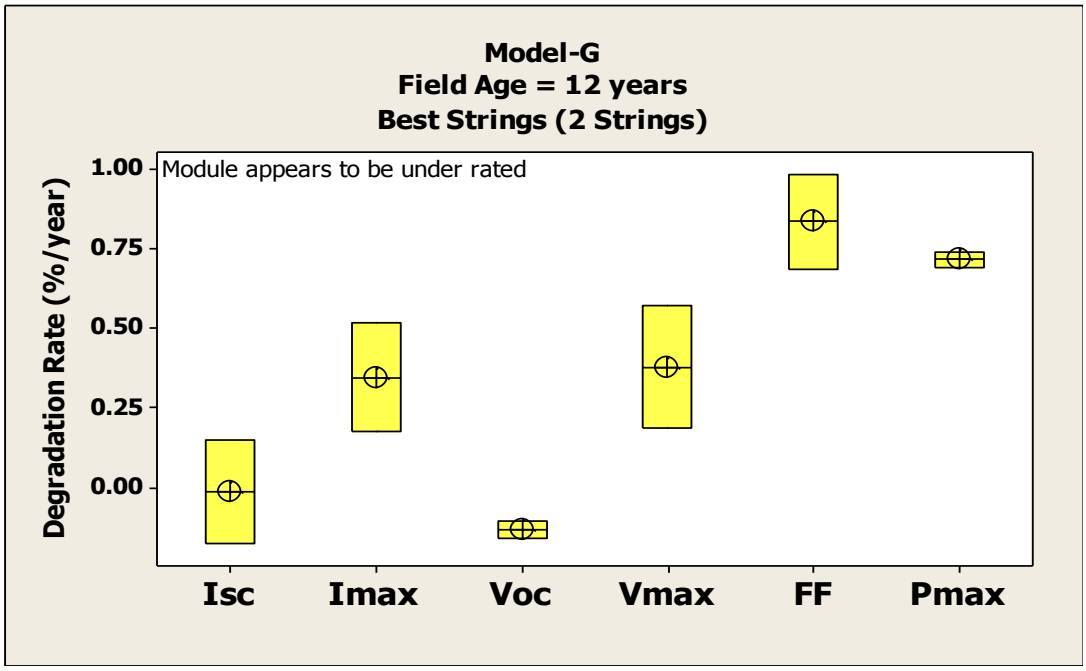

Figure A 6 Plot for various I-V parameter degradation (%/year) for Best String

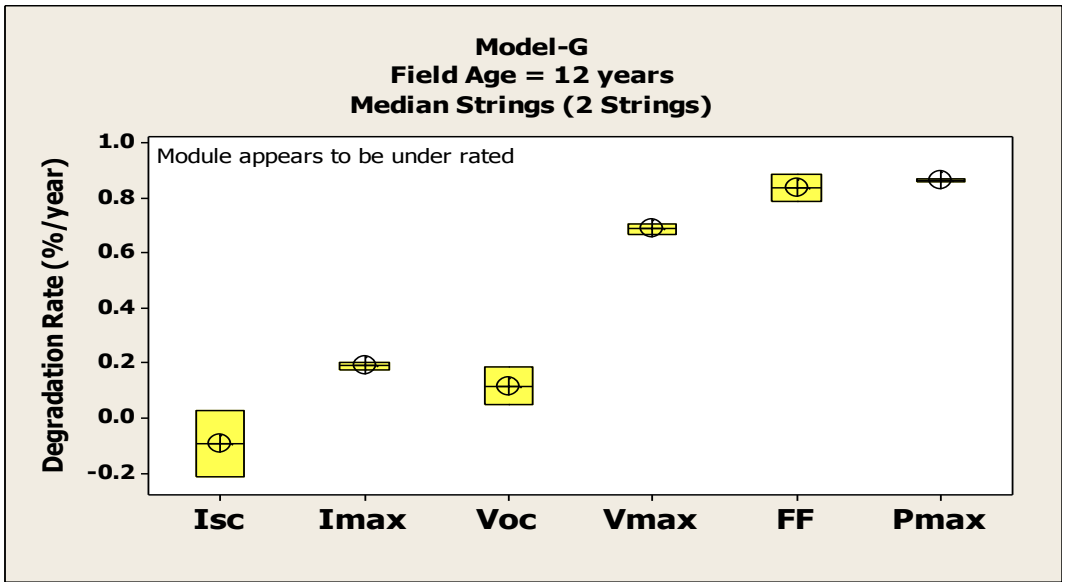

Figure A 7 Plot for various I-V parameter degradation (%/year) for median strings

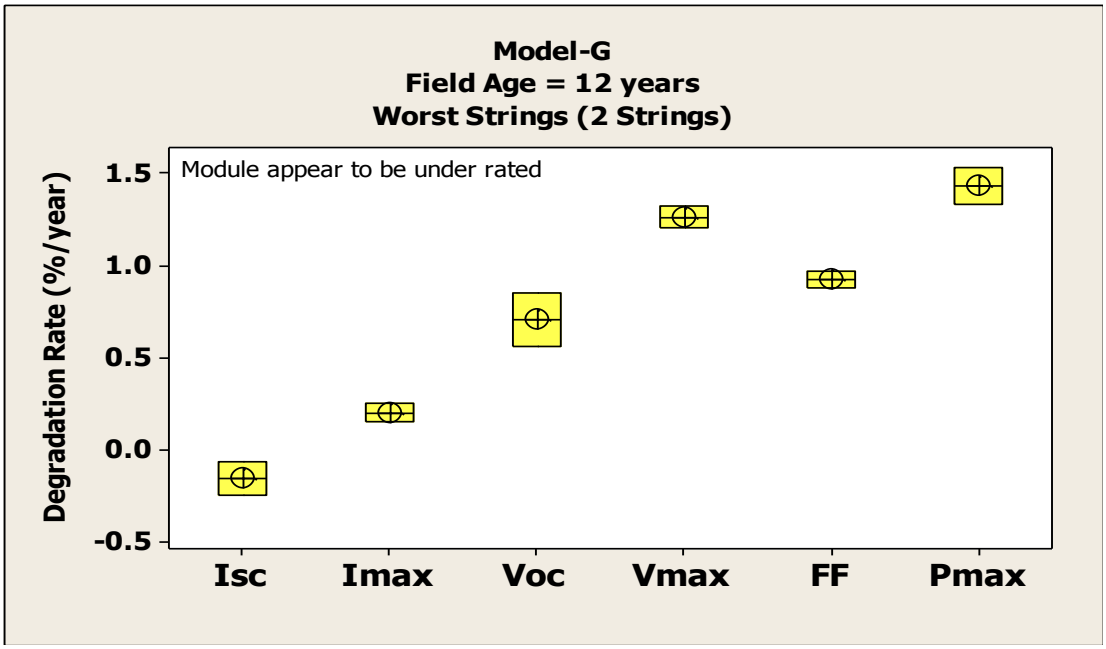

Figure A 8 Plot for various I-V parameter degradation (%/year) for worst strings

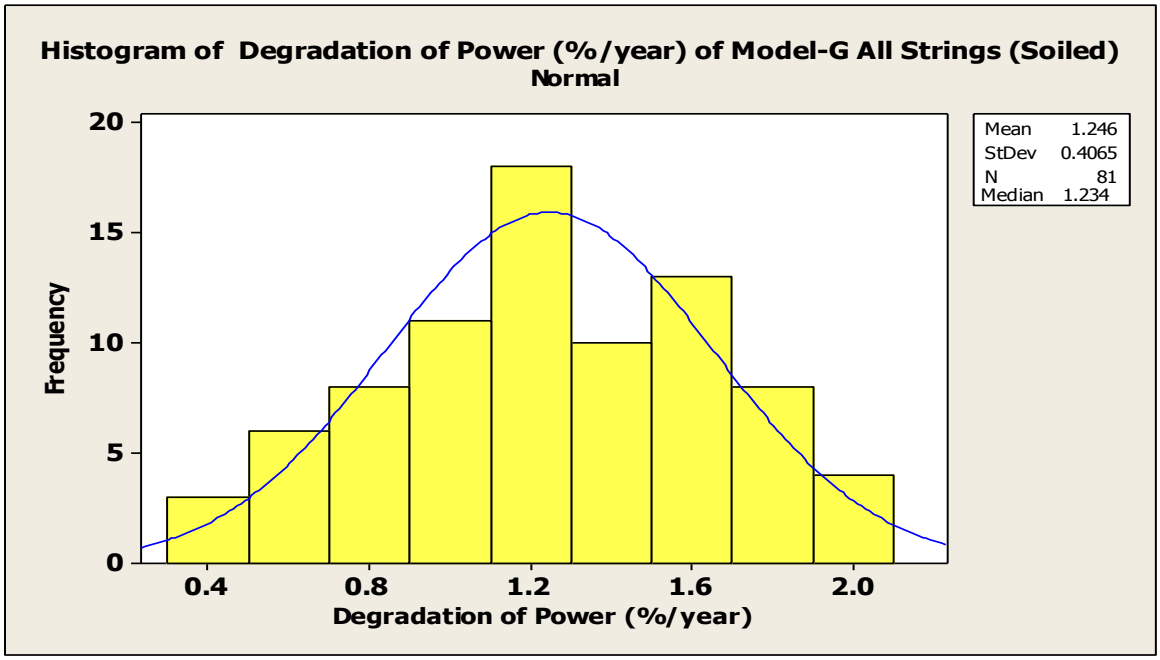

Figure A 9 Histogram of Power Degradation (%/Year) for Model-G strings (Soiled)

APPENDIX B

SITE 4C PLOTS FOR VARIOUS I-V PARAMETERS

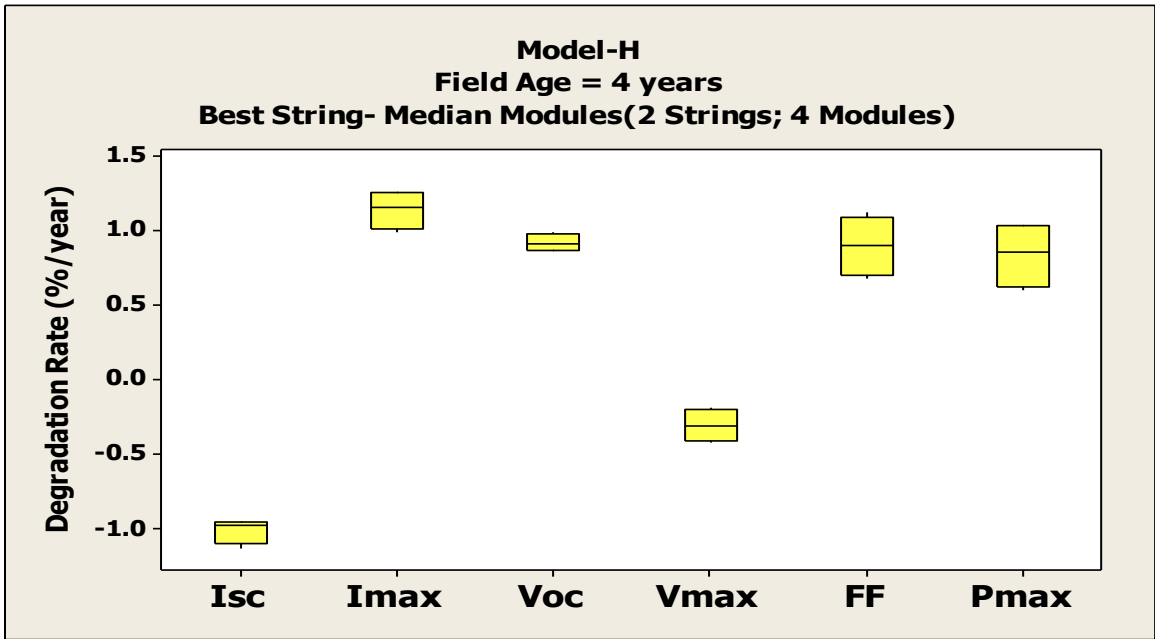

Figure B 1 Plot for various I-V parameter degradation (%/year) for best string- median modules

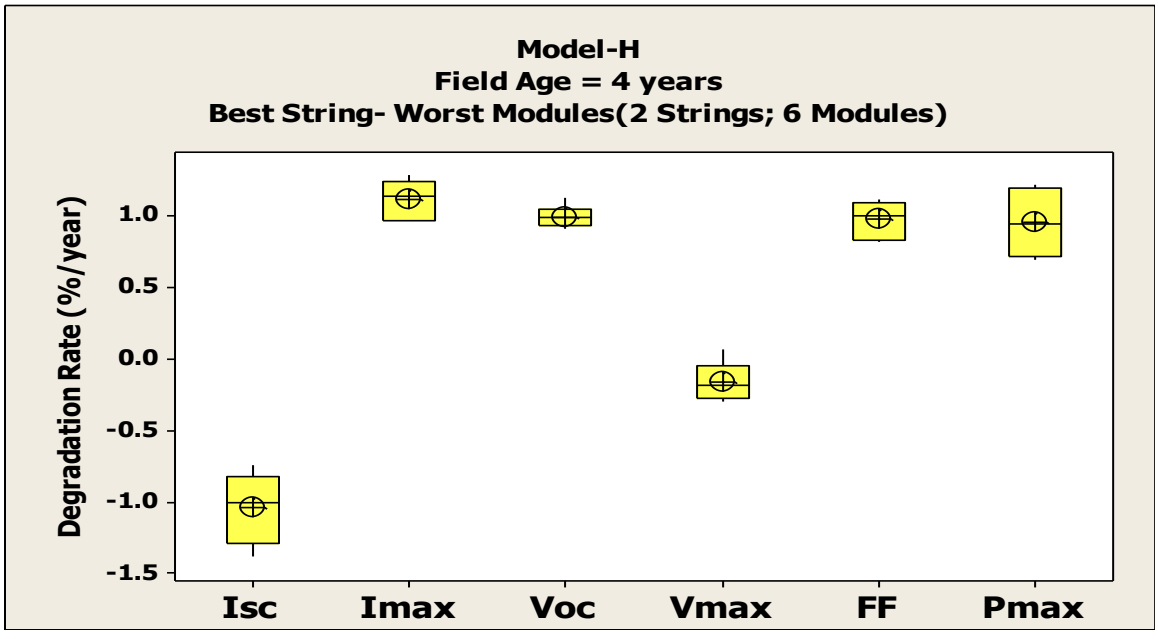

Figure B 2 Plot for various I-V parameter degradation (%/year) for best string- worst modules

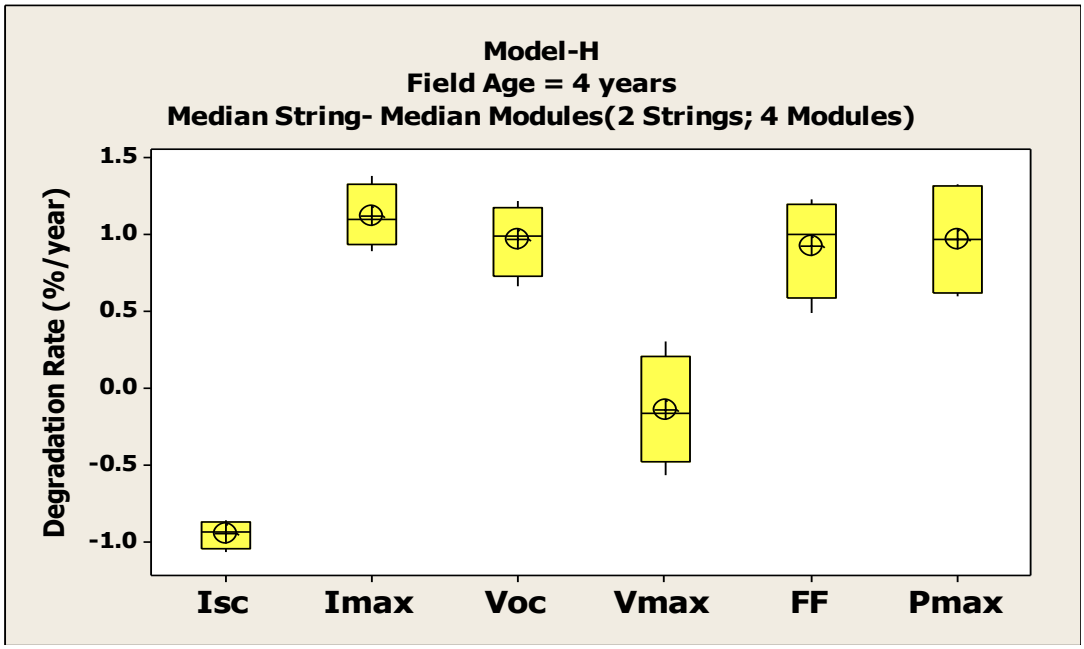

Figure B 3 Plot for various I-V parameter degradation (%/year) for median string- median modules

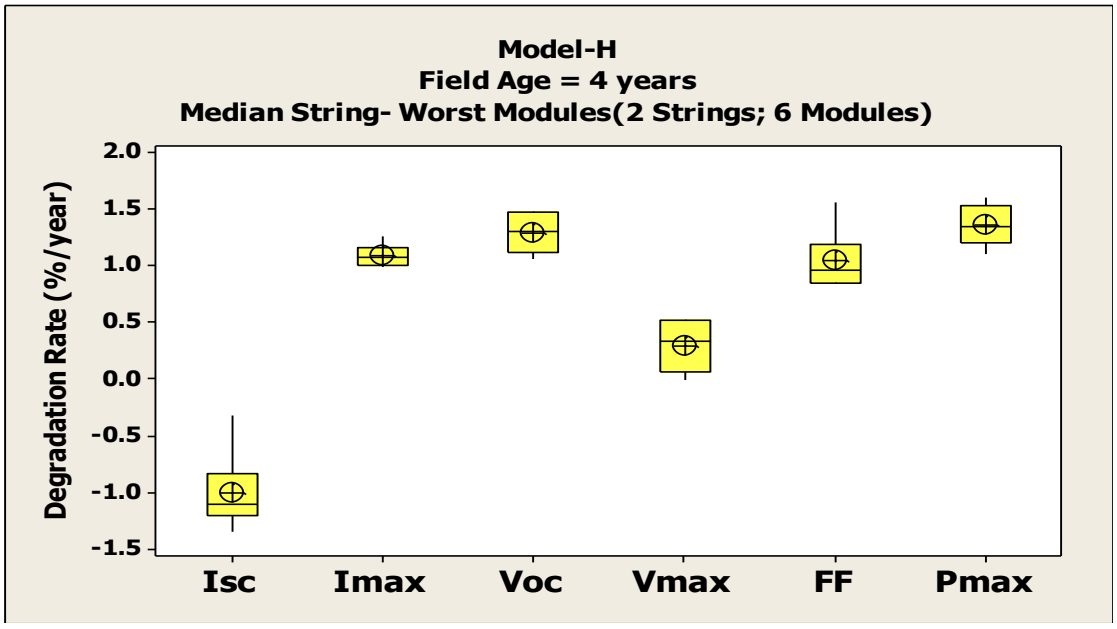

Figure B 4 Plot for various I-V parameter degradation (%/year) for median string- worst modules

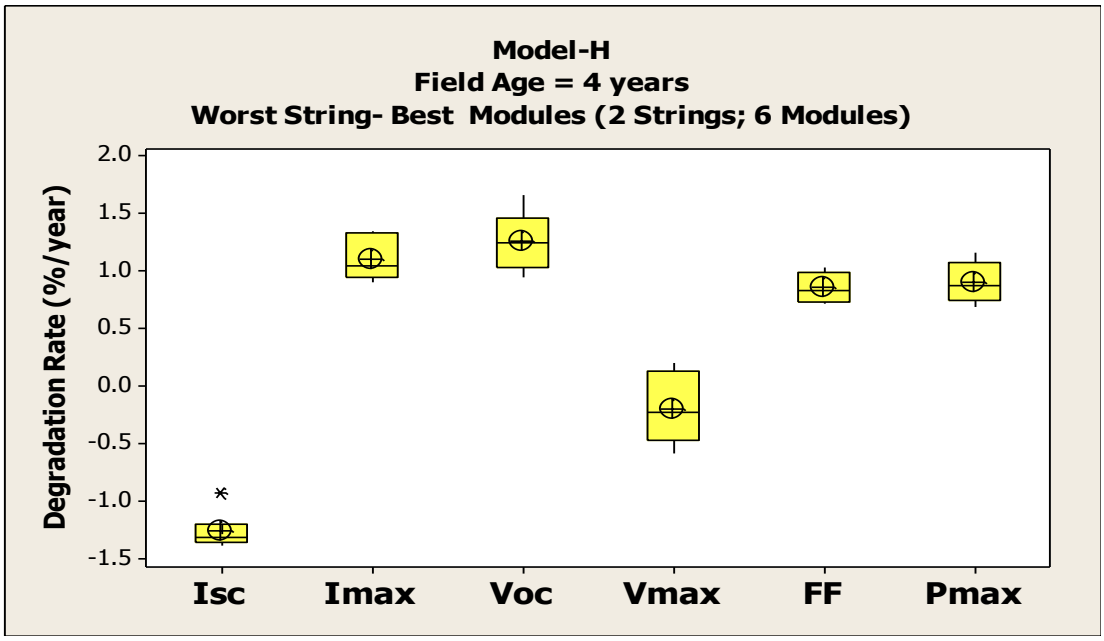

Figure B 5 Plot for various I-V parameter degradation (%/year) for worst string- best modules

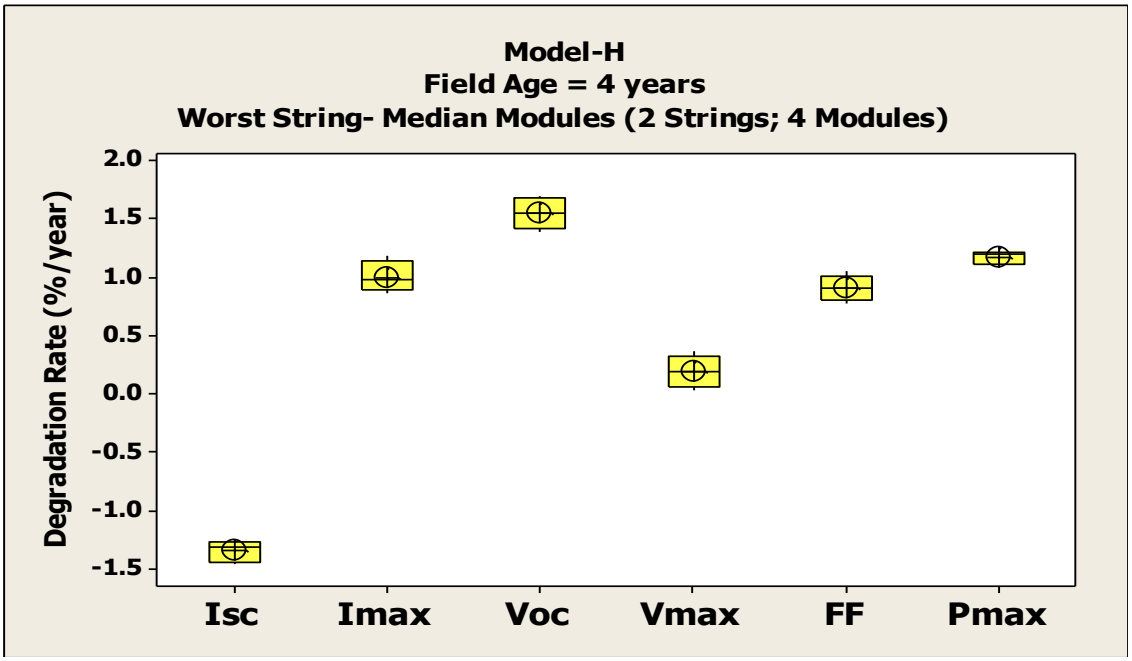

Figure B 6 Plot for various I-V parameter degradation (%/year) for worst string- median modules

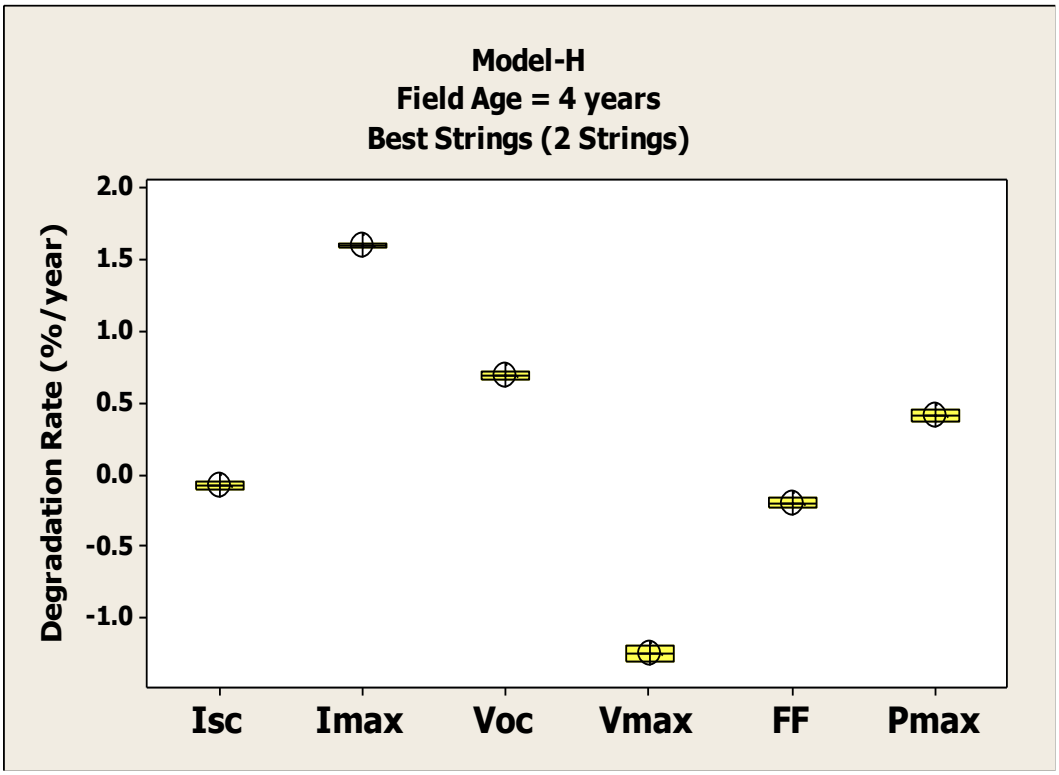

Figure B 7 Plot for various I-V parameter degradation (%/year) for best strings

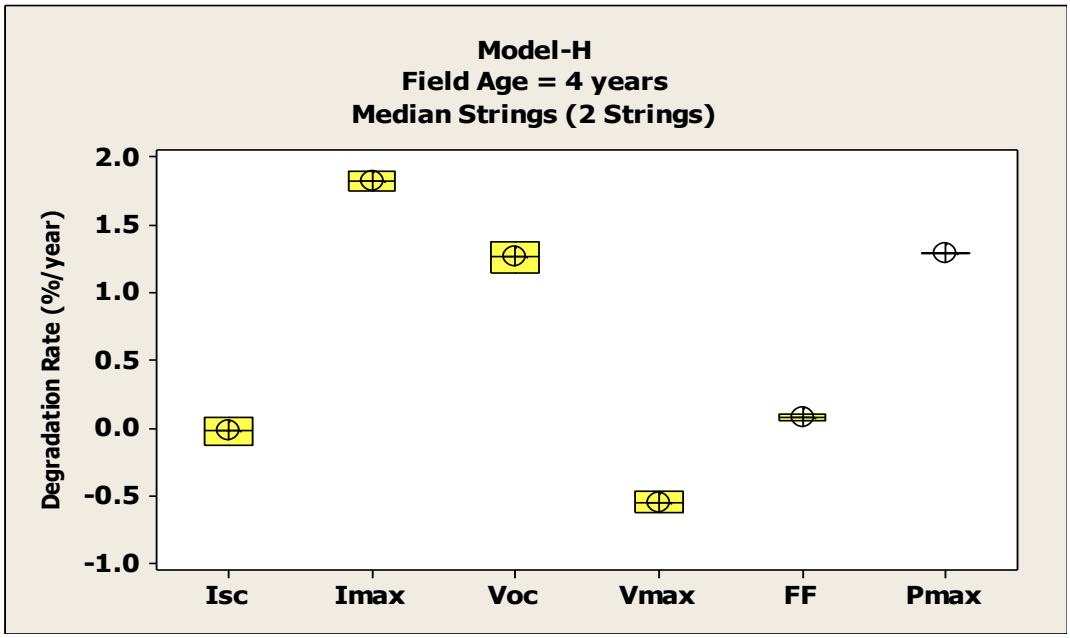

Figure B 8 Plot for various I-V parameter degradation (%/year) for median strings

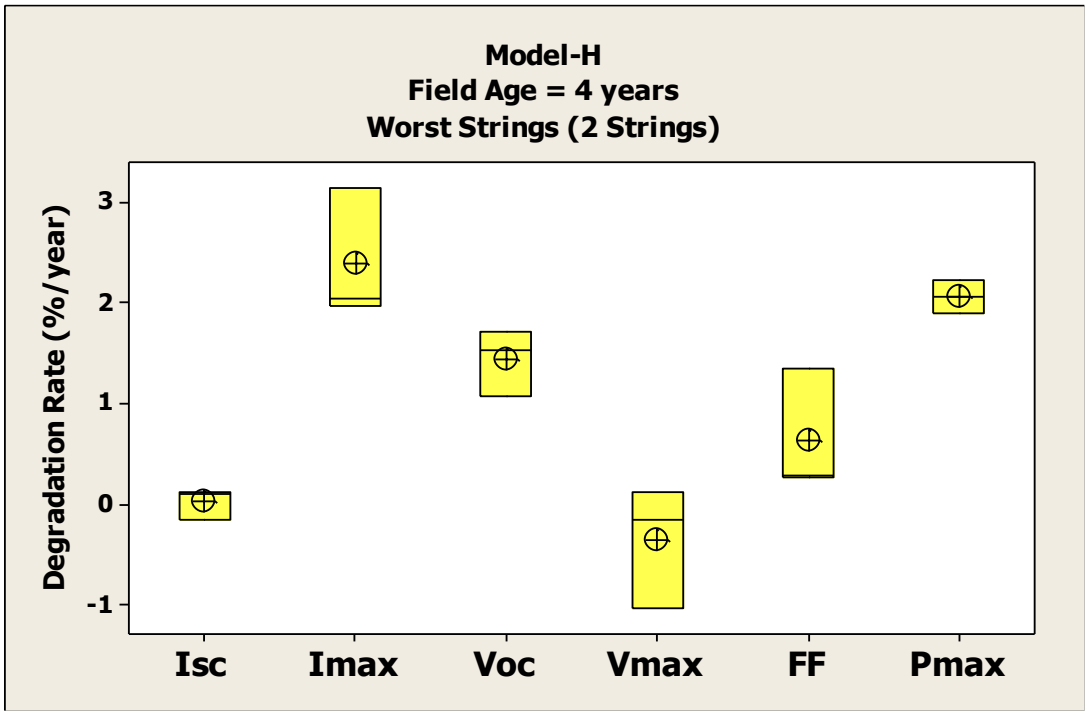

Figure B 9 Plot for various I-V parameter degradation (%/year) for worst strings

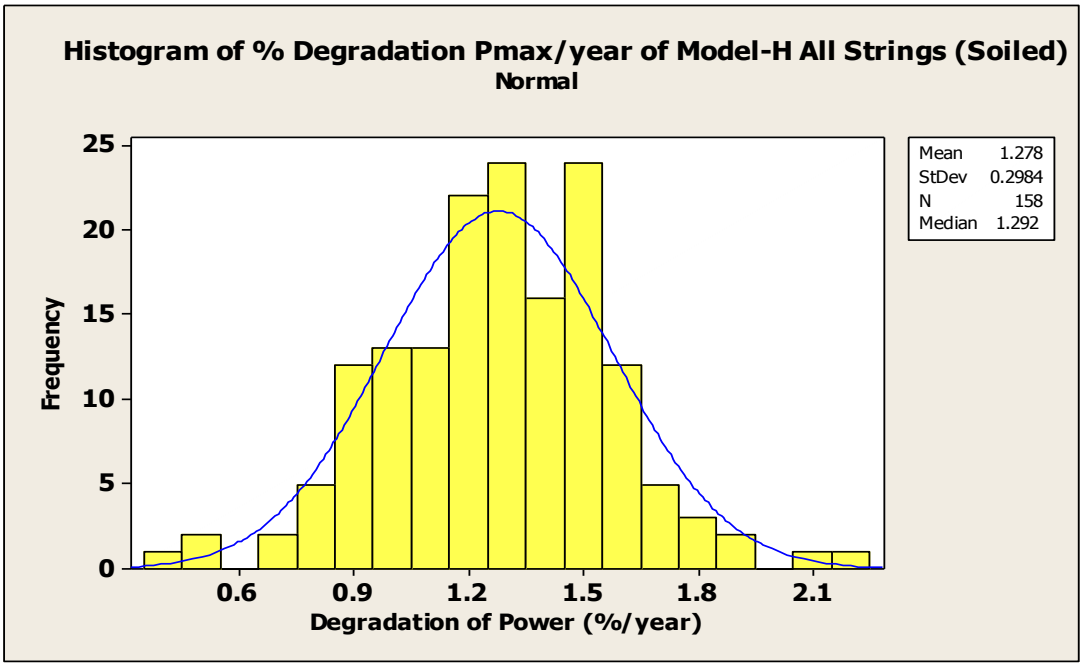

Figure B 10 Histogram of Power Degradation (%/Year) for Model-H strings (Soiled)